CENTRO DE INVESTIGACIÓN Y DE ESTUDIOS AVANZADOS DEL INSTITUTO POLITÉCNICO NACIONAL

Unidad Mérida

DEPARTAMENTO DE FÍSICA APLICADA

"ELABORACIÓN Y CARACTERIZACIÓN DE MATERIALES DE QUITOSANO CON EXTRACTOS DE PLANTAS PARA APLICACIÓN BIOMÉDICA"

Tesis

Que presenta

Isabel Otilia Caamal Herrera

Para obtener el grado de

Doctora en Ciencias

en

Fisicoquímica

Director de Tesis:

Dr. José Antonio Azamar Barrios

Mérida, Yucatán, México Diciembre de 2018

CENTRO DE INVESTIGACIÓN Y DE ESTUDIOS AVANZADOS DEL INSTITUTO POLITÉCNICO NACIONAL

Unidad Mérida

DEPARTAMENTO DE FÍSICA APLICADA

"ELABORATION AND CHARACTERIZATION OF MATERIALS OF CHITOSAN WITH PLANT EXTRACTS FOR BIOMEDICAL APPLICATION"

Thesis

Presented by:

Isabel Otilia Caamal Herrera

To obtain the degree of

Doctor of Science

in

Physical Chemistry

Thesis Director:

Dr José Antonio Azamar Barrios

Mérida, Yucatán, México December 2018

ACKNOWLEDGEMENTS

First of all, thanks to **God** for giving me life, family, friends and the opportunity to reach this goal in my professional and personal career.

I would like to express my gratitude to my advisor **Dr Jose Antonio Azamar Barrios** for his support, patience and trust to develop this project. I thank very much **Dra Leydi Carrillo Cocom** for her expert knowledge, support and for sharing with me the fascinating world of cellular tests. Thank you so much **MC Araceli Gonzalez Burgos** and **MC Diana Escalante Rendiz** for your valued time in the supervision of the microbiological tests and for your constructive comments. I also want to thank my collaboration partners: **Dr David Muñoz Rodriguez** for his support with the Gas Chromatographic techniques and identification of metabolites; **Dr Tomas Madera Santana** for his valued time in the supervision of the present work and his support in the material characterization. Thank you so much **Dr Mario Moises Alvarez** for giving me the opportunity to realize my doctorate stay, to open the doors of his laboratory and to know the fantastic world of the cellular tests. I would like to thank to reviewers: **Dra Patricia Quintana Owen**, **Dr Rodrigo Patiño Díaz** and **Dr Geonel Rodriguez Gattorno** for your valued comments that helped to improve the present work.

I am very grateful for the **Faculty of Chemical Engineering at Universidad Autónoma de Yucatán, FEMSA Biotechnology Center at Instituto Tecnológico y de Estudios Superiores de Monterrey**, **Campus Monterrey, Instituto Tecnológico de Mérida and Cinvestav Mérida** for the facilities provided during the research. Also, to the **Herbarium at Natural Resources Unit of the Center of Scientific Research of Yucatán (CICY)** for the support provided during the process of classification and identification of the specimens of plant material.

Special thanks to the personnel in charge and technical staff of the **Laboratory of Microbiology and Biotechnology** (**QI Karla Ku Duran, IBT Eric Ic Caamal, MC Alejandra Cabañas Sandoval** for your support and friendship); **Laboratory of Instrumental**, **QI Robert Sosa** for your support with the GC/MS equipment; **Laboratory of Cell Culture, LBG Diana Araiz Hernandez,** for the support with the fibroblast cells. You along with **Ilse, Cinthia, Dilore** and **Felipe** made me feel at home during my stay in

Monterrey. Thanks to **Laboratory of Fermentations**, **Dra Odri Sosa** for your support with the equipment for cellular test. SEM, TGA, DSC and DMA measurements were performed at **LANNBIO Cinvestav Mérida**, under support from projects **FOMIX-Yucatán 2008-108160 CONACYTLAB-2009-01-123913, 292692, 294643, 188345 y 204822**. Technical help is acknowledged to **MC Cristobal Ramos**, **MC Dora Huerta** and **IQI Andrea Loria**.

Thank you so much to the **Consejo Nacional de Ciencia y Tecnología (CONACYT)** for the financial support (**through the scholarship number 222612**) during the doctorate studies. Finally, my gratitude to **CINVESTAV Mérida** for giving me the great opportunity to realize my doctoral grade, and for the support during this phase of my professional and personal development.

I thank my family for all their love, unconditional support and understanding of my absences. To my mother, **Lilia**, you are the principal motivation. To my sisters **Lourdes**, **Cristina,** and **Lilia** for your support at all time, especially in the difficult moments. To my **nephews** and **nieces** who made me feel loved at all time. For my brother **Roger,** thanks for the example of perseverance. For my beautiful angel **Margarita†**, you will be always my best example of love and devotion. For the constant friendship, unconditional support and love of my friends, especially **Lupita, Swe, Jael, Alba**, thank you so much for understanding my absences and staying with me in the darker days of my life. Finally, to all those people who, in one way or another, have been present in my personal and professional growth.

LIST OF ABBREVIATIONS

AAE: Aqueous extract of *Ocimum micranthum* Willd leaves

ATCC: American Type Culture Collection

A. indica: *Azadirachta indica* A. Juss

B. subtilis: *Bacillus subtilis*

C. officinalis: *Calendula officinalis*

C.albicans: *Candida albicans*

CHO-K1: Chinese hamster ovary cells

DMA: Dynamic mechanical analysis

DMSO: Dimethylsulfoxide

DSC: Differential scanning calorimetry

E. coli: Escherichia coli

EEA: Ethanolic extract of *Ocimum micranthum* Willd leaves

EOA: Essential oil of *Ocimum micranthum* Willd leaves

GC/MS: Gas chromatography–mass spectrometry

HAECa: Hydro-alcoholic extract of *Calendula officinalis* flowers

HAET: Hydro-alcoholic extract of *Mimosa tenuiflora* bark

hFB: Human fibroblast cells

INT: *P*-iodonitrotetrazolium;

MIC: Minimal inhibitory concentration

M. tenuiflora: *Mimosa tenuiflora*

MTT: 3-(4,5-dimethylthiazol-2-yl)-2,5-diphenyltetrazolium bromide

O. micranthum: *Ocimum micranthum* Willd

P. aeruginosa: *Pseudomonas aeruginosa*

S. aureus: *Staphylococcus aureus*

SD: Standard Deviation

SEM: Scanning electron microscopy

SPE: Solid phase extraction

TGA: Thermogravimetric analysis

t_R: Retention time

WVTR: Water vapor transmission rate.

LIST OF TABLES

LIST OF FIGURES

CONTENT

ABSTRACT

In México there are several medicinal plants such as *Ocimum micranthum* Willd (wild basil), *Calendula officinalis* (marigold), *Mimosa tenuiflora* (tepezcohuite) and *Azadirachta indica* A. Juss (neem), which possess antimicrobial, antioxidant, healing and anti-inflammatory activities, suitable characteristics for biomedical applications. Chitosan is a natural polymer with cationic and film-forming properties, so that has been used to develop active films and membranes incorporating essential oils, silver nanoparticles, and drugs. Recently, it has been developed a tendency to integrate extracts from plants in films and nanoparticles of chitosan; the goal is to take advantages of the medicinal properties that these natural extracts possess and that these films may have biomedical applications, especially in the treatment of wounds and burns. Therefore, this work aimed to study the effect of the incorporation of extracts from these plants on the physical, thermal and mechanical properties as well as the antimicrobial activity and human cell (hFB) proliferative behavior in the chitosan films.

A chemical characterization by GC/MS analysis was realized in essential oil, ethanolic and aqueous extract from leaves of *Ocimum micranthum* Willd, hydro-alcoholic extract of *Calendula officinalis* flowers, hydro-alcoholic extract of *Mimosa tenuiflora* bark and oil from seeds of *Azadirachta indica* A. Juss. The antimicrobial activity and the proliferative effect on hFB cell line also were evaluated in these extracts and oils. These assays showed that the hydro-alcoholic extract of *Calendula officinalis* flowers (HAECa) and the aqueous extract of *Ocimum micranthum* Willd leaves (AAE) possess special activity against *Candida albicans* at same concentration (80 µl/ml). Those extracts also showed a minor anti-proliferative effect on hFB cell line at concentrations evaluated.

The hydro-alcoholic extract of *C. officinalis* flowers (HAECa), and the aqueous extract of *O. micranthum* Willd leaves (AAE) were added in 8, 10, 12% (v/v) and 2, 4, 6% (v/v) respectively into chitosan matrix for prepare films by the casting method. The mechanical characterization of the films was performed using a universal testing machine and a texturometer at 25° C. The relaxation modulus was measured with dynamic mechanical analyzer. The surface free energy of chitosan films with extracts was performed by static contact angle measurements carried out by the sessile drop method. The water vapor transmission rate (WVTR) was carried out by the ASTM-E96-95 method. Thermal analysis was carried out through Differential Scanning Calorimetry (DSC) and Thermogravimetric analysis (TGA) tests under a nitrogen atmosphere. The antimicrobial activity against *Staphylococcus aureus*, *Bacillus subtilis*, *Pseudomonas aeruginosa* and *Candida albicans* was determined through the agar disc-diffusion method. The cell proliferation assay was carried out

using human fibroblast cell line (hFB). The proliferative behavior and cell morphology were monitored by optical microscopy and scanning electron microscopy (SEM). The cell viability of human fibroblast was observed by fluorescent microscopy.

The tensile strength values of chitosan films with HAECa decreased significantly ($p < 0.05$) when the concentration of this extract increased in the formulation. The elongation at break values showed a significant decrease in all films that incorporated natural extracts. The Young's modulus was not affected significantly by the incorporation of extracts. All formulations had a reduction of the value of the relaxation modulus when the temperature was increased.

The chitosan films with HAECa had values of contact angle below 50° and were different significantly ($p<0.05$) to the control and to the films with AAE (90°). The addition of HAECa at 12% exert a significant increase in the WVTR value of chitosan films, while the addition of AAE extract did not cause a significant effect.

In the exothermic phase, the DSC study showed that HAECa caused in the chitosan films a displacement to high decomposition temperature and higher decomposition enthalpies than control and them films incorporated with AAE. This behaviour was confirmed in the TGA study.

The chitosan films with HAECa presented an effect by contact against *Pseudomonas aeruginosa*, while the films with AAE showed the same effect against *Bacillus subtilis*. The addition of HAECa into the chitosan matrix permitted the cell adhesion of human fibroblasts which was observed using optical and SEM microscopy. This cell line also showed viability, which was observed through fluorescent microscopy.

These results indicate that the chitosan films with HAECa could be used for biomedical, although before is necessary confirming its proliferative behavior on hFB cell line through of *in vivo* models and clinical assays.

By other hand, the other extracts and oils from *O. micranthum*, *Mimosa tenuiflora* and *A. indica* that showed anti-proliferative effect on hFB cell line could be evaluated in other kind of cell line, for example cancer cells.

RESUMEN

En México hay diversas plantas medicinales como *Ocimum micranthum* Willd (wild basil), *Calendula officinalis* (marigold), *Mimosae tenuiflorae* (tepezcohuite) and *Azadirachta indica* A. Juss (neem), las cuales poseen actividades antimicrobianas, antioxidantes, curativas e inflamatorias; características idóneas en aplicaciones biomédicas. El quitosano es un polímero con propiedades catiónicas y formadoras de película, por lo que se ha utilizado en el desarrollo de envases funcionales incorporándole aceites esenciales, nano partículas de plata y fármacos. Recientemente, se ha incrementado el interés por integrar extractos de plantas en películas y membranas de quitosano; el propósito es aprovechar las propiedades medicinales de estos y que dichos materiales puedan tener una aplicación biomédica, especialmente en el tratamiento de heridas y quemaduras. El objetivo del presente trabajo fue estudiar el efecto de los extractos de estas plantas en las propiedades físicas, térmicas, mecánicas, así como en la actividad antimicrobiana y el comportamiento proliferativo de células humanas (fibroblastos) en las películas de quitosano.

Se realizó una caracterización química por análisis de GC/MS en aceite esencial, extracto etanólico y acuoso proveniente de hojas de *Ocimum micranthum* Willd, extracto hidroalcoholico de flores de *Calendula officinalis*, extracto hidroalcoholico de corteza de *Mimosa tenuiflora* y aceite de semillas de *Azadirachta indica* A. Juss. La actividad antimicrobiana y el efecto proliferativo sobre fibroblastos humanos también fueron evaluados en estos extractos y aceites. Estos ensayos mostraron que el extracto hidroalcoholico de flores de *C. officinalis* (HAECa) y el extracto acuoso de hojas de *O. micranthum* Willd poseen actividad especial contra *Candida albicans* a la misma concentración (80 µl/ml). Estos extractos también mostraron un efecto anti-proliferativo menor contra la línea celular de fibroblastos humanos a las concentraciones evaluadas.

El extracto hidro-alcohólico de flores de *C. officinalis* (HAECa) y el extracto acuoso de hojas de *O. micranthum* Willd (AAE) fueron adicionados a una matriz de quitosano en concentraciones de 8, 10, 12 % (v/v) y 2, 4 y 6% (v/v), respectivamente, para preparar películas por método de vaciado. La caracterización mecánica de las películas se realizó empleando una maquina universal de pruebas y un texturómetro a una temperatura de 25° C. El módulo de relajación se midió en un equipo DMA. Se determinó la energía libre de superficie de las películas de quitosano incorporadas con extractos se obtuvo midiendo el ángulo de contacto por el método de goteo. Se determinó la velocidad de transmisión de vapor de agua (WVTR) bajo el método ASTM-E96-95. En los análisis térmicos de calorimetría de barrido diferencial (DSC) y termogravimetría (TGA) se usaron los equipos correspondientes bajo una atmósfera de nitrógeno. Se determinó la

actividad antimicrobiana contra *Staphylococcus aureus*, *Bacillus subtilis*, *Pseudomonas aeruginosa* and *Candida albicans* se determinó a través del método difusión en agar. El ensayo de proliferación celular fue realizado usando una línea celular de fibroblastos humanos (hFB). Se monitoreó el comportamiento proliferativo y la morfología celular mediante microscopia óptica y microscopia electrónica de barrido. Se observó la viabilidad celular de los fibroblastos humanos por microscopia de fluorescencia.

El valor de la fuerza de tensión de las películas de quitosano con HAECa disminuyó significativamente ($p < 0.05$) al incrementar la concentración del extracto. En todas las películas a las que se les incorporó el extracto, el valor de elongación a la ruptura mostró una caída significativa ($p < 0.05$) El valor de módulo de Young en las películas de quitosano no se vio afectado significativamente ($p > 0.05$) por la presencia de los extractos. En todas las formulaciones se presentó una reducción del valor de módulo de relajación al incrementar la temperatura,

Las películas de quitosano con HAECa tuvieron valores de ángulo de contacto menores a 50° y fueron significativamente diferentes ($p < 0.05$) a las películas control y aquellas con AAE (90°). La adición de HAECa al 12% (v/v) ejerció un incremento significativo ($p < 0.05$) de valor de WVTR; mientras que la adición de AAE no causó un efecto significativo ($p > 0.05$).

La fase exotérmica del estudio DSC mostró que el HAECa causó en las películas de quitosano un desplazamiento de la temperatura de descomposición y valores mayores de entalpia de descomposición en comparación con las películas control (sin extracto) y las películas incorporadas con AAE. Este comportamiento fue confirmado en el estudio TGA.

Las películas de quitosano con HAECa mostraron un efecto por contacto contra *Pseudomonas aeruginosa*, mientras que las películas con AAE mostraron el mismo efecto contra *Bacillus subtilis*. La adición de HAECa dentro de la matriz de quitosano permitió la adhesión de las células de fibroblastos humanos en las películas, lo cual se observó mediante microscopía óptica y microscopía electrónica de barrido. Por otra parte, la viabilidad de dicha células fue constatada a través de microscopía fluorescente.

Estos resultados indican que las películas de quitosano con HAECa podrían ser utilizadas para aplicación biomédica, pero antes sería necesario verificar el efecto proliferativo sobre hFB a través de modelos *in vivo* y estudios clínicos.

Por otra parte los extractos y aceites provenientes de *O. micranthum*, *M. tenuiflora* y *A. indica* que mostraron efecto antiproliferativo sobre hFB podrían ser evaluados en otros tipos de líneas celulares, por ejemplo, células cancerosas.

HYPOTHESIS

It is known that the *Ocimum micranthum* Willd (wild basil), *Calendula officinalis* (marigold), *Mimosa tenuiflora* (tepezcohuite), and *Azadirachta indica* A. Juss (neem) are plants with medicinal properties that to help in the regeneration of skin wounds and burns because have antimicrobial, antioxidant, healing and anti-inflammatory activities. Chitosan is a biopolymer with film-forming, healing, antimicrobial, and antifungal properties. If we extract the active components of these plants and we add them to chitosan, then it is very likely that the healing function will be potentiating improving the healing process and time.

By the other hand, if we add these extracts to chitosan, we could achieve a high interaction grade at molecular level that could modify the physical, chemical, thermal and mechanical original properties of this biopolymer.

INTRODUCTION

The plants represent the main therapeutic resource in the practice of the traditional and alternative medicine. The interest in the use of plants with anti-inflammatory, antioxidant, antibacterial, and proliferative activity is due to the importance of these properties in the treatment of wound, burns and skin diseases, because help to improve the time and healing process. For example, people with *diabetes mellitus* have strong tendency to suffer wound chronic of difficult healing as a consequence of high sugar levels in blood damaging the blood vessels that carry oxygen and nutrients.

The extracts and oils of some plants, such as *Calendula officinalis* and *Mimosa tenuiflora* have been used topically in products such as creams and ointments. The main characteristics of these extracts are the anti-inflammatory effect and the increment of the rate of re-epithelialization, the formation of granular tissue, and regeneration of dermal collagen in skin wounds. In Yucatán, there are plants with the similar potential such as the case of *Ocimum micranthum* Willd and *Azadirachta indica* A. Juss.

Diverse polymeric matrices have been studied to carry the secondary metabolites of the plants so that they maintain the curative effects and properties. Among the most suitable polymers is the chitosan, a polymer of natural origin obtained from the crustacean's chitin. The chitosan, because its particular characteristics, such as biodegradability, biocompatibility, non-toxicity and antimicrobial properties, has been used in wound healing, tissue repair, cell adhesion, drug delivery, and food packaging.

The incorporation of the extracts may produce changes on the chitosan matrix and as a consequence of its properties. Therefore, the primary objective of this work was to study the effect of the presence of the aqueous extract *of Ocimum micranthum* (AAE) leaves and the hydro-alcoholic extract *of Calendula officinalis* flowers (HAECa) on the physical, chemical, thermal, and mechanical properties, as well as the antimicrobial activity and human cell (hFB) proliferative behavior in the chitosan films.

Chapter 1

Identification of volatile compounds in extracts of *Ocimum micranthum* Willd leaves, *Calendula officinalis* L. flowers, *Mimosa tenuiflora* bark and *Azadirachta indica* A. Juss seeds using GC/MS.

1.1 Introduction

Currently, traditional medicine is a health system that is being revalorized rapidly with great potential, it is used worldwide, and medicinal plants constitute its principal therapeutic resource [1]. The plants have medicinal properties, owing to their secondary metabolites, which can be located in leaves, flowers, stems, seeds or roots. In México, there are several medicinal plants such as wild basil, marigold, tepezcohuite and neem, which possess antimicrobial, antioxidant, healing and anti-inflammatory activities; suitable characteristics for biomedical applications [2-5].

Ocimum micranthum Willd is the scientific name of the wild basil, which belongs to the family of Lamiaceae/Labiatae. On the Yucatan's peninsula, it has been known as Cacaltún or Xkakaltun (Mayan names), and it has been used for its medicinal and culinary virtues for many years. Mayan people used a decoction of the flowers to treat gastrointestinal, respiratory and nervous diseases, as well as to relieve earache, headache, swelling, or constipation. The stem of this plant has also been used in the process of maceration in alcohol to treat neck pain problems, rheumatism, sprains, and cramps [6]. The decoction of the leaves of the plant has been used to treat stomach pain, rheumatism, gout, fever, high blood pressure, toothache, sores, ulcers, grains, insomnia, and menstrual regulation as well as a postpartum bath and mosquito repellent [6, 7].

Previous studies showed that *O. micranthum* Willd leaves contain saponins, flavonoids, tannins and essential oil [8, 9]. This last fraction has a profile of volatile compounds with activity against human pathogens such as bacteria (*Escherichia coli, Pseudomonas aeruginosa, Staphylococcus aureus, Mycobacterium tuberculosis*) and fungi (*Candida albicans, Cryptococcus neoformans, Microsporum canis, Microsporum gypseum, Trichophyton mentagrophytes, Trichophyton rubrum*) [6, 9]. In the essential oil, there were also discovered functional activities such as anaesthetic, analgesic, and anti-inflammatory, with potential application in both traditional and conventional medicine [9, 10].

Concerning the functional properties of ethanolic extracts from the genus *Ocimum*, the *O. micranthum* species showed activity against the insect *Culex quinquefasciatus* [6], *Ocimum sanctum* Linn leaves exert a positive effect on wound healing in rats, and the ethanolic extract of *Ocimum ubasilicum* leaves had antimicrobial activity against *Acinetobacter spp, Bacillus, Escherichia*,

Staphylococcus and *Candida albicans* [11,12]. However, the chemical composition and profile of volatile compounds of the ethanolic and aqueous extracts of the leaves of the *Ocimum micranthum* Willd species has not been reported.

Calendula officinalis (marigold) is a plant native from southern Europe that, over time, has extended to many countries throughout Europe and America. It is widely used for its healing, anti-inflammatory and antiseptic properties [13]. The marigold flower is abundant in flavonoids, phenolic acids, and saponins. It also contains carotenoids, free or esterified triterpene alcohols and unsaturated fatty acids, such as calendic acid, which has shown anti-inflammatory properties *in vivo* and inhibitory properties *in vitro* [14, 15]. Among the identified antioxidants in *C. officinalis* are flavaxanthin, luteoxanthin, ß-carotene, lycopene, α-carotene, rutinoside, isorhamnetin, and narcissin [13]. The essential oils of the *Calendula officinalis* flower have shown antibacterial activity against *Escherichia coli*, *Staphylococcus aureus* and *Streptococcus faecalis* as well as antifungal activity against *Candida albicans* [13]. The particular interest in the biomedical applications of *C. officinalis* is due to its ability to heal external and opened wounds, lacerations, and ulcers through the promotion of granulation tissue. It has been used to treat ulcers in the stomach and intestines, haemorrhages, and chronic skin lesions such as burns [16]. Concerning applications of extracts from *Calendula officinalis* flowers, the effect of the hydro-alcoholic extract in the treatment of acne was tested [17]; the authors observed an antimicrobial effect against *Staphylococcus aureus*, *Staphylococcus faecalis*, *Escherichia coli* and *Klebsiella pneumonia*, as well as an antifungal effect against *Candida mannose*. Moreover, it was reported that the butanol fraction of the extract of the plant flowers has antioxidant activity, and the aqueous extract obtained by the decoction of the plant has an anti-inflammatory effect [18, 19].

M. tenuiflorae is a plant belonging to the *Mimosaceae* family; its bark has been used in traditional medicine for the treatment of burns and skin wounds [3]. Previous studies have shown that aqueous and ethanolic extracts of the dried bark of *M. tenuiflorae* contain tannins, steroidal saponins and phenolic compounds [20]. Since its successful application to burn victims of various catastrophic events in 1980 in Mexico, *M. tenuiflorae* bark has received a considerable focus within scientific research on skin treatments. In traditional Mexican ethno-medicine, the bark has been used directly on lesions of the skin and in the form of aqueous extracts. Furthermore, it has exhibited mitogenic and anti-ulcerative effects, primarily in extracts that have been prepared with ethanol [3]. The use of aqueous extracts from *M. tenuiflorae* bark in the treatment of leg venous ulceration has also been reported [20]. Among the pre-clinical studies of aqueous and alcoholic extracts of the bark of *M. tenuiflorae* are healing and the treatment of severe skin ulcers; its effect on the inflammation induced by *Tityus serratu*s scorpion venom is the latest clinical application

reported [21]. In this study, an aqueous extract obtained by a decoction of the bark and fractionation with dichloromethane, ethyl acetate and *n*-butanol was used. The activities of the hydro-alcoholic extract and its applications have not previously been reported in a scientific context.

Azadirachta indica A. Juss is a plant native of the India with use in folk medicine due to immunomodulatory, anti-inflammatory, antimicrobial, antifungal, and anticarcinogenic properties [22]. Also, it has been observed its effect for decreasing high pressure and cholesterol levels, as well as in the treatment of burns, gastric ulcers and digestive diseases [23]. In this plant, it has been found more of 100 terpenoid compounds such as the limonoids azadirachtin, meliantriol, nimbin, and salannin [24].

Although there is information about the composition of the essential oil and the aqueous extract of the flowers of *C. officinalis* as well as the aqueous and ethanolic extracts of the bark of *M. tenuiflora*, the profile of volatile compounds in the hydro-alcoholic extracts of both plants have not yet been published. In the case of *A. indica* A. Juss oil obtained by ethanolic extraction from seeds, the profile of volatile compounds has been neither reported.

Therefore, this part of the thesis is focused on the analysis of extracts from *O. micranthum* Willd leaves, *C. officinalis* flowers, *M. tenuiflora* bark and *A. indica* seeds using GC/MS to identify and quantify the content of major volatile compounds using the normalization method. The results contribute to a knowledge of which volatile compounds could be involved in the medicinal properties of these extracts and to propose possible mechanisms of action.

1.2 Experimental Methods

Plant material.

The *O. micranthum* Willd was taxonomically identified and classified by the biologist José L. Tapia of the Herbarium at The Natural Resources Unit of the Center of Scientific Research of Yucatán, Mérida, Yucatán, México. A specimen was deposited in this same Herbarium with a number 68785. The leaves were collected during the winter season between December 2013 and February 2014 at 100 m around the point 21°9'10.91" North latitude and 89°5'4.58" West longitude in the town of Cansahcab, Yucatán, México. Harvested leaves were washed and dried in a convection oven at 50°C for 16 h. Finally, the leaves were ground in a mill (Ika, model A11) [22].

Preparation of essential oil and aqueous extract from *O. micranthum* Willd leaves.

The essential oil was obtained by hydro-distillation of ground leaves of *O. micranthum* Willd, using a Clevenger trap [7, 8, 22]. The essential oil fraction was recovered by density and stored at 4°C in glass vials sealed with Teflon tape, and covered with aluminium until its characterization. The aqueous phase was collected in plastic containers and filtered using a

membrane of 0.22 μm, finally it was stored at 4°C. This phase was called the aqueous extract (AAE) [23, 24].

Preparation of ethanolic extract from *O. micranthum* Willd leaves.

The ethanolic extract was obtained by Soxhlet extraction of ground leaves of *O. micranthum* Willd, using reagent-grade ethanol (JT Baker). The ethanol was recovered through as Büchi rotary evaporator (model R-215) with a vacuum controller (V-850) coupled to a cooling unit. The extract was filtered through a filtration system comprising a stainless-steel base and a Millipore filter (0.22 μm), and stored in glass bottles. Finally, the ethanolic extract was labelled and refrigerated at 4°C until its analysis.

Hydro-alcoholic extracts of *C. officinalis* L. flowers and *M. tenuiflorae* bark

The commercial fluid hydro-alcoholic extracts from *C. officinalis* flowers and *M. tenuiflorae* bark used in this study were acquired in REDSA S.A de C.V. (production batch EFM012280114 and EFT003122113 respectively). These extracts were obtained by the process of maceration in ethanol solution [25, 26].

Oil extraction of *A. indica* A. Juss seeds

The oil was obtained by Soxhlet extraction of dried and ground seeds of *A. indica* A. Juss, using reagent-grade ethanol (JT Baker) as the solvent [27]. The ethanol was recovered through the Büchi rotary evaporator (model R-215) with a vacuum controller (V-850) coupled to a cooling unit. The oil was centrifuged and then filtered through a filtration system comprising a stainless-steel base and a Millipore filter (0.22 μm). Finally, the oil extract was stored in glass bottles, labelled and refrigerated at 4°C until its analysis.

Sample preparation for GC/MS analysis of essential oil, aqueous and ethanolic extracts from *O. micranthum* Willd.

The essential oil was diluted (1:500) in HPLC-grade dichloromethane [7, 8]. The ethanolic extract was diluted (1:10) in HPLC-grade dichloromethane. The aqueous extract was centrifuged at 2000 rpm for 10 minutes to remove particles that could interfere in the process of solid-phase extraction [28] which was performed with two separate C18 SPE cartridges (500 mg, Alltech, Deerfield IL). This extraction was performed to pre-concentrate the compounds present in the extract, to change the solvent and subsequently to inject the sample directly into the chromatograph. In this extraction, was passed 5 mL of methanol through both cartridges, followed by 5 mL of ethanol: water (70:30) for conditioning; then, were injected 10 mL of the aqueous extract, before the cartridges were dried with air flow and one cartridge was eluted with 1 mL of isooctane and the other with 1 mL of acetonitrile.

Sample preparation for GC/MS analysis of hydro-alcoholic extracts of *C. officinalis* L. flowers and *M. tenuiflorae* bark.

The hydro-alcoholic extracts of *C. officinalis* flowers, and *M. tenuiflorae* bark were centrifuged at 2000 rpm for 10 minutes in order to remove particles that could interfere with the process of solid-phase extraction [28] which was performed in two C18 SPE cartridges (500 mg, Alltech, Deerfield IL); this kind of extraction was carried out in order to pre-concentrate the extract, to change the solvent and, subsequently, to be able to inject directly into the chromatograph. In such an extraction, were passed 5 mL of methanol through both cartridges, followed by 5 mL of ethanol:water (70:30) for conditioning, and then 10 mL of aqueous extract, after which the cartridges were dried with an air flow and, finally, one cartridge was eluted with 1 mL of isooctane and the other with 1 mL of acetonitrile; this procedure was performed in duplicate, and a control of each solvent was used to detect the signals attributable to the solvent or cartridge in the chromatogram of each sample.

Sample preparation for GC/MS analysis of *A. indica* A. Juss

The oil was diluted (1:5) in HPLC-grade dichloromethane.

GC/MS description and conditions

The extracts were analyzed with a gas chromatograph (Agilent Technologies, Santa Clara, California, USA) model 7890A, coupled to a mass spectrometer (Model 5975C, same brand). A Zebron ZB-5HT INFERNO capillary column (5 % phenyl-95 % polydimethylsiloxane, 30 m × 0.25 mm and a film thickness of 0.25 μm) from Phenomenex (Torrance, California, USA) was used for the separation of compounds. USP-grade helium was used as the carrier gas with a flow of 1 mL/min. The injection temperature was 280 ºC.

A volume of 0.2 μL of the dilution of the essential oil with dichloromethane was injected into the chromatograph with a split ratio 1:100. In the case of ethanolic extract, 1 μL of the dilution was injected with a split ratio of 1:100. A volume of 1 μL of the dilution of the aqueous extract with both solvents (isooctane and acetonitrile) was injected into the chromatograph using splitless mode. The described procedure was performed in duplicate, and a blank of each solvent was used. Concerning hydro-alcoholic extracts, 1 μL of the elution of both extracts with isooctane and acetonitrile was injected using mode splitless. In the case of oil of *Azadirachta indica* A. Juss, a volume of 1 μl of the dilution (1:5) was injected with a split ratio of 1:100. The oven temperature program and the chromatographic conditions varied according to the extract (**Table 1.1**). The typical operating conditions of the mass spectrometer were optimized with the software option "auto-tune". The ionization mode was electron impact (70 eV) and the mass of the ions was

monitored between 50 and 800 m/z. The temperatures of the ion source and the quadrupole were 250 and 150 °C, respectively.

The compounds were identified by comparing experimental mass spectra with those of the electronic library NIST/EPA/NIH Mass Spectral Database (NIST 11) using the NIST MS Search Program for Windows (Version 2.0) software. For quantification, only major compounds were considered, which had a percentage area greater than or equal to 1 % of the peak relative to the total area of the chromatogram. The normalization method was applied, in which the results were expressed as the area percentage contribution of each of the signals of interest concerning the total area of the chromatographic signals. Signals (peaks) of the siloxanes from the C18 SPE cartridge were not considered when calculating the percentage peak area.

Table 1.1 Oven temperature programs used in the analysis of the extracts by GC/MS.

Extract	Rate (°C/min.)	Temperature (°C)	Hold time (min.)	Post-run
Essential oil	-	60	0	280°C 5 min.
	0.7	68	7	
	10	100	0	
	5	130	7	
	1	135	6	
Aqueous and ethanolic extracts	-	60	0	280°C 5 min.
	0.7	68	7	
	10	100	0	
	5	130	7	
	1	135	20	
Calendula officinalis L.	-	40	2	280°C 5 min.
	5	155	0	
	2.5	170	5	
	2.5	180	4	
	10	210	5	
Mimosa tenuiflora	-	50	2	280°C 5 min.
	5	155	0	
	1.5	290	3	
Azadirachta indica A. Juss	-	80	0	320°C 5min.
	3	180	5	
	3	205	0	
	20	285	0	
	5	305	15	

Post-run: Conditions of the thermal cleaning of the column.

1.3 Results and Discussion

1.3.1 GC/MS analysis of essential oil, ethanolic and aqueous extracts of *Ocimum micranthum* Willd leaves.

Essential oil

For the essential oil, a total of 39 chromatographic signals were detected, but only 24 were identified, and 15 of these offered more than a 1 % contribution to the total area of the chromatogram (**Table 1.2**). Three compounds showed a higher percentage contribution to the total area: caryophyllene (27 %), methyl-eugenol (14 %), and eugenol (12 %). The chemical structure of these compounds can be observed in **Figure 1.1**.

Table 1.2 Identified compounds in the essential oil of *Ocimum micranthum* Willd leaves

No	t_R (min)	Compound	Area (%)
1	6.863	α-pinene	< 1
2	7.475	Camphene	< 1
3	8.772	β-pinene	< 1
4	9.578	β-myrcene	< 1
5	11.858	D-Limonene	8
6	11.992	Eucalyptol	2
7	12.664	Trans-β-Ocimene	< 1
8	21.241	(-)-Alcanfor	3
9	21.879	Isoborneol	2
10	23.374	α-Terpineol	< 1
11	**28.994**	**Eugenol**	**12**
12	29.617	α-copaene	< 1
13	30.251	levo-β-Elemene ó β-Elemene	< 1
14	**30.778**	**Methyl-eugenol**	**14**
15	**31.363**	**Caryophyllene**	**27**
16	32.085	Trans-α-Bergamotene	< 1
17	32.938	Humulene ó α-Caryophyllene	4
18	33.297	Aromandendrene	1
19	34.402	D-Germacrene	2
20	35.288	γ-Elemene	10
21	35.790	levo-β-Elemene ó β-Elemene	1
22	36.060	β-Bisabolene	8
23	40.424	(-)-Spathulenol	3
24	40.728	Caryophyllene oxide	3

<: Minor; **Bold**: Three major compounds (more abundant); t_R: Retention time

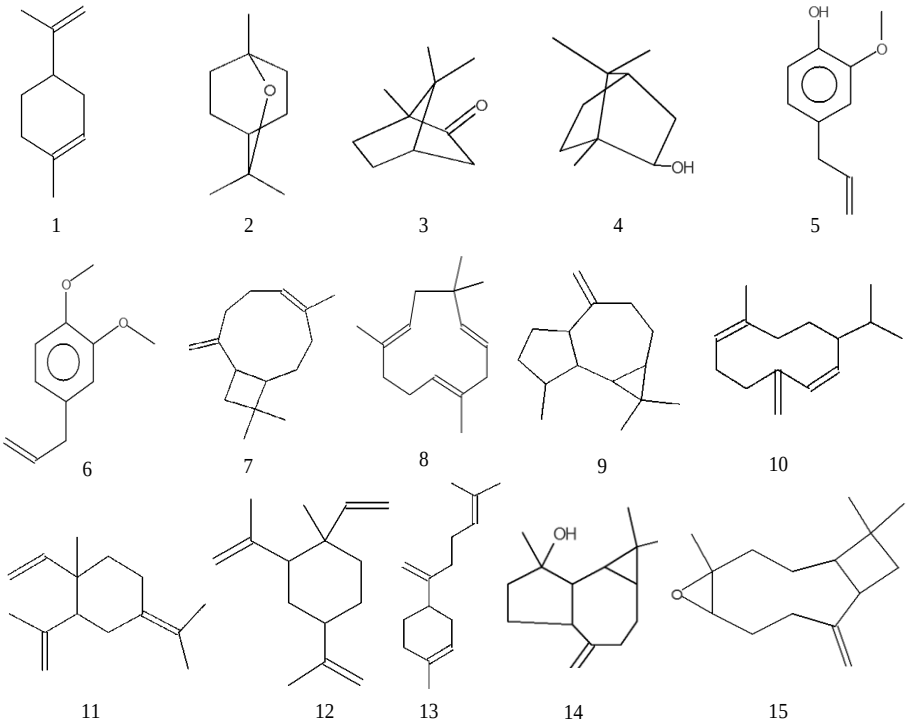

Figure 1.1. Chemical structures of major compounds identified in the essential oil of *Ocimum micranthum* Willd leaves. (1) D-limonene, (2) eucalyptol, (3) -(-) alcanfor, (4) isoborneol, (5) eugenol, (6) methyl-eugenol, (7) caryophyllene, (8) humulene, (9) aromadendrene, (10) D-germacrene, (11) γ-elemene, (12) β-elemene, (13) β-bisabolene, (14) –(-)spathulenol, (15) caryophyllene oxide.

From the identified and quantified compounds, only five were consistent with those reported by other authors [7] in this same variety of basil (**Table 1.3**) that is, eucalyptol, eugenol, caryophyllene, β-elemene, and γ-elemene. The first three of these were major components, but of the major compounds in the present study, only eugenol and caryophyllene coincided with those of the previous research. Furthermore, these authors [7] identified and quantified α-pinene, β-pinene, camphene, myrcene, *trans*-β-ocimene, and α-terpineol, although these compounds were minor in this study. Concerning other reviews [10], only eight identified and quantified compounds coincided; these were caryophyllene, eugenol, β-elemene, D-germacrene, spathulenol, caryophyllene oxide, eucalyptol, and humulene, from which the former two compounds were major in both studies. Those authors [10], reported the identification and quantification of α-pinene, β-pinene, camphene, myrcene, *trans*-β-ocimene, α-terpineol, and *trans*-*α*-bergamotene, which were just minor compounds in this study. Moreover, in other studies, [9] only five identified and quantified compounds coincided with our reseach; these were eugenol, caryophyllene, eucalyptol, α-humulene, and aromadendrene.

Eugenol and caryophyllene were major compounds in both studies. These authors [9] also identified linalool (0.7 %), bicyclogermacrene (8.1 %) and germacrene A (2 %), which were minor compounds.

Table 1.3 Identified and quantified compounds in the essential oil of *Ocimum basilicum* and *Ocimum micranthum* Willd leaves.

No	Compound	Composition%[a]				
		O.*m*[b]	O.*m*[c]	O.*m*[d]	O.*m*[e]	O.*b*[f]
1	*α-pinene*	< 1	0.24	0.24	-	-
2	*Camphene*	< 1	0.04	0.07	-	-
3	*β-pinene*	< 1	1.33	0.75	-	0.10
4	*β-myrcene*	< 1	0.13	0.26	-	-
5	D-Limonene	8	-	-	-	0.10
6	Eucalyptol	2	20.02	5.35	1.50	4.00
7	*Trans-β-Ocimene*	< 1	0.73	0.35	-	-
8	(-)-Alcanfor	3	-	-	-	-
9	Isoborneol	2	-	-	-	-
10	*α-Terpineol*	< 1	1.10	0.45	-	1.00
11	**Eugenol**	**12**	**20.50**	**46.55**	**64.80**	**5.90**
12	*α-copaene*	< 1	-	-	-	-
13	levo-β-Elemene ó β-Elemene	< 1	-	-	-	-
14	**Methyleugenol**	**14**	-	-	-	**3.10**
15	**Caryophyllene**	**27**	**19.26**	**11.94**	**14.30**	**0.30**
16	*Trans-α-Bergamotene*	< 1	-	0.13	-	-
17	Humulene ó α-Caryophyllene	4	-	2.40	2.30	0.20
18	Aromandendrene	1	-	-	0.70	0.10
19	D-Germacrene	2	-	0.13	-	0.30
20	γ-Elemene	10	1.55/ 14.44	-	-	-
21	levo-β-Elemene ó β-Elemene	1	0.51	9.06	-	0.30
22	β-Bisabolene	8	-	-	-	-
23	(-)-Spathulenol	3	-	1.15	-	0.80
24	Caryophyllene oxide	3	-	1.23	-	-

O.*m., Ocimum micrantum; O.b., Ocimum basilicum* (-): Not detected <: Minor
[a] The percentage composition is expressed as the percentage of the total area of the essential oil composition
Bold: Major compounds (more abundant) [b] Present study [c] Charles *et al.,* 1990 [d] Sachetti *et al.,* 2004
[e] Vieira *et al.,* 2014 [f] Politeo *et al.,* 2007

In the previous studies (see **Table 1.3**), which the hydro-distillation method was used a Clevenger trap for essential oil extraction, the content of eugenol in the essential oil of *Ocimum micranthum* was higher than that observed in the present study (12 %). In contrast, the content of caryophyllene (27 %) was higher in this variety, and methyl-eugenol (14 %) was identified and quantified as a major component. These differences may be related to the geographical origin of the plant [29], to the culture conditions [30], the state of vegetative development [31], the nutritional status of the plants [32, 33] and seasonal variations in the plant [34].

The profile of compounds in essential oils from plants of the *Ocimum* genus changes according to the species and variety. For example, *basilicum* (basil common or domestic) species has the caryophyllene (0.3 %) and eugenol (5.9 %) content lower than *micranthum* species [35]. However, its major components were linalool (28.6 %), which is a terpene, and estragole (21.7 %), which is an aromatic ether compound, and these are not usually present in the *O. micranthum* species.

Most of the compounds identified in the essential oil of *Ocimum micranthum* Willd belongs to sesquiterpenes, monoterpenes and monoterpene alcohol groups, except for eugenol (an allylbenzene) and methyl-eugenol (a phenylpropanoid); this agrees with the study reported by other authors, which detail the types of volatile compounds that can generally be found in the essential oil of any plant [36,37]. Additionally, nine signals in the essential oil were identified, which correspond to α-pinene (1), β-pinene (3), camphene (2), β-myrcene (4), *trans*-β-ocimene (7), α -terpineol (10), α-copaene (12), β-elemene (13) and *trans*-α-bergamotene (16), as can be seen in **Figure 1.2**, which were considered minor compounds.

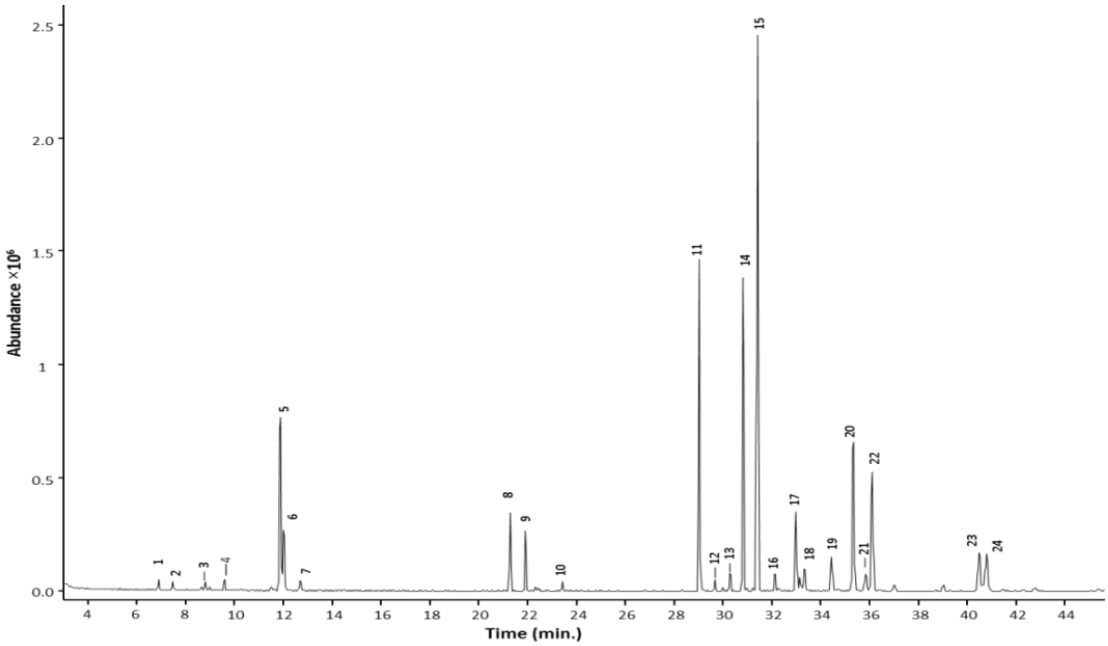

Figure 1.2 Chromatogram of the essential oil of *Ocimum micranthum* Willd leaves

Comparing the minor compounds found in the present study with those reported by other authors for the same variety [7] the content of β-pinene and α-terpineol were slightly above 1 % in this case (**Table 1.3**), which could be attributed to the fact that we identified and quantified fewer compounds. Therefore, the distribution area ratio was slightly higher. A study reported for the species *O. basilicum* that the area ratio of the trans-α-bergamotene compound was 2.2 %, which could be attributed to differences between species [23]. The α-copaene was not identified in other studies [7, 8, 35].

Ethanolic extract

In the ethanolic extract, 25 chromatographic signals were detected, of which only ten were considered for the quantification. Six minor signals were identified as 2-chlorocyclohexanol (1), trans-α-bergamotene (8), humulene (9), aromadendrene (10), 2, 4-di-tert-butylphenol (13) and caryophyllene oxide (16) (**Figure 1.3**).

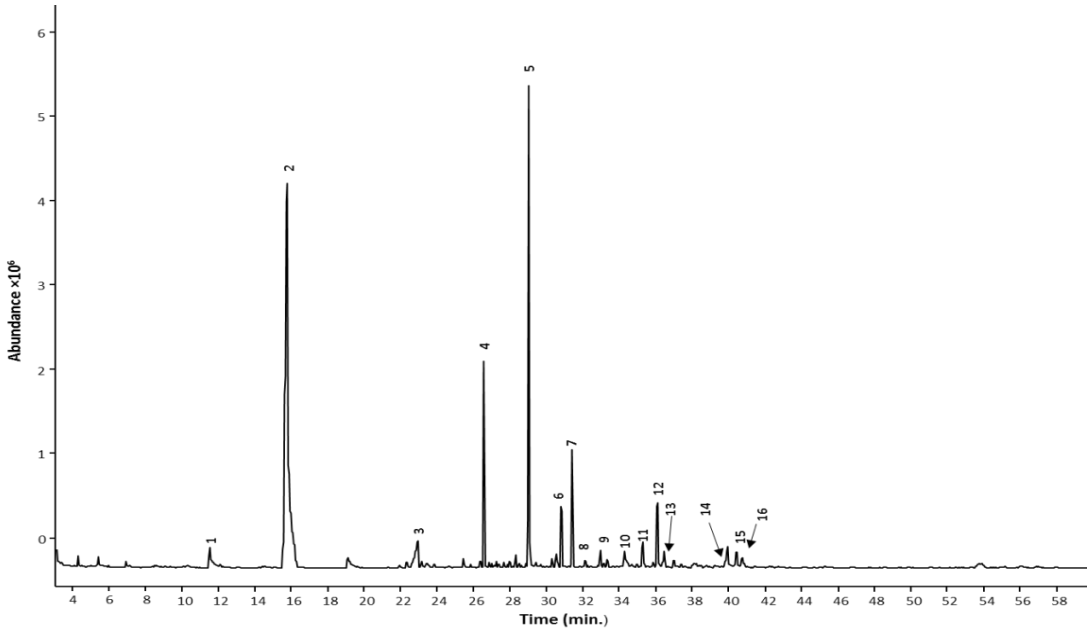

Figure 1.3 Chromatogram of the ethanolic extract of *Ocimum micranthum* Willd leaves.

The *trans*-α-bergamotene compound had a minor presence in the essential oil and the ethanolic extract, indicating a difference between species when compared to the *O. basilicum* species, in whose essential oil the content of this compound was reported 2 %. On the other hand, the content of caryophyllene oxide and humulene in the essential oil was 3 and 4 %, respectively, whereas these compounds only represented a minor percentage in the ethanolic extract. It could be related to the lipophilic nature of both isoprenoid compounds, which is the major part of the essential oil fraction.

The most representative compounds in the ethanolic extract are shown in **Table 1.4**. The two compounds with the highest contribution to the percentage area were *n*-octyl alcohol (55 %) and eugenol (18 %). Also, eight compounds (two unidentified) showed an area percentage of 1.0–7 %, that is, benzoic acid, methyl-eugenol, caryophyllene, β-bisabolene, dodecanoic acid, and (-) -spathulenol. The chemical structure of these compounds can be observed in **Figure 1.4**.

Table 1.4 Compounds present in the ethanolic extract of *Ocimum micranthum* Willd leaves.

No	**t_R (min.)**	Compound	Area (%)
1	11.471	2-chlorocyclohexanol	< 1
2	**15.704**	**n-Octyl alcohol ó alfol 8**	**55**
3	22.867	Benzoic acid	3
4	26.488	*f*	7
5	**28.981**	**Eugenol**	**18**
6	30.746	Methyl-eugenol	2
7	**31.334**	**Caryophyllene**	**6**
8	32.054	trans-α-bergamotene	< 1
9	32.905	Humuleno/α Caryophyllene	< 1
10	33.266	Aromandendrene	< 1
11	35.227	*f*	2
12	36.015	β-Bisabolene	4
13	36.374	2,4 Di-tert-butylphenol	< 1
14	39.889	Dodecanoic acid	2
15	40.354	(-)-Spathulenol	1
16	40.671	Caryophyllene oxide	< 1

<: Minor; **Bold**: Major compounds (more abundant); ***f:*** unidentified compound t_R: Retention time

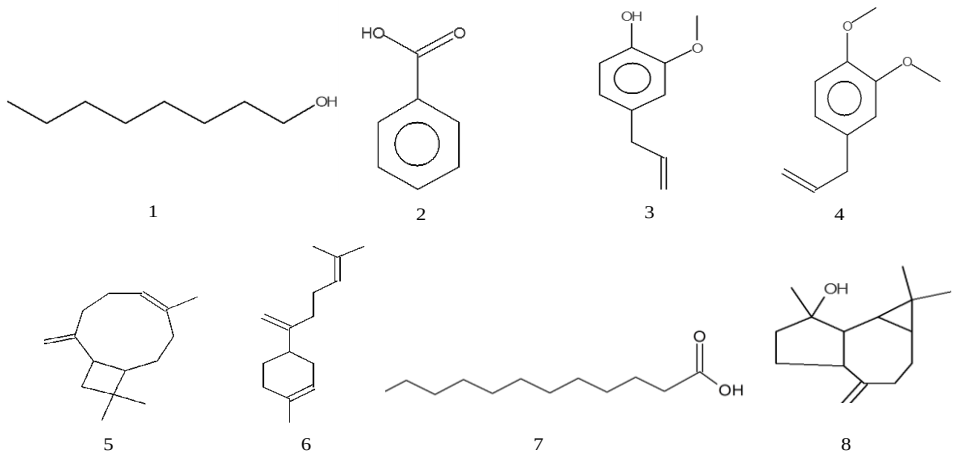

Figure 1.4 Chemical structures of some major compounds identified in ethanolic extract of *Ocimum micranthum* Willd leaves. (1) *n*-octyl alcohol, (2) benzoic acid, (3) eugenol, (4) methyl-eugenol, (5) caryophyllene, (6) β-bisabolene, (7) dodecanoic acid, (8) (-) -spathulenol.

Regarding the types of compounds that could commonly be present in the ethanolic extracts of the *Ocimum* genus, diverse authors mentioned phenolic compounds, flavonoids, saponins, tannins, anthraquinone glycosides and alkaloids [38]. However, in this study, the presence of eugenol, methyl-eugenol, caryophyllene, *trans*-α-bergamotene, humulene, aromandendrene, β-bisabolene, and spathulenol were detected in both the essential oil, and in the ethanolic extract of *Ocimum micranthum* Willd leaves; in both cases, eugenol was the second most abundant compound. Information about the volatile compounds in the ethanolic extracts of the *Ocimum micranthum* Willd species have not been reported yet; therefore, it is important to point out that the presence of these compounds in this extract is typically found in the essential oils. This result indicates that one may recover these compounds by different extraction techniques, because the essential oil was obtained by hydro-distillation and the ethanolic extract by Soxhlet method.

Aqueous extract

The aqueous extract was passed through a C18 SPE cartridge to retain the compounds that were present and, subsequently, to elute these in an appropriate solvent for introduction into the gas chromatograph. For the elution, isooctane and acetonitrile were used, owing to the different elution strengths in the reverse phase of these solvents. In the elution of the C18 SPE cartridge with isooctane, only eugenol (97.2%) and methyl-eugenol (2.8%) were observed in the extract (**Figure 1.5**). Both compounds also were found in the ethanolic extract and essential oil, in which the major compound was eugenol.

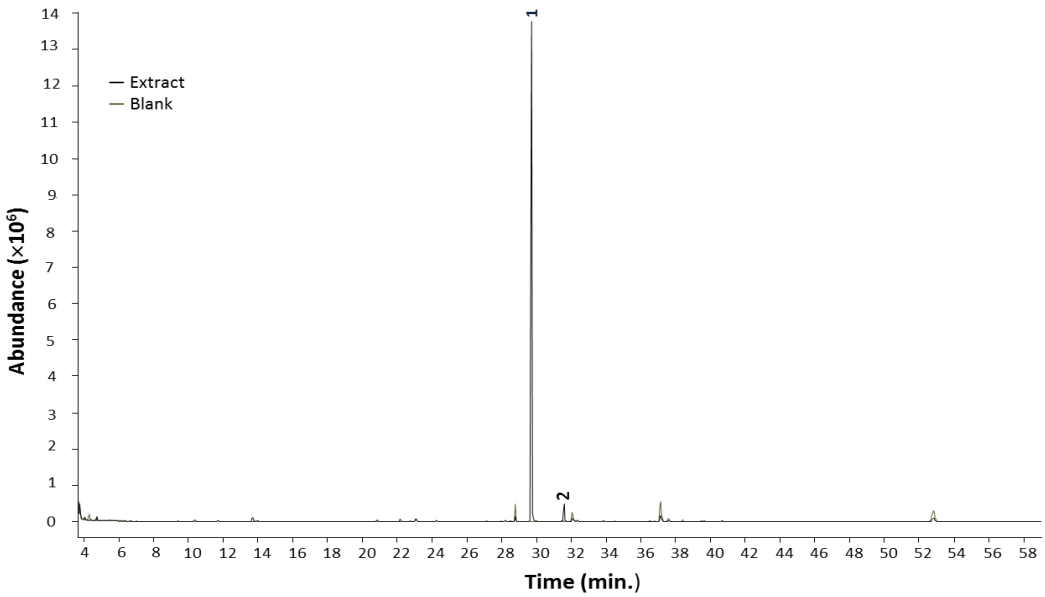

Figure 1.5 Chromatogram of isooctane eluate obtained after passing the aqueous extract of *Ocimum micranthum* Willd leaves through a C18 SPE cartridge. (1) eugenol, t_R 29.721 min. (2) methyl-eugenol, t_R 31.566 min.

Concerning other species of the *Ocimum* genus a *kilimandscharicum*, volatile compounds such as camphor, 1,8-cineole, limonene, trans-caryophyllene, camphene, 4-terpenol, myrtenol, α-terpineol, endoborneol and linalool were identified in the aqueous extract from leaves [39]; flavonoids, saponins, sterols, carbohydrates, proteins, and triterpenes also were identified. The difference in the profile of volatile compounds identified in the aqueous extract reported by other authors and in the aqueous extract of the leaves of *Ocimum micranthum* Willd, can be ascribed to the fact that the species are different [39]. In the *Ocimum kilimandscharicum* species, the major components of the essential oil of the leaves were camphor (56.07 %) and D-limonene (13.56 %); these compounds too were identified in the aqueous extract as major components. Whereas, eugenol and methyleugenol were observed in the profile of volatile compounds of the aqueous extract from *Ocimum micranthum* Willd species eluted with isooctane and acetonitrile which were also major components in the essential oil of this plant. These results appear to show that the identified volatile compounds in the essential oil of the leaves of the plant of the *Ocimum* genus are too present in the corresponding aqueous extracts.

Nine major compounds were quantified in the aqueous extract of *Ocimum micranthum* Willd leaves when the C18 SPE cartridge was eluted with acetonitrile (**Table 1.5**); the structure for some of these compounds is shown in **Figure 1.6**. Eugenol (9) presented the greatest contribution to the area percentage (59 %) followed by two compounds, (11) and (12), that could not be identified. The remaining six compounds showed a percentage between 1 and 4 %; one of these was not identified. Additionally, three minor components (area < 1 %) were identified, which were 4-vinylphenol (5), 2-hydroxy-1,8-cineole (6), and 2-methoxy-4-vinylphenol (8) (**Figure 1.7**).

Table 1.5 Major compounds eluted with acetonitrile after passing aqueous extract of *Ocimum micranthum* Willd leaves though a C18 cartridge.

No	t_R (min.)	Compound	Area %
1	7.516	***f***	< 1
2	20.598	2,2-Dimethyl-4-(methylethyl)-2H-imidazole	4
3	20.946	Phenethyl alcohol	2
4	24.627	Catechol	1
5	25.216	4-vinylphenol	< 1
6	25.292	2-Hydroxy-1,8-cineole	< 1
7	27.523	***f***	< 1
8	28.161	2-Methoxy-4-vinylphenol	< 1
9	**29.775**	**Eugenol**	**59**
10	31.563	Methyleugenol	2
11	33.423	***f***	11
12	**35.296**	***f***	**18**
13	48.205	3-Oxo-α-ionol	1
14	56.533	***f***	2

<: Minor; **Bold**: Major compounds (more abundant); ***f:*** unidentified compound
t_R: Retention time

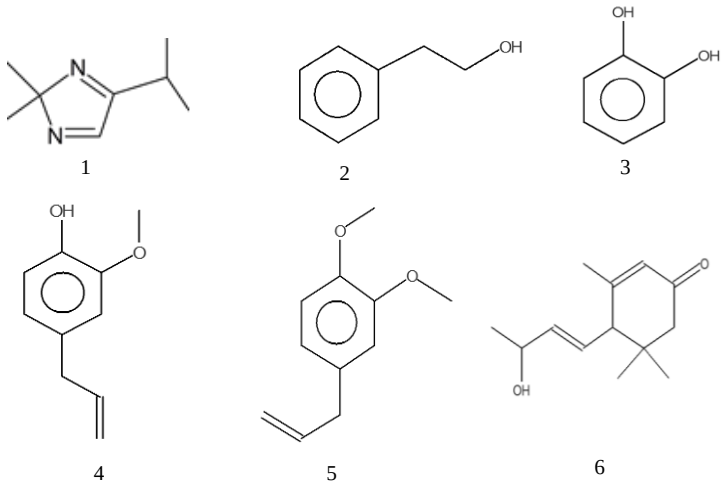

Figure 1.6 Chemical structures of some major compounds identified by MS in the acetonitrile eluate obtained after passing the aqueous extract of *Ocimum micranthum* Willd though a C18 SPE cartridge (1) 2,2-dimethyl-4-(methylethyl)-2H-imidazole, (2) phenethyl alcohol, (3) catechol, (4) eugenol, (5) methyleugenol, (6) 3-oxo-α-ionol.

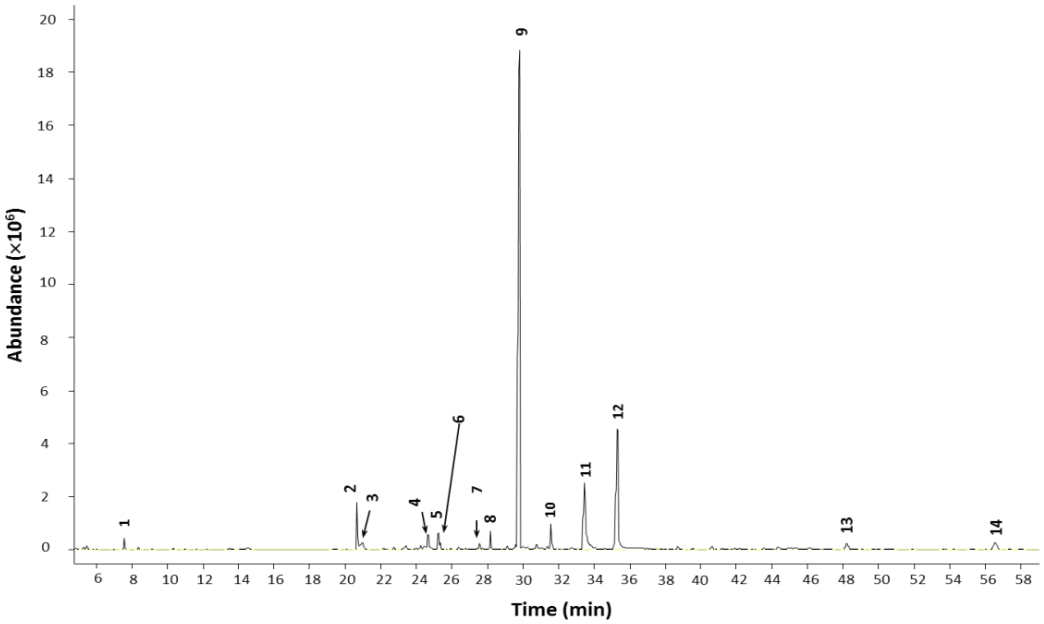

Figure 1.7 Chromatogram of acetonitrile eluate obtained after passing the aqueous extract of *Ocimum micranthum* Willd leaves through a C18 SPE cartridge.

In the aqueous fraction that was eluted with a polar solvent (acetonitrile); eugenol and methyl-eugenol were identified again; the retention time of both compounds was the same. The range of compounds recovered and identified was major using this polar solvent comparing with isooctane.

1.3.2 GC/MS analysis of Hydro-alcoholic extracts of *Calendula officinalis* L. flowers and *Mimosae tenuiflorae* bark.

Hydro-alcoholic extract of *Calendula officinalis* flowers.

In the elution of the C18 SPE cartridge with isooctane, eight major compounds were quantified (**Table 1.6**), of which α-thujone, 4-terpineol, α-cadinol, and bornyl acetate showed the highest contribution to the percentage of the total area. The chemical structures of these compounds can be observed in **Figure 1.8**.

Table 1.6 Major compounds eluted with isooctane after passing the hydro-alcoholic extract of *Calendula officinalis* flowers though C18 SPE cartridge.

No.	t_R (min.)	Compound	Area (%)
5	12.634	eucalyptol	9
8	**14.912**	**α-thujone**	**36**
9	15.209	β-thujone	7
12	**17.016**	**4-terpineol**	**12**
18	**20.060**	**(-)-bornyl acetate**	**11**
23	29.571	α-epi-muurolol	6
24	**29.956**	**α-cadinol**	**12**
25	32.570	***f***	7

f : Unidentified compound; **Bold**: Major compound (more abundant); t_R: Retention time.

The profile of identified volatile compounds in the hydro-alcoholic extract of the *Calendula officinalis* flowers, at least in the fraction eluted with isooctane, agrees in some compounds with the profile obtained previously by GC/MS in essential oils from the flowers of this species, as well as other *Calendula* species.. Concerning the *Officinalis* species, it was previously reported the presence of the α-cadinol (8.3%), 4-terpineol (0.4%), and α-muurolol (0.8%) [40], whereas other authors reported the identification of sesquiterpenes, sesquiterpenols, α-cadinol, δ-cadinene [41], and eucalyptol [42]. In other kinds of extracts from *Calendula officinalis* flowers (ethanolic and aqueous extracts) it was identified the presence of linalool, α-terpineol, α-thujone and α-cadinol [43]. The presence of 4-terpineol, α-thujone, and α- cadinol in the *arvensis* species also was reported [44].

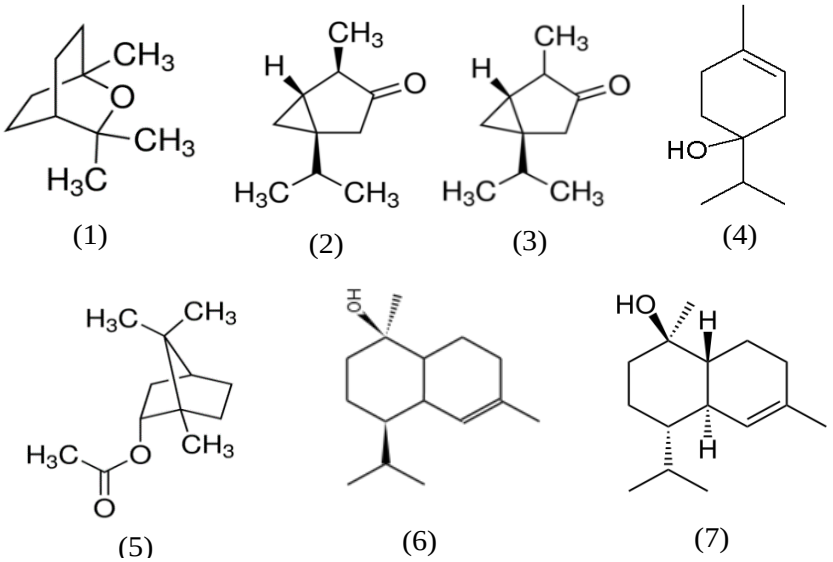

Figure 1.8 Chemical structure of major compounds identified by MS in the isooctane eluate obtained after passing the hydro-alcoholic extract of *Calendula officinalis* L. flowers though C18 SPE cartridge. (1) eucalyptol, (2) α-thujone, (3) β-thujone, (4) 4-terpineol, (5) (-)-bornyl acetate, (6) α-epi-muurolol, (7) α-cadinol.

It is interesting to note that compounds with lipophilic characteristic (**Table 1.6**) were recovered from the hydro-alcoholic extract, as these compounds are usually found in the essential oil. This indicates that these compounds may be recovered using various forms of extraction, as the essential oils are obtained by hydro-distillation or supercritical-fluid extraction, whereas hydro-alcoholic extracts are regularly obtained by maceration. The rest of the major volatile compounds of the hydro-alcoholic extract of the flowers of *Calendula officinalis* showed a percentage area of 6–9%; one of these compounds could not be identified. Additionally, 20 minor compounds (area <1%) were identified, as can be observed in **Table 1.7**

Table 1.7 Minor compounds eluted with isooctane after passing the hydro-alcoholic extract of *Calendula officinalis* flowers though C18 SPE cartridge.

No.	t_R (min.)	Compound	Area (%)
1	6.812	(3R)-3-phenyl-2,3-dihydro-1H-isoindol-1-one	< 1
2	7.501	ethyl 2-methyl butanoate	< 1
3	10.482	ethyl β-methylvalerate	< 1
4	11.092	1-octene-3-ol	< 1
6	14.364	L-fenchone	< 1
7	14.704	L-linalool	< 1
10	16.042	(-)-camphor	< 1
11	16.677	1-borneol	< 1
13	17.395	α-terpineol	< 1
14	17.516	ethyloctanoate	< 1
15	17.570	(-)-myrtenol	< 1
16	17.593	p-allylanisole	< 1
17	19.641	ethyloctanoate	< 1
19	21.759	α-terpinenyl acetate	< 1
20	21.979	eugenol	< 1
21	26.482	2,6,6-trimethyl-2-hydroxycyclohexylidene)acetic, acid lactone	< 1
22	27.927	(E)-ethyl 3-ciclohexyl-2-methylpropenoate	< 1
26	33.995	1,3,4,5-tetrahydro-7,8-dimethoxypyrrolo[4,3,2-de]quiniline	< 1
27	44.318	ethyl palmitate	< 1
28	45.336	4bS*8aS*)-2,4-dimethoxy-3-hydroxy-4b-methyl-4b,5,6,7,8,8a-hexahydro-9H-fluorene	< 1

<: Minor product; t_R: Retention time.

On the profile of the minor compounds identified in the hydro-alcoholic extract of *Calendula officinalis* flowers, some compounds coincided with those compounds identified in the essential oil of these flowers. The presence of α-terpineol (<0.1%), linalool (0.1%) and ethyl palmitate (0.1%) were previously identified [40], whereas other authors identified camphor [42]. The compound linalool also was identified in the essential oil of flowers of the *arvensis* species [44]. In these studies, the percentage areas of the compounds identified in the essential oil were also low, so it is inferred that these compounds have only a minor presence in the flowers.

Figure 1.9 represents the chromatographic profile obtained for the hydro-alcoholic extract from *Calendula officinalis* flowers eluted with isooctane as well as the major and minor components observed. Red signals denote the siloxanes present in the C18 SPE cartridge.

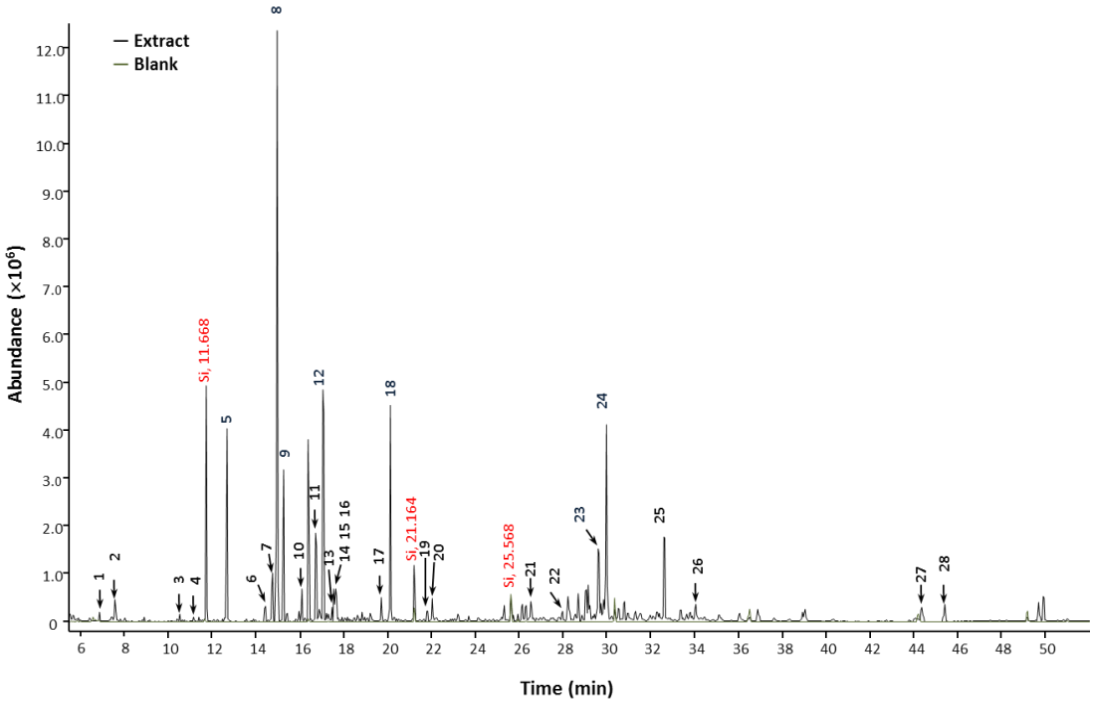

Figure 1.9 Chromatogram of isooctane eluate obtained after passing the hydro-alcoholic extract of *Calendula officinalis* flower through C18 SPE cartridge.

When the C18 SPE cartridge was eluted with acetonitrile, 20 major compounds (**Table 1.8**) were quantified. Three compounds showed the most significant contributions to the percentage of the total area; two compounds (22 and 13%) were not identified, and the another was α-thujone (12%). The rest of the compounds showed a percentage area of 2–8%, of which four were unidentified. The chemical structures of some of these compounds can be observed in the **Figure 1.10**.

Table 1.8 Major compounds eluted with acetonitrile after passing the hydro-alcoholic extract of *Calendula officinalis* flowers though C18 SPE cartridge.

No.	t_R (min.)	Compound	Area (%)
13	11.585	9-(methylthio)-8H-acenaphtho[1,2-c]pyrrole-7-carboxylic acid	2
14	12.558	eucalyptol	3
18	**14.848**	**α-thujone**	**12**
19	15.175	β-thujone	2
21	16.660	1-borneol	3
22	16.987	4-terpineol	4
27	20.049	(-)-bornyl acetate	4
29	21.827	2-methoxy-3-methylhydroquinone	2
34	28.186	***f***	2
35	28.639	***f***	2
36	29.570	α-epi-muurolol	3
37	**29.947**	**α-cadinol**	**8**
38	**32.598**	***f***	**22**
39	**35.165**	***f***	**13**
40	36.851	***f***	2
41	38.554	***f***	2
42	43.797	3-(3-hydroxy-3-methyl-1-butenyl)-4-methoxyacetophenone	3
43	44.325	ethyl hexadecanoate	2
45	49.661	***f***	4
46	49.879	***f***	5

f: Unidentified compound; **Bold**: Major compound (more abundant); t_R: Retention time.

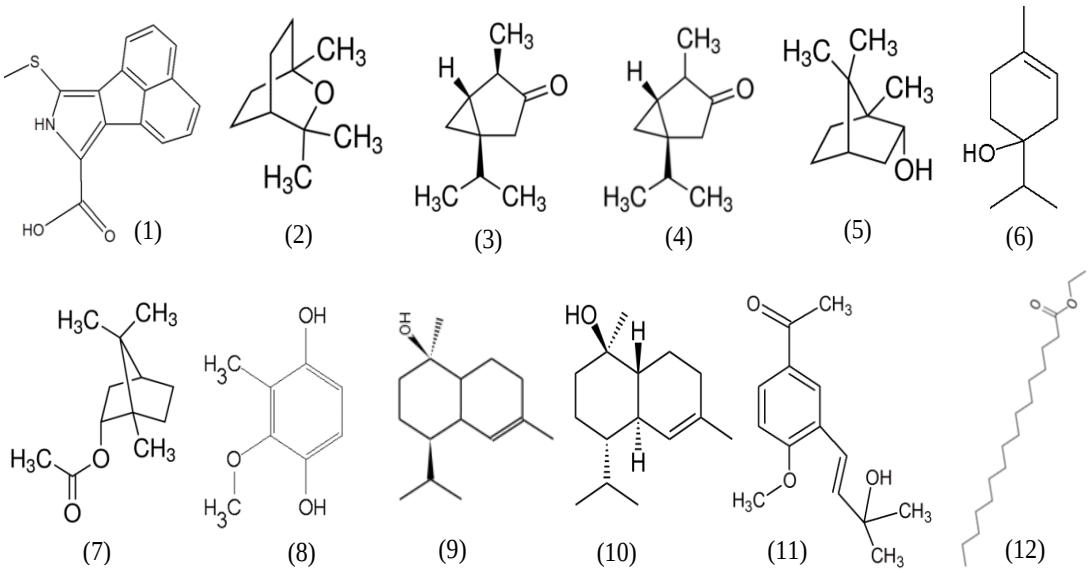

Figure 1.10. Chemical structure of major compounds identified by MS in the acetonitrile eluate obtained after passing the hydro-alcoholic extract of *Calendula officinalis* L. flowers though C18 SPE cartridge. (1) 9-(methylthio)-8H-acenaphtho[1,2-c]pyrrole-7-carboxylic acid (2) eucalyptol, (3) α-thujone, (4) β-thujone, (5) 1-borneol, (6) 4-terpineol, (7) (-)-bornyl acetate, (8) 2-methoxy-3-methylhydroquinone, (9) α-epi-muurolol, (10) α-cadinol, (11) 3-(3-hydroxy-3-methyl-1-butenyl)-4-methoxyacetophenone, (12) ethyl hexadecanoate.

For the elution with acetonitrile, we again observed the presence of eucalyptol, α-thujone, β-thujone, 4-terpineol, (-) -bornylacetate, α-cadinol and α-muurolol, but with lower percentage areas in comparison with the percentages obtained in the elution with isooctane. This may be associated with the fact that, in the elution with acetonitrile, more compounds were obtained experimentally, so a higher distribution of the total area was realized and, therefore a reduction in the area of each compound compared to that observed in the elution with isooctane, where only eight compounds had a percentage area over 1%. Additionally, 26 minor compounds (**Table 1.9**) were identified.

Table 1.9 Minor compounds eluted with acetonitrile after passing the hydro-alcoholic extract of *Calendula officinalis* flowers though C18 SPE cartridge.

No.	t_R (min.)	Compound	Area (%)
1	4.186	diethyl(2-propenyloxymethyl) amine	< 1
2	4.261	methyl-(3R)-(-)-5-oxo-3 propylpentanoate	< 1
3	4.396	3-(3'-butenoxy)propanoic acid	< 1
4	5.947	5,5-dimethyl-2-(1,1,dimethyl)-2-hydroxyethyl-4-hydroxy-1,3 dioxane	< 1
5	7.315	1,1-dimethoxycyclobutane	< 1
6	7.726	2-methylbutanoi Acid	< 1
7	7.768	*n*-hexanol	< 1
8	8.204	N-methylcyclopentane 1,1 dicaboxiamide	< 1
9	9.320	methyl 3-hydroxy -2(p-toluenesulfunyloxy)methyl-10-tetrahydropyranilloxydecanoate	< 1
10	9.555	3-amino-5-methyllisoxazole	< 1
11	10.997	hep-1-en-3-ol	< 1
12	11.215	phenol	< 1
15	12.960	phenyl acetaldehyde	< 1
16	14.386	*cis*-3-methoxyphenyl)-1,2,4-trioxollane	< 1
17	14.655	α-terpinolen	< 1
20	16.042	(-)-camphor	< 1
23	17.398	α-terpineol	< 1
24	18.186	4-vynylphenol	< 1
25	19.160	2-isopropyl-2,5-dihydrofuran	< 1
26	19.646	ethyl o-hydroxybenzoate	< 1
28	20.837	2-methoxy-4-vynylphenol	< 1
30	25.569	(+)-ledene	< 1
31	26.248	δ-cadinene	< 1
32	27.248	4 vynyl-syringol	< 1
33	27.322	methyl-4-hydroxy-4-methyl-2-pentynoate	< 1
44	45.336	(4bs*-8as*)-2,4-dimethoxy-3-hydroxy-4b-methyl-4b,5,6,7,8,8a-hexahydro-9H-fluorene	< 1

<: Minor product; t_R: Retention time.

Both (-)-camphor and α-terpineol were minor compounds in the elution with acetonitrile (**Table 1.9**) and isooctane. Also, it is important to refer of the presence of δ-cadinene, (+) ledene and 4-vynil-syringol as minor compounds. The first two compounds are present in the essential oil extracted of the plant *Melaleuca alternifolia*, and this oil has been used in the treatment of Demodex ocular [45], whereas the latter compound have been studied for application in the food area [46].

Figure 1.11 represents the chromatographic profile obtained for the hydro-alcoholic extract from *Calendula officinalis* flowers eluted with acetonitrile; major and minor components were observed. Red signals denote the siloxanes present in the C18 SPE cartridge.

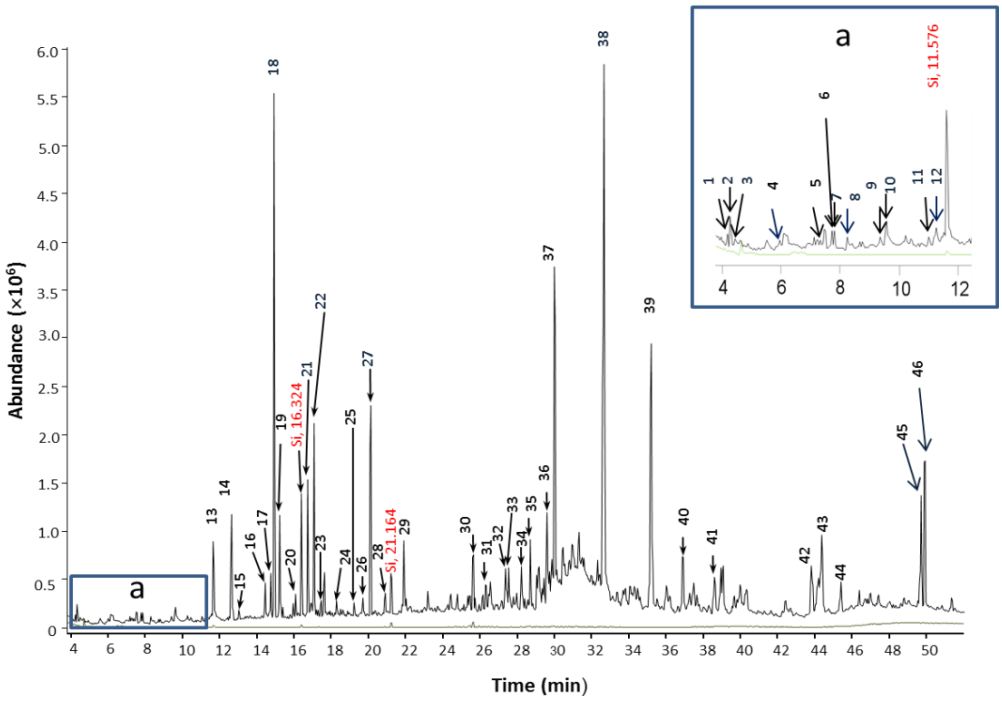

Figure 11. Chromatogram of acetonitrile eluate obtained after passing the hydro-alcoholic extract of *Calendula officinalis* flower through C18 SPE cartridge.

Hydro-alcoholic extract of *Mimosae tenuiflorae* bark.

For the C18 SPE cartridge eluted with isooctane, ten major compounds were quantified in the hydro-alcoholic extract of *Mimosae tenuiflorae* bark (**Table 1.10**). Three compounds showed a higher percentage contribution to the total area, which were camphor (44%), 2-amino-3, 5-dicyano-6-(4-methoxy-phenoxy) pyridine (20%), and ethyl 3-phenylpropanoate (11%). Also, seven compounds had a percentage area of 2–6%, and one them was not identified. **Figure 1.12** shows the chemical structures of these compounds.

Table 1.10 Major compounds eluted with isooctane after passing the hydro-alcoholic extract of *Mimosae tenuiflorae* bark though C18 SPE cartridge.

No.	t_R (min.)	Compound	Area (%)
1	10.742	eucalyptol	6
3	**14.073**	**camphor**	**44**
4	14.702	endo-borneol	6
5	15.037	(-)-4-terpineol	3
8	20.025	trimethyl benzaldehyde	4
9	**23.524**	**ethyl 3-phenylpropenoate**	**11**
10	26.300	***f***	2
11	27.093	ethyl p-methoxycinnamate	1
12	**29.752**	**2-amino-3,5-dicyano-6-(4-methoxyphenoxy)-pyridine**	**20**
13	30.892	ribenone	2

f: Unidentified compound; **Bold**: Major compound (more abundant); t_R: Retention time.

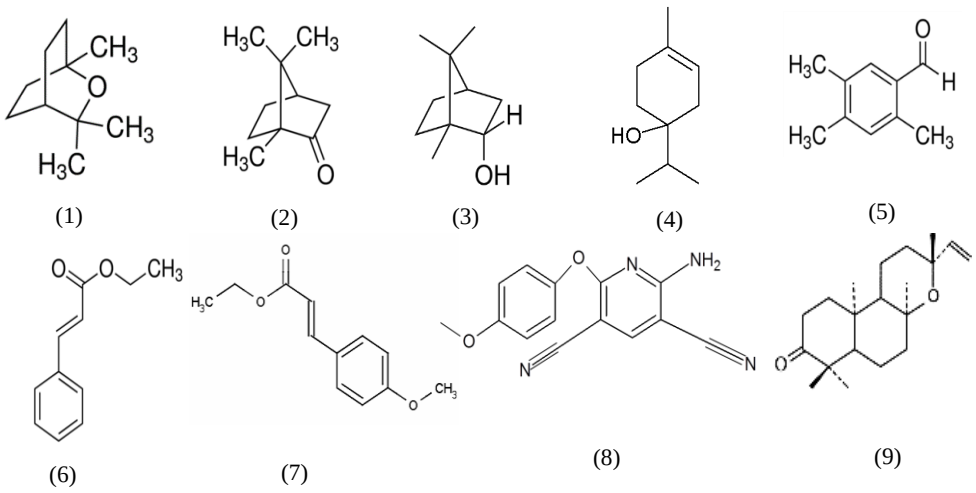

Figure 1.12 Chemical structure of some major compounds identified by MS in the isooctane eluate obtained after passing the hydro-alcoholic extract of *Mimosae tenuiflorae* though C18 SPE cartridge. (1) eucalyptol, (2) camphor, (3) endoborneol, (4) (-)-4-terpineol, (5) trimethyl benzaldehyde, (6) ethyl 3-phenylpropenoate, (7) ethyl p-methoxycinnamate, (8) 2-amino-3,5-dicyano-6-(4-methoxyphenoxy)-pyridine, (9) ribenone.

Among the compounds identified in the hydro-alcoholic extract of *M. tenuiflorae* bark, eucalyptol, camphor, endo-borneol, and (-)-4-terpineol stand out, as these compounds are typically reported in essential oils obtained by hydro-distillation or supercritical-fluid extraction [47,48].

However, they have not been reported previously in the profile of volatile compounds of the hydro-alcoholic extract, only the presence of tannins, flavonoids proanthocyanidins, and triterpenoid saponins in the extract have been reported [49,50]. Other authors have identified the presence of polyphenols in the methanolic extract of the bark of this plant [51].

Additionally, the compounds β-thujone (2), α-terpineol (6), α-terpinyl acetate (7), and ω-(1',2',4'-triazol-1'-yl)-[(ω-phenyl)-hydrazono]-acetophenone (14) were identified, and the percentage areas of these compounds were lower than 1%. Signals corresponding to the siloxane (Si) of the C18 cartridge used in SPE (**Figure 1.13**) also were obtained.

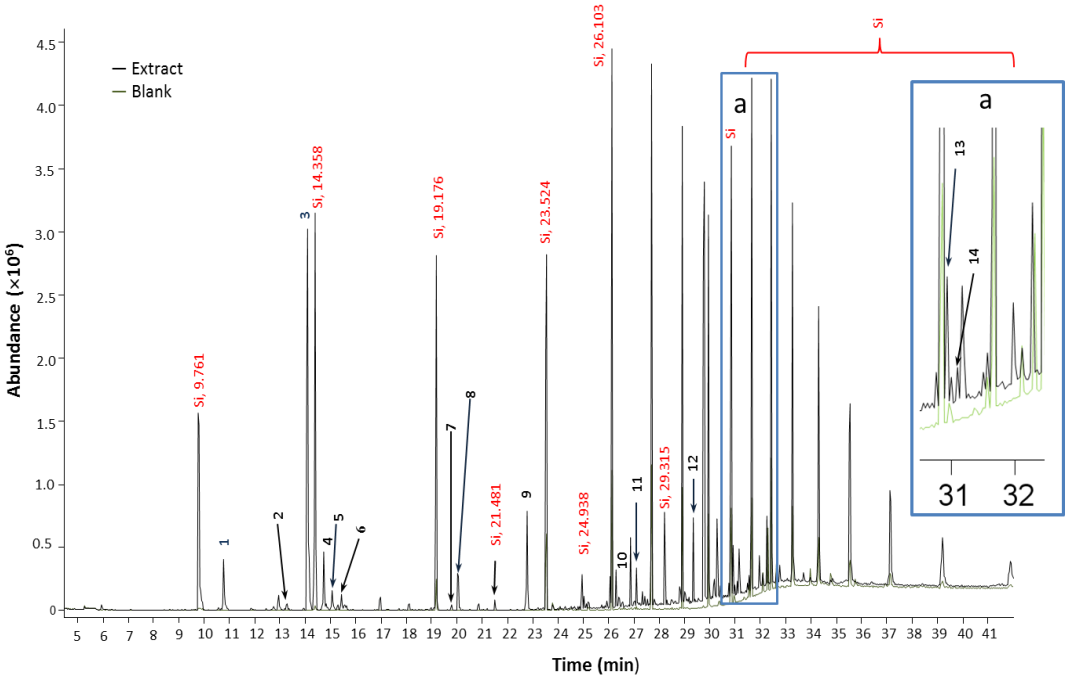

Figure 1.13 Chromatogram of isooctane eluate obtained after passing the hydro-alcoholic extract of *Mimosae tenuiflorae* bark through C18 SPE cartridge.

β-thujone, a monoterpene ketone, stands out in the minor compounds, as it have been identified previously as a major constituent of essential oils from a great variety of plants [52]. Also, it has applications in herbal medicine, cosmetics and the food and beverage industries in a regulated manner, owing to its adverse effects (possesses analeptic and convulsing action) in high concentrations (> 45 mg/kg). For this reason, the European Union has regulated its use [52, 53]. The monoterpenes α-terpineol and α-terpinyl acetate have been identified frequently with the essential oil fraction of various plants; the first compound has been studied due to its functional activities potential [54], whereas the second compound has been used in the fragrance industry, specifically in soaps [55].

In the elution with acetonitrile, ten major compounds (**Table 1.11**) were quantified. Compounds that showed a percentage contribution to the total area greater than 10% were resorcinol (29%), (+)-2-bornanone (22%), 2-(5-acetyl-2-furyl)-1,4 naphthoquinone (13%), and N,N-dimethyltryptamine (12%). The rest of the compounds showed a percentage area among 2–

10%. Within this group, eucalyptol and endo-borneol were identified, which were also previously identified in the C18 SPE cartridge that was eluted with isooctane. **Figure 1.14** shows the chemical structures of these compounds.

Table 1.11 Major compounds eluted with acetonitrile after passing the hydro-alcoholic extract of *Mimosae tenuiflorae* bark though C18 SPE cartridge.

No.	t_R (min.)	Compound	Area (%)
1	10.753	eucalyptol	3
2	12.519	2-methoxyphenol	2
4	**14.088**	**(+)-2-bornanone**	**22**
5	14.720	endo-borneol	5
8	**18.03**	**resorcinol**	**29**
13	20.700	***f***	10
14	21.429	2-ethyl-3-methylnaphtho[2,3-b]thiophene-4,9-dione	3
20	**27.515**	**N,N-dimethyltryptamine**	**12**
21	28.517	ethyl (2E)-3-(4-hydroxy-3-methoxyphenyl)-2-propenoate	2
22	**29.751**	**2-(5-acetyl-2-furyl)-1,4-naphthoquinone**	**13**

f: Unidentified compound; **Bold**: Major compound (more abundant); t_R: Retention time.

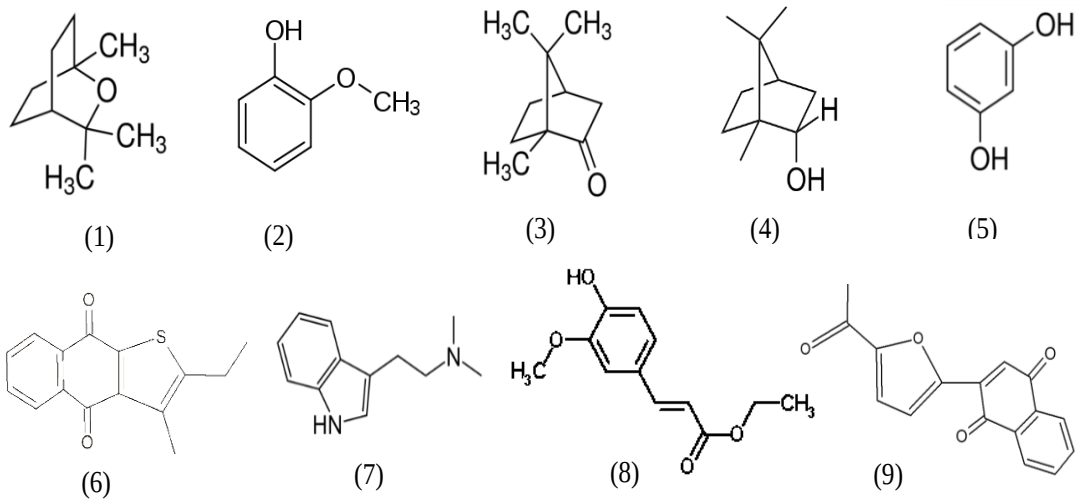

Figure 1.14 Chemical structure of some major compounds identified by MS in the acetonitrile eluate obtained after passing the hydro-alcoholic extract of *Mimosae tenuiflorae* though C18 SPE cartridge (1) eucalyptol, (2) 2-methoxyphenol, (3) (+)-2-bornanone, (4) endo-borneol, (5) resorcinol, (6) 2-ethyl-3-methylnaphtho[2,3-b]thiophene-4,9-dione, (7) N,N-dimethyltryptamine, (8) ethyl (2E)-3-(4-hydroxy-3-methoxyphenyl)-2-propenoate, (9) 2-(5-acetyl-2-furyl)-1,4-naphthoquinone.

In the present study, the presence of the alkaloid N, N-dimethyltryptamine within the major compounds stands out, which was previously identified by GC/MS in the hexanic eluate of *Mimosae tenuiflorae* bark obtained by matrix solid-phase dispersion extraction using silica as the solid support [56]. In our study, N, N-dimethyltryptamine was only identified in the C18 SPE cartridge eluted with acetonitrile, owing to its polar character. It is also important to note the

presence of resorcinol, a compound with a polar character had been detected previously in extracts from the bark of *Taiwan acacia* and *China Fir* [57] and Awa-Ban sheets [58]. In one of these studies, a co-polymer resin of resorcinol–tannin–formaldehyde was obtained to offer it as an alternative resin to provide tackiness in the manufacturing of plywood.

Additionally, 14 minor compounds (area <1%) were identified in the acetonitrile-eluted C18 SPE cartridge (**Figure 1.15**). Of these compounds, terpineol-4 (6), the α-terpineol (7) and ethyl p-methoxy cinnamate (19) are also present in the elution with isooctane, which shows the affinity of these compounds for both solvents and that their content in the bark of the *Mimosae tenuiflorae* is limited, owing to the percentage areas obtained in this study.

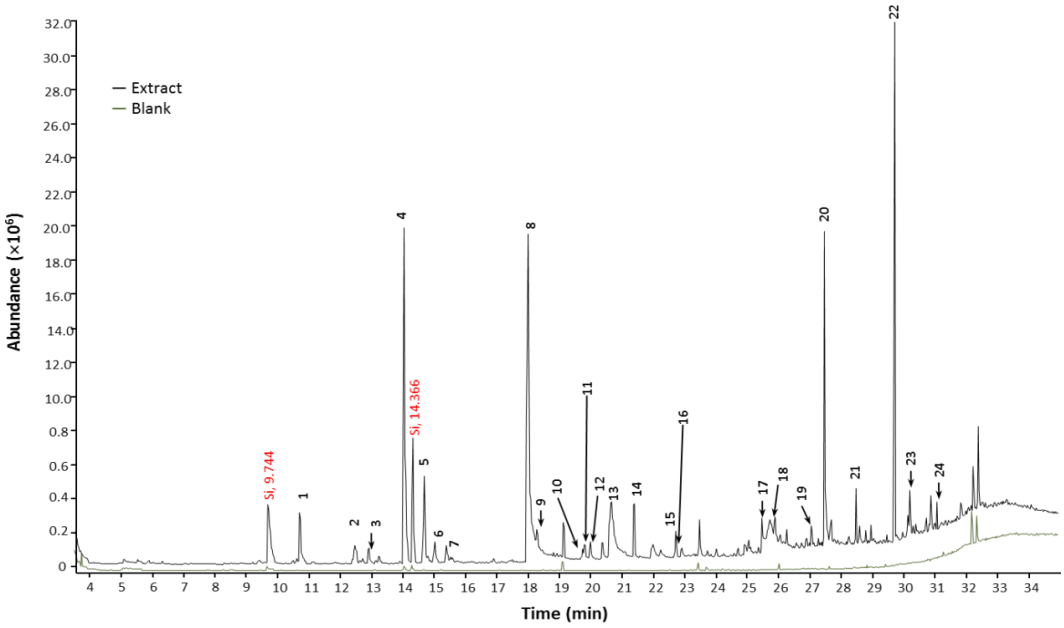

Figure 1.15 Chromatogram of acetonitrile eluate obtained after passing the hydro-alcoholic extract of *Mimosae tenuiflorae* bark through C18 SPE cartridge.

1.3.3 GC/MS analysis of *Azadirachta indica* A. Juss.

The **Table 1.12** shows the compounds identified in the seed oil of *Azadirachta indica* A. Juss obtained by Soxhlet extraction with ethanol. Among these are fatty acids as stearic acid, derived from fatty acids as ethyl palmitate, ethyl oleate and ethyl-9, 12-octadecadienoate, triterpenes as squalene, phytosterols as γ-sitosterol and a carotenoid as γ-tocopherol. The **Figure 1.16** shows to the chromatogram obtained by GC/MS.

Table 1.12 Major compounds in oil of *Azadirachta indica* A. Juss seeds using dichloromethane as solvent in GC/MS analysis.

No.	t_R (min.)	Compound	Area (%)
1	40.141	Ethyl palmitate ó Ethyl n-hexadecanoate	5
2	46.883	**Ethyl-9,12-octadecadienoate**	8
3	47.095	**Ethyl Oleate ó Ethyl cis-9-octadecenoate**	15
4	47.759	Octadecanoic acid, ethyl ester ó Stearic acid, ethyl ester	6
5	52.293	***f***	3
6	53.171	**Squalene**	7
7	54.937	γ-Tocopherol ó 7,8-Dimethyltocol	2
8	56.391	***f***	2
9	56.722	***f***	1
10	57.051	***f***	8
11	57.732	**γ-Sitosterol ó Clionasterol**	17
12	59.469	***f***	4
13	64.829	***f***	2
14	67.565	***f***	2
15	67.809	***f***	5
16	68.990	***f***	14

f: Unidentified compound; **Bold**: Major compound (more abundant); t_R: Retention time.

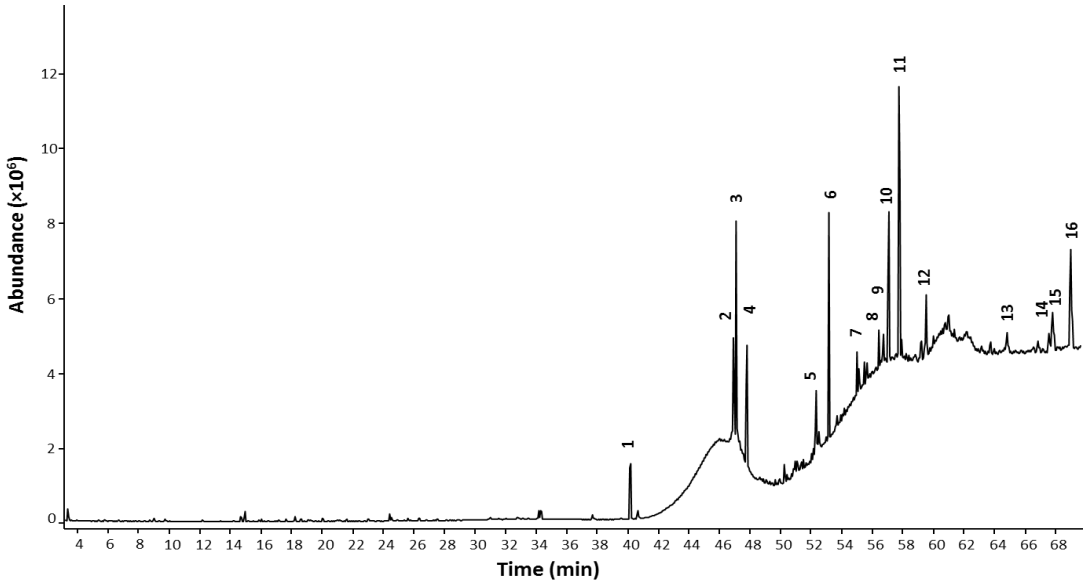

Figure 1.16 Chromatogram of the oil *Azadirachta indica* A. Juss seeds obtained by ethanolic extraction.

Among the major identified compounds by GC/MS is γ-sitosterol, which is a kind phytosterol that has shown antidiabetic activity [59] and apoptotic effect on breast and lung cancer cells [60]. Another compound identified in the oil is the squalene, an intermediate in the biosynthesis of phytosterol or cholesterol in plants, animals and humans, which has been also identified in the oil of other plants as olive, soybean, grape seeds, hazelnuts, peanuts, corn, sunflower, palm and amaranthus [61]; the squalene plays an important role in skin hydration, repairing of the damaged skin and rejuvenating the ageing skin. Also, its antibacterial property is

used for preparing a cooling formulation for the local treatment of burns. Finally, γ-tocopherol was identified. It was present in a low percentage. Γ-tocopherol is the most prevalent form of vitamin E in plant seeds [62] has it shown anti-inflammatory activity *in vitro* and *in vivo* [63]. In addition, this compound has also exhibited an anti-proliferative and apoptotic effect on cancer cells, but not on normal epithelial cells [64].

Few studies about the profile of volatile compound in seeds and oil seeds of *Azadirachta indica* A. Juss by GC/MS have been reported previously. In one of these studies [65], the seeds were analyzed by head space solid phase microextraction combined with GC/MS and the most abundant volatile components were (Z)-9,7-octadecadienal and palmitic acid; several kinds of compounds were also identified as alcohols, carbonyl compounds (ketones, aldehydes, and esters), terpenes, nitrogen and sulfur compounds among others. Other authors [66] obtained the oil by soxhlet extraction with hexane as a solvent and identified mainly fatty acids as oleic acid (67%), stearic acid (15%) and palmitic acid (16.60%); with reverse-phase HPLC method they identified the presence of Azadirachtin, Nimbin and Salannin.

1.4 Conclusions

Eugenol and methyl-eugenol are major volatile compounds in the leaves of the plant *Ocimum micranthum* Willd, owing to the presence of these components in essential oil, ethanolic extract and aqueous extract. The application of solid-phase extraction with a C18 SPE cartridge and subsequent elution with isooctane allowed to analyze the aqueous extract of *Ocimum micrantum* Willd leaves by GC/MS and to extract only eugenol and methyleugenol. The presence of eugenol and methyl-eugenol in different extracts of *Ocimum micrantum* Willd leaves, as well as other compounds (caryophyllene, humulene and eucalyptol) with functional activities reported by some previous studies, can explain the use of this plant in the traditional medicine. Therefore, any of the three extracts analyzed in this study could be attractive for pharmaceutical and biomedical applications.

The acetonitrile allowed the elution of a higher number of volatile compounds from the C18 SPE cartridge in both of the hydro-alcoholic extracts, which, in some cases, were complementary to the compounds eluted with isooctane. However, in the hydro-alcoholic extract of *Calendula officinalis* flowers, α-thujone, β-thujone, 4-terpineol, (-)-bornylacetate, eucalyptol, α-cadinol, and α-epi-muurolol were eluted from the SPE cartridge with both solvents; α-thujone was the compound with the highest percentage of the area. In contrast, in the hydro-alcoholic extract of *Mimosae tenuiflorae* bark, the only compound that was eluted in this way was eucalyptol; additionally, resorcinol and N,N-dimethyltryptamine were solely obtained in the elution with acetonitrile, and

these were major compounds together with (+)-2-bornanone. Therefore, for the identification of volatile compounds in a hydro-alcoholic extract using SPE (for pre-concentration and solvent change), it is important to make the right selection of solvent in the elution step, as it will determine the information that can be obtained in the GC/MS analysis. For this reason, it is convenient to choose solvents of low, medium and high polarity to elute compounds of different polarities. It is important to mention that anti-tumour, anti-inflammatory, antioxidant, antibacterial and antifungal properties shown in previous studies by some of the volatile compounds identified in the present study, support the medicinal properties that have been given to these compounds in the empirical use of the extracts of *Calendula officinalis* flowers and *Mimosae tenuiflorae* bark in traditional medicine.

Finally, due to the functional properties of some compounds identified in the oilseeds of *Azadirachta indica*, it could be used in the biomedical area and not only in the agroindustry.

1.5 References

1. Méndez-González ME, Durán-García R, Campos-Bobadilla SM, Dorantes-Euan A. Flora Medicinal. Uso de la flora y la fauna silvestre. Biodiversidad y Desarrollo Humano en Yucatán. CICY, PPD-FMAM, Conabio, Seduma. Mérida, Yuc. 2010; 349–352.
2. Altiok D, Altiok E, Tihnminlioglu F. Physical, antibacterial and antioxidant properties of chitosan films incorporated with thyme oil for potential wound healing applications. J. Mater. Sci. Materials in Medicine. 2010; 21: 2227–2236.
3. Zippel J, Deters A, Hensel A. Arabinogalactans from Mimosa tenuiflora (Willd). Poiret bark as active principles for wound-healing properties: Specific enhancement of dermal fibroblast activity and minor influence on HaCaT keratinocytes. J. Ethnopharmacol. 2009; 124: 391-396.
4. Sánchez-Medina A, García-Sosa K, May-Pat F, Peña-Rodríguez LM. Evaluation of biological activity of crude extracts from plants used in Yucatecan Traditional Medicine. Part1. Antioxidant, antimicrobial and β-glucosidase inhibition activities. Phytomedicine. 2001; 8: 144–151.
5. González-Elizondo M, López-Enríquez L, González-Elizondo S, Tena-Flores J. Plantas Medicinales del Estado de Durango y Zonas Aledañas. CIIDIR Durango. Instituto Politécnico Nacional. México, D.F. 2004: 12–13.
6. Morataya-Morales MA. Caracterización Farmacopéica de cuatro plantas aromáticas nativas de Guatemala Albahaca de monte (*Ocimum micranthum*), Orégano (*Lippia graveolens*), Salvia sija (*Lippia alba*) y Salviyá (*Lippia chiapasensis*). Tesis de Licenciatura. Facultad de Ciencias Químicas y Farmacia. Universidad de San Carlos de Guatemala. 2006; 3-7.

7. Charles DJ, Simon JE, Wood KV. Oil constituents of *Ocimum micranthum* Willd. J. Agric. Food Chem. 1990; 38: 120–122.
8. Charles DJ, Simon JE. Comparison of extraction methods for the rapid determination of essential oil content and composition of Basil. J. Amer. Soc. Hort. Sci. 1990; 115 (3), 458–462.
9. Vieira P, M de Morais S, Bezerra HQF, Travassos-Ferreira PA, Oliveira IR, Silva MGV. Chemical composition and antifungal activity of essential oils from *Ocimum* species. Ind. Crop. Prod. 2014; 55: 267–271.
10. Saccheti G, Medici A, Maletti S, Radice M, Muzzoli MV, et al. Composition and functional properties of the essential oil of Amazonian Basil, *Ocimum micranthum* Willd *Labiatae* in comparison with commercial essential oils. J. Agric. Food Chem. 2004; 52: 3486–3491.
11. Shetty S, Udupa S, Udupa L. Evaluation of antioxidant and wound healing effects of alcoholic and aqueous extract of *Ocimum sanctum* Linn in rats. Evid. Based Complement. Alternat. Med.: eCAM. 2008; 5: 95–101. doi:10.1093/ecam/nem004.
12. Adigüzel A, Güllüce M, Sengüil M, Ögütcü H, Sahin T, Karaman I. Antimicrobial effects of *Ocimum basilicum* (Labiatae) extract. Turk. J. Biol. 2005; 29: 155–160.
13. Domínguez-Marín L. Efecto de la aplicación del extracto hidroalcohólico de flores de caléndula *(Calendula officinalis*) en la estabilización del color y vida útil en pulpa de frutas. Universidad Nacional de Colombia. Maestría en Ciencia y Tecnología de Alimentos. Programa Interfacultades. Bogota, Colombia. 2012; 22–41.
14. Butnariu M, Coradini MA. Evaluation of biologically active compounds from *Calendula officinalis* flowers using spectrophotometry. Chem Cent. J. 2012; 35 (6):1–2.
15. Hamburger M, Adler S, Baumann D, Förg A, Weinreich B. Preparative purification of the major anti-inflammatory triterpenoid esters from Marigold (*Calendula officinalis*). Fitoterapia. 2003; 74: 328–338.
16. Patrick KFM, Kumar S, Edwarson PAD, Hutchinson JJ. Induction of vascularization by an aqueous extract of the flowers of *Calendula officinalis* L. The European Marigold. Phytomedicine. 1996; 3(1): 11–18.
17. Priyanka M, Patidar A, Gupta A, Agrawal S. Treatment of acne with herbal remedy *Calendula officinalis*: An overview. Int J Pharm Biol Arch. 2011; 2(4): 1020–1023.
18. Córdova CAS, Siqueira IR, Netto CA, Yunes RA, Volpato AM, Filho VC, et al. Protective properties of butanolic extract of the Calendula officinalis L. (marigold) against lipid peroxidation of rat liver microsomes and action as free radical scavenger. Redox Rep. 2002; 7(2): 95–102. DOI: 10.1179/135100002125000325.

19. Lagarto A, Bueno V, Guerra I, Valdés O, Vega Y, Torres L. Acute and sub-chronic oral toxicities of Calendula officinalis extract in Wistar rats. Exp. Toxicol Pathol. 2011; 63:387–391.
20. Rivera-Arce E, Chávez-Soto MA, Herrera-Arellano A, Arzate S, Agüero J, Feria-Romero I, et al. Therapeutic effectiveness of a Mimosae tenuiflorae cortex extract in venous leg ulceration treatment. J Ethnopharmacol. 2007; 109: 523–528.
21. Oliveira-Bitencourt MA, Jerônimo de Souza Lima MC, Torres-Rêgo M, Morais-Fernandes J, Da Silva-Junior AA, Vilarinho-Tambourgi D, et al. Neutralizing effects of Mimosa tenuiflora extracts against inflammation caused by Tityus serrulatus Scorpion venom. Biomed Res Int. 2014; 1–8. DOI:10.1155/2014/378235.
22. Rodríguez-Álvarez M, Alcaraz-Meléndez L, Real-Cosío SM. Procedimientos para la extracción de aceites esenciales en plantas aromáticas. Edit. Centro de Investigaciones Biológicas del Noroeste, S.C. La Paz, Baja California Sur, México. 2012; 24-29.
23. Aziba PI, Bass D, Elegbe Y. Pharmacological Investigation of Ocimum gratissimum in Rodents. Phytother. Res. 1999; 13: 427-429.
24. Chiu C-C, Huang C-Y, Chen T-Y, Kao S-H, Liu J-Y, et al. Beneficial effects of Ocimum gratissimum aqueous extract on rats with CCl4-induced acute liver injury. Evid. Based Complement. Alternat. Med.: eCAM. 2012; 2012:736752. doi:10.1155/2012/736752
25. Fabricación de extractos fluidos y secos. Laboratorio de remedios herbolarios. Rosa Elena Dueñas S.A de C.V. Conferencia on line Web site. http://www.redsa.com.mx. Updated November 20, 2015. Accessed November 20, 2015.
26. Issara-Amphorn J, T-Thienprasert NP. Preliminary in vitro pro-apoptotic effects of Cratoxylum formosum crude leaf extracts. Int J Appl Res Nat Prod. 2014; 7(4):27.
27. Joshi B, Sah GP, Basnet BB, Bhat MR, Sharma D, et al. Phytochemical extraction and antimicrobial properties of different medicinal plants: Ocimum sanctum (Tulsi), Eugenia caryophyllata (Clove), Achyranthes bidentata (Datiwan) and Azadirachta indica (Neem). J. Microbiol. Antimicrob. 2011; 3(1):1-7.
28. Advances in Method Development for SPE. Agilent Technologies. Web site. https://www.agilent.com/cs/library/slidepresentation/Public/Advances%20in%20Method%20Development%20SPE.pdf. Published October, 2009. Updated November 23, 2015. Accessed November 23, 2015.
29. Arvy MP, Gallouin F. Especias, aromatizantes y condimentos. MundiPrensa Libros. Madrid, España. 2007; 36-37.

30. Viña A, Murillo E. Essential oil composition from twelve varieties of basil (*Ocimum spp*) grown in Colombia. J. Braz. Chem. Soc. 2003; 14: 744–749.
31. Fleisher A. Essential oils from two varieties of Ocimum basilicum L., grown in Israel. J. Sci. Food Agric. 1981; 32: 1119–1122.
32. Özcan M, Chalchat JC. Essential oil composition of Ocimum basilicum L. and Ocimum minimum L. in Turkey. Czech. J. Food Sci. 2002; 20: 223–228.
33. Sajjadi SE. Analysis of the essential oils of two cultivated basil (Ocimum basilicum L.) from Iran. DARU J. Pharm. Sci. 2006; 14: 128–130.
34. Hussain AI, Anwar F, Hussain-Sherazi ST, Przybylski R. Chemical composition, antioxidant and antimicrobial activities of basil (Ocimum basilicum) essential oils depend on seasonal variations. Food Chem. 2008; 108: 986–995.
35. Politeo O, Jukic M, Milus M. Chemical composition and antioxidant capacity of free volatile aglycones from basil (Ocimum basilicum L.) compared with its essential oil. Food Chem. 2007; 101: 379–385.
36. Miele M, Dondero R, Ciarallo G, Mazzei M. Methyleugenol in Ocimum basilicum L. Cv. Genovese Gigante. J. Agric. Food Chem. 2001; 49: 517–521.
37. Wossa SW, Rali T, Leach DN. Volatile chemical constituents of three Ocimum species (Lamiaceae) from Papua New Guinea. SPJNS. 2008; 26: 25–27.
38. Oboh, G. Antioxidant and antimicrobial properties of ethanolic extracts of Ocimum gratissimum leaves. J Pharmacol. Toxicol. 2010; 5: 396–402.
39. Narwal S, Rana AC, Tiwori V, Gangwani S, Sharma R. Review on chemical constituents and pharmacological action of Ocimum kilimandscharicum. Indo. Global J. Pharm. Sci. 2011; 1: 287–293.
40. Crabas N, Marongiu B, Piras A, Pivetta T, Porceddaa S. Extraction, separation and isolation of volatiles and dyes from Calendula officinalis L. and Aloysia triphylla (L'Her.) britton by supercritical CO2. J Essent Oil Res. 2003; 15 (5): 350–355.
41. Gazim ZC, Rezende CM, Fraga SR, Svidzinski TIE, Cortez DAG. Antifungal activity of the essential oil from Calendula officinalis L. (asteraceae) growing in Brazil. J Braz Microbiol. 2008; 39(1): 61–63. DOI:10.1590/S1517-838220080001000015.
42. Mishra AK, Mishra A, Chattopadhyay P. Assessment of in vitro sun protection factor of Calendula officinalis L. (Asteraceae) essential oil formulation. J Young Pharm. 2012; 4(1): 18–20.
43. Re TA, Mooney D, Antignac E, Dufour E, Bark I, Srinivasan V, et al. Application of the threshold of toxicological concern approach for the safety evaluation of calendula flower

(Calendula officinalis) petals and extracts used in cosmetic and personal care products. Food Chem Toxicol. 2009; 47: 1246–1254.

44. Paolini J, Barboni T, Desjobert JM, Djabou N, Muselli A. Chemical composition, intra-species variation and seasonal variation in essentials oils of Calendula arvensis L. Bioch Syst Ecol. 2010; 38: 865–874.
45. Tighe S, Gao Y-Y, Tseng SCG. Terpinen-4-ol is the most active ingredient of tea tree oil to kill Demodex mites. Transl Vis Sci Technol. 2013; 2(7): 2. DOI:10.1167/tvst.2.7.2.
46. Wang XY, Yang D, Zhang H, Jia YS, Lee KT. Antioxidant activity of soybean oil containing 4-Vinylsyringol obtained from decarboxylated synaptic acid. J Am Oil Chem Soc. 2014; 9: 1543–1550.
47. Saccheti G, Medici A, Maletti S, Radice M, Muzzoli MV, Manfradini S, et al. Composition and functional properties of the essential oil of Amazonian Basil, Ocimum Micrantum Willd Labiatae in comparison with commercial essential oils. J Agric Food Chem. 2004; 52: 3486–3491.
48. Vieira P, M de Morais S, Bezerra HQF, Travassos-Ferreira PA, Oliveira IR, Silva MGV. Chemical composition and antifungal activity of essential oils from Ocimum species. Ind Crop Prod. 2014; 55: 267–271.
49. Anton R, Jiang Y, Weniger B, Beck JP, Rivier L. Pharmacognosy of Mimosa tenuiflora (Willd) Poiret. J Ethnopharmacol. 1993; 38:153–157.
50. Rivera-Arce E, Gattuso M, Alvarado R, Zárate E, Agüero J, Feria I, et al. Pharmacognostical studies of the plant drug Mimosae tenuiflorae cortex. J Ethnopharmacol. 2007; 113: 400–408.
51. Lammoglia-Ordiales L, Vega-Memije ME, Herrera-Arellano A, Rivera-Arce E, Agüero J, Vargas-Martinez F, et al. A randomised comparative trial on the use of a hydrogel with tepescohuite extract (Mimosae tenuiflorae cortex extract 2G) in the treatment of venous leg ulcers. Int Wound J. 2012; 9: 412–418.
52. Pelkonen O, Abass K, Wiesner J. Thujone and thujone containing herbal medicinal and botanical products: Toxicological assessment. Regul Toxicol Pharm. 2013; 65: 100–107.
53. NTP. Toxicology and carcinogenesis studies of alpha, betathujone (CAS No. 76231-76-0) in F344/N rats and B6C3F1 mice (gavage studies). National Toxicology Program. Natl Toxicol. Program Tech. Rep. Ser. 2011a; 570: 1–260.
54. Hassan SB, Gali-Muhtasib H, Göransson H, Larsson R. Alpha terpineol: A potential anticancer agent which acts through suppressing NF-kB signalling. Anticancer Res. 2010; 30: 1911–1920.
55. Gainsford G, Hosie CF, Weston RJ. Conversion of α-pinene to terpinyl acetate over H-beta zeolites. Appl Catal A Gen. 2001; 209: 269–277.

56. Gaujac A, Aquino A, Navickiene S, Bittencourt de Andrade J. Determination of N,N-dimethyltryltamine in *Mimosa tenuiflora*, inner barks by matrix solid-phase dispersion procedure and GC-MS. J Chromatogr B. 2012; 881–882: 107–110.
57. Lee WJ, Lan WC. Properties of resorcinol-tannin formaldehyde copolymer resins preparated from the bark extracts of Taiwan acacia and China fir. Bioresource Tech. 2006; 97: 257–264.
58. Hiasa M, Kurokawa M, Ohta K, Tomoyuki E, Akita H, Niki K, et al. Identification and purification of resorcinol, an antioxidant specific to *Awa-ban* (pickled and anaerobically fermented) tea. Food Res Int. 2013; 54: 72–80.
59. Balamurugan R, Duraipandiyan V, Ignacimuthu S. Antidiabetic activity of γ-sitosterol isolated from *Lippia nodiflora* L. in streptozotocin induced diabetic rats. Eur J Pharmacol. 2011. 667: 410-418.
60. Sundarraj S, Thangam R, Sreevani V, Kaveri K, Gunasekaran P, Achiraman S, Kannan S. γ-Sitosterol from *Acacia nilotica* L. induces G2/M cell cycle arrest and apoptosis through c-Myc suppression in MCF-7 and A549 cells. J Ethnopharmacol. 2012 Jun 14: 141(3):803-9.
61. Popa O, Băbeanu NE, Popa I, Niță S, Dinu-Pârvu CE. Methods for Obtaining and Determination of Squalene from Natural Sources. BioMed Res Int. 2015. doi:10.1155/2015/367202
62. Jiang Q, Christen S, Shigenaga MK, Ames BN. γ-Tocopherol, the major form of vitamin E in the US diet, deserves more attention. Am J Clin Nut. 2001. 74: 714-22.
63. Reiter E, Jiang Q. Christen S. Anti-inflammatory properties of α and γ-tocopherol. Mol Aspects Med. 2007. 28(5-6): 668–691.
64. Jiang Q, Elson-Schwab I, Courtemanche C, Ames BN. Gamma-tocopherol and its major metabolite, in contrast to alpha-tocopherol, inhibit cyclooxygenase activity in macrophages and epithelial cells. Proc Natl Acad Sci USA 2000. 97(21):11494–9.
65. Shivashankar S, Roy TK, Moorthy PNK. Headspace Solid Phase Micro Extraction and GC/MS Analysis of the Volatile Components in Seed and Cake of *Azadirachta indica* A. juss. Chem. Bull. "POLITEHNICA" Univ. (Timisoara). 2012. 57(71)
66. Kumar J, Parmar BS. Physicochemical and Chemical Variation in Neem Oils and Some Bioactivity Leads against *Spodoptera litura* F. J. Agric. Food Chem. 1996. 44 (8): 2137–2143.

Chapter 2

"Antimicrobial and proliferative activity of extracts of *Ocimum micranthum* Willd leaves, *Calendula officinalis* L. flowers, *Mimosae tenuiflorae* bark and *Azadirachta indica* A. Juss seeds"

2.1 Introduction

In traditional medicine, the use of herbal products or extracts of plants in the treatment of several diseases, as well as in the treatment of cuts, cutaneous infections, wounds and burns is a regular practice [1, 2]. Among the plants that have been used for this purpose are *Ocimum micranthum* Willd, *Mimosa tenuiflora, Calendula officinalis* and *Azadirachta indica* [3, 4, 5, 6]. The antimicrobial, antioxidant, anti-inflammatory properties of some crude extracts of plants have shown a positive effect on the wound healing process [7].

O. micranthum Willd is an herbaceous native plant belonging to tropical and subtropical regions of America and the West Indies [8]. In México, this plant is distributed in the states of Campeche, Chiapas, Colima, Jalisco, Oaxaca, Puebla, Querétaro, Quintana Roo, Sinaloa, Tabasco, Tamaulipas, Veracruz and Yucatán [9]. Previous studies have indicated that the essential oil of this species has activity against human pathogens, fungi, insects, and larvae in addition to its antioxidant, antiprotozoal, anti-inflammatory and contraceptive properties [10]. The essential oil of *Ocimum micranthum* Willd leaves contain volatile compounds such as eugenol, β-elemene, γ-elemene β-caryophyllene, isoeugenol and methyl-eugenol [11, 12]. The eugenol and methyl-eugenol are phenolic compounds with antiseptic, antibacterial and analgesic properties that have also been identified in aqueous and ethanolic extracts of this plant [12]. In particular, the effect of eugenol, it has been reported on mast cells and melanoma cells [13] and due to the broad field of application of this compound, it will be essential to know its action on healthy human cells, such as skin cells (fibroblast and keratinocytes) [14]. For other species of the genus *Ocimum* such as *sanctum Linn, gratissimum Linn, kilimandscharicum*, it has been reported the wound healing properties of its crude extracts, and essential oil [15, 16, 17]. The crude extracts of *micranthum* species it has been that support it therapeutic benefits on wound healing and cutaneous infections through *in vitro* tests on healthy cell lines. Moreover, studies have not addressed the potential antimicrobial activity of these extracts against pathogenic microorganisms.

C. officinalis is a medicinal plant native from southern Europe with yellow or orange flowers. It is used in folk medicine medicinally how infusion, tinctures, liquid extracts, creams or ointments; the plant contains polysaccharides, flavonoids, triterpene alcohols, phenol acids, tannins, glycosides, sterols, carotenoids and saponosides [18, 19]. The essential oils of the *C. officinalis*

flowers have shown antibacterial activity against *Escherichia coli, Staphylococcus aureus* and *Streptococcus faecalis* as well as antifungal activity against *Candida albicans* [20]. The particular interest in the biomedical applications of this plant is due to its ability to heal external and opened wounds, lacerations, and ulcers through the promotion of granulation tissue. It has been used to treat ulcers in the stomach and intestines, haemorrhages, and chronic skin lesions such as burns [21, 22].

M. tenuiflora is a plant belonging to the *Mimosaceae* subfamily, a common shrub/tree that is distributed in areas of tropical deciduous forests in the Americas from the southeastern regions of México to northern Brazil and Venezuela [23]; its bark has been used in traditional medicine for the treatment of burns and skin wounds [24,25]. Previous studies have shown that aqueous and ethanolic extracts of the dried bark of *M. tenuiflora* contain tannins, steroidal saponins and phenolic compounds [26].

A. indica A. Juss (neem) belongs to the family *Meliaceae* and is original of Southeast Asian. This plant is also found in tropical and semitropical regions of India, Bangladesh, Pakistan and Nepal [27]. Among the active compounds that have been identified in neem are including azadirachtin, nimbolinin, nimbin, nimbidin, nimbidol, sodium nimbinate, gedunin, salannin, and quercetin [28]. Several biological and pharmacological activities have been reported, including antibacterial [29, 30], antifungal [31], anti-inflammatory and immunomodulatory [32]. The effect of the crude neem oil on wound healing has been reported in animal cases [33] but has not been reported *in vitro* or *in vivo* studies with human cells.

There are not scientific reports that support the bioactivities and the therapeutic use of extracts from *Ocimum micranthum* Willd, *Mimosa tenuiflora*, *Calendula officinalis* and *Azadirachta indica* in the traditional medicine for the treatment of cutaneous infections and wound healing.

The aim of the present study aimed to assess the crude extracts of these plants for antimicrobial activity against some pathogenic microorganisms. Also, the proliferative activity was evaluated *in vitro* on a healthy human cell line (hFB) and the CHO-K1 cell line with the purpose of providing evidence (research-based) about its bioactivity and effects on a healthy cell line associated with the process of wound healing.

2.2 Experimental Methods

The complete description of the plant material and procedure of extraction of diverse extracts and oils is located in Chapter 1.

Microbial strains

The antimicrobial activity of the extracts was evaluated through the determination of minimal inhibitory concentration (MIC) using the microdilution technique on a 96 well plate and by staining with a solution of iodonitrotetrazolium chloride (INT). The microorganisms used in this study consisted of two Gram-positive strains (*Staphylococcus aureus* ATCC® 25973TM and *Bacillus subtilis* ATCC® 465 TM); one Gram-negative strain (*Pseudomonas aeruginosa* ATCC ® 27853 TM) and one yeast-fungus strain (*Candida albicans* ATCC® 14053 TM).

Growth kinetics

For the McFarland turbidimetric analysis [37], a wavelength of 590 nm was used. The absorbance values of this test were correlated with the absorbance values from the growth kinetics of each microorganism tested. This correlation was used to calculate the time taken by each microorganism to reach the exponential phase and also the concentration of microorganism necessary to carry out for the microdilution test. The value recorded in the present study was 0.50 on the McFarland scale which is equivalent to 1.5 x 10^8 CFU/mL. In the growth kinetics, a pre-inoculum of each microorganism was incubated for 20-21 h at 35°C under stirring. The culture medium used for this purpose was brain heart infusion (BHI) broth for *S. aureus* and *B. subtilis*, nutritive broth (*P. aeruginosa*) and sabouraud broth (*C. albicans*). The absorbance was measured every 2 h during a period of 16 h using a spectrophotometer model GENESYS 20 (Thermo Scientific) at a wavelength of 590 nm.

Minimal Inhibitory Concentration (MIC)

Twelve concentrations of the extracts (ethanolic, aqueous, and essential oil) of *Ocimum micranthum* Willd leaves were analyzed. Six of these concentrations were chosen through the evaluation of the results of osmolality and pH assays that were performed to avoid interferences in the tests with mammalian cells. The dilutions of the extracts were prepared with 5 % dimethylsulfoxide (DMSO) solution (D8418-500mL ® Sigma Aldrich). This concentration of the reagent was selected based on the results of a preliminary test where different concentrations of DMSO were evaluated to measure its toxicity on the microorganisms utilized in the present study and to eliminate the possibility of interference by the concentration of DMSO. Positive controls such as amikacin (4 mg/L) and nystatin (2 mg/mL), control of culture medium, color control of each extract concentration and positive control of growth of each microorganism were used. In the test, 100 µL of each microorganism suspension at a concentration of 1.5 x10^8 CFU/mL (0.5 of the

McFarland scale) was inoculated in the 96 well microplates, and then 100 µL of each extract solution were added. The microplates were incubated at 35°C for 20-21 h in the case of *S. aureus, B. subtilis,* and *P. aeruginosa*; in the case of *C. albicans*, the incubation time was 40-42 hours. Once the incubation period had lapsed, 20 µL of a solution of iodonitrotetrazolium chloride 0.25 mg/mL (58030-1g-F ®Sigma Aldrich) were added to the 96 well microplates, which were incubated at 35 °C for 1 hour [38]. Subsequently, the MIC was determined visually; an aliquot of 50 µL was taken from the wells that did not present a color change and it was used to inoculate a Petri dish with a medium corresponding to the evaluated microorganism. On the Petri dish, an extension technique using a digralski spreader was carried out, after the Petri dishes were incubated at 35°C for 24 h (*S. aureus, B. subtilis, and P. aeruginosa*) and 48 h (*C. albicans*). Finally, the microplates were read in a microplate reader (model Stat Fax 4200 (® Awareness Technology) at a wavelength of 492 nm.

The MIC was reported for each microorganism in every extract. The MIC was defined as the lowest concentration that led to growth inhibition, which was visually observed, as no color change in the colorimetric test. The growth of some microorganisms in the Petri dishes indicated a bacteriostatic effect, while no growth of the microorganism indicated a bactericidal effect of the extracts. Concerning *Candida albicans*, the terms that were applied were either a fungistatic or fungicide effect respectively.

Measurement of pH and osmolality

The pH and osmolality of the culture media supplemented with the extracts were evaluated before to the MTT assay, with the goal of verifying that the values were in the optimum range and to avoid cytotoxic effects of osmotic shock or pH and, in this way, assess only the effect of the extracts on the cell lines. The osmolality measurements were performed with an osmometer (Advanced Instrument Inc. model 3320) using the freezing point depression method. The pH measurements were carried out with a VWR® SB90M5 pH meter. The optimum range of osmolality for cell growth was 230 to 400 mOsm/kg, and the optimum range of pH was 6.60 to 7.80 [39].

Cell lines and cell culture

In the present study, two cell lines were used, healthy human breast-derived fibroblasts (hFB) and adherent Chinese hamster ovary cells (CHO-K1, Gibco, USA). This last cell line is a classic model of cytotoxic tests and proliferative assays due to its capacity of adaptation in adherent mode or suspension [40]. Both cell lines were routinely grown in DMEM F12 medium (Gibco, USA) supplemented with 10% fetal bovine serum (Gibco, USA) at 37 °C in a humidified atmosphere of 5% CO_2.

MTT assay

The effect of the extracts on CHO-K1 and hFB cell lines was assessed using the tetrazolium colorimetric MTT assay [41]. The cells were seeded at a density 2 x 10^4 cells/well in 96-well microtiter plates and incubated at 37°C and 5% CO_2 in a humidified environment for 24 h. Subsequently, 100 µL of six different concentrations of each extract were added to the wells, and the plates were incubated for 48 h. After that, 10 µL of MTT solution (5 mg/ml in RPMI-1640 without phenol red, Sigma Aldrich®) were added to each well, and the plates were incubated at 37°C for 2 h. After the incubation period, the culture medium was retired and 100 µL of MTT solvent (0.1N HCl in anhydrous isopropanol) were added to the wells to solubilize the formazan crystals. Multiskan FC (Thermo Scientific) microplate reader at 570 nm was used for the measurement of the absorbance. The measurement of the color control of all concentrations of each extract was carried out to ensure that no interference occurred in the measurement of each well. The percentage of relative cell proliferation was calculated based on a comparison with untreated cells (control) as [extract absorbance/control absorbance] x 100. Microscopic viewing of the cell cultures was performed before and after the assay using an inverted microscope (Axio Vert 200) coupled with a video camera (Carl Zeiss).

Trypan blue exclusion assay

The trypan blue exclusion assay is a visual method used for the direct counting of viable cells. Therefore, it was chosen to evaluate the proliferative activity of the extracts on hFB cell line and for comparison with a colorimetric method such as MTT. The cells were seeded in a 24 well plate (cell density of 2 x 10^4 cells/well) and incubated at 37°C in an atmosphere of 5% CO_2 and a humidified environment for 24 h. The next day, cells were treated with six different concentrations of each extract for 48 h. The morphological changes of treated and untreated cell line (control) were compared by monitoring using an inverted microscope (Carl Zeiss, Axio Vert 200 model). After the morphological assessment, the cell viability was evaluated. For this, the cells were rinsed with 1 mL of phosphate buffered saline (PBS 1X, Gibco) and trypsinized with 0.50 mL of 0.025% trypsin-EDTA (Gibco). Then, trypsin was neutralized by the addition of 0.50 mL of growth medium. Samples were taken and stained with 0.04% Trypan blue dye solution (Sigma Aldrich). Within two minutes, the cells were loaded in a Neubauer chamber, and the number of viable and non-viable cells per 1 x 1 mm square were counted under a phase contrast microscope. The relative cell proliferation was determined as [No. of viable cells in the cells treated/ No. of viable cells in the cells not treated (control)] x 100.

Statistical Analysis

Results of MTT and Trypan Blue test were presented as the Mean ± Standard deviation (SD). The data were subjected to one-way analysis of variance (ANOVA) using STATGRAPHICS PLUS 5.1 statistical program. Duncan's Method was used in the multiple comparisons in the cases where the ANOVA detected a significant difference ($p < 0.05$).

2.3 Results and discussion

2.3.1 Minimal Inhibitory Concentration

Essential oil, ethanolic and aqueous extracts of *Ocimum micranthum* Willd leaves

The results of the MIC test (**Table 2.1**) suggested that the fungi *C. albicans* was the more susceptible microorganism to the ethanolic and aqueous extracts. The essential oil exerted the least antimicrobial effect which showed the highest value of MIC in all tested microorganisms. The ethanolic and aqueous extracts showed the same antimicrobial effect against *S. aureus, B. subtilis* and *P. aeruginosa*, microorganisms with different Gram, and therefore different cell wall chemistry. The positive controls, amikacin, and nystatin showed an antimicrobial effect at 4 mg/L and 2 mg/L respectively, seeing that there was no color change when the solution of iodonitrotetrazolium chloride was added during the MIC assay.

Table 2.1 MIC of essential oil and extracts of *Ocimum micranthum* Willd leaves.

Plant	Extract	Minimal Inhibitory Concentration (µL/mL)			
		Staphylococcus aureus	***Bacillus subtilis***	***Pseudomonas aeruginosa***	***Candida albicans***
Ocimum micranthum	**Ethanolic**	125	125	125	5
	Aqueous	125	125	125	80
	Essential oil	500	250	500	125

The essential oil and the extracts (ethanolic and aqueous) of *O. micranthum* leaves showed a bacteriostatic effect against *S. aureus, B. subtilis,* and *P. aeruginosa*. The bacteriostatic effect against Gram-positive and Gram-negative bacteria, at the same concentration, suggests that the chemical composition of the extracts and its mechanism of action had a bacteriostatic effect that was independent of the chemistry of the cell wall of the microorganisms, which in other studies has been reported to be a factor.

On the other hand, only essential oil showed a fungicide effect against *C. albicans*, since its growth was not observed in the Petri dishes. These results suggest that the essential oil and the extracts of this plant may produce a fungicide or fungistatic effect at low concentrations in comparison with the levels that are necessary to cause a bacteriostatic effect. These last results are relevant since the majority of studies that have used the microdilution technique to calculate the MIC have not reported complementary tests necessary to verify the bactericide, bacteriostatic, fungicide or fungistatic effects of the extracts.

Some studies have reported the antimicrobial activity of essential oil from diverse species of the *Ocimum* genus, such as *micranthum* and *basilicum* using the diffusion disc method [42]. In these studies the essential oil from *micranthum* species showed higher antimicrobial activity against *C. albicans* (0.069 mg/L) and *P. aeruginosa* (0.173 mg/L) than essential oil from the *basilicum* species, however, *basilicum* species showed higher antimicrobial activity against *S. aureus* (0.057mg/L) than *micranthum* species (0.104 mg/L). Other authors [43] have reported antimicrobial activity of ethanolic extract from *Ocimum basilicum* using the micro-well dilution method, where this extract had a MIC of 250 μg/mL against *S. aureus*; however, activity was not demonstrable against *C. albicans*. These authors also used the diffusion disc method, where the ethanolic extract showed activity against *S. aureus* (8 mm) and *Bacillus subtilis* at a concentration of 300 μg/disc, but the extract did not manifest activity against *P. aeruginosa* and *C. albicans.*

Other studies [44] have observed the antimicrobial activity of the ethanolic extract from *Ocimum gratissimum* leaves against *P. aeruginosa, S. aureus* and antifungal activity against *C. albicans*; this activity was increased when the concentration of the extract also increased. Other authors [45] have reported antimicrobial activity against *S. aureus,* and *P. aeruginosa* exerted by the ethanolic extract from *Ocimum sanctum* using the diffusion disc method. There is a study that indicated higher inhibitory activity of the ethanolic extract from *Ocimum basilicum* against *S. aureus* and *E. coli* at 200 mg/L using the hole-plate diffusion method [46].

Other authors carried out a study of the antifungal activity of essential oils derived from different species of the *Ocimum* genus (*americanum*, *basilicum* variety *purpurascens*, *basilicum* variety *minimum*, *micranthum*, *selloi)* against different species of the *Candida* genus using broth microdilution method, in accordance with the Clinical and Laboratory Standards Institute-CLSI [47]. In this study, it was observed that essential oil from *americanum*, *basilicum* variety *purpurascens* and *basilicum* variety *minimum* species did not display inhibitory activity against *C. albicans* (ATCC 3719). The essential oil from *americanum* and *basilicum* variety *purpurascens* had high MIC values (5000 μg/mL) against *C. albicans* (ATCC 11006), while *basilicum* variety

minimum did not show inhibitory activity. The essential oil from *selloi* species showed inhibitory activity against *C. albicans* (ATCC 3719) and *C. albicans* (ATCC 11006) at a concentration of 1250 µg/mL. The essential oil from the *micranthum* species displayed inhibitory activity against *C. albicans* 3719 and *C. albicans* (ATCC 11006) at concentrations of 1250 µg/mL and 625 µg/mL, respectively.

The variation of the antimicrobial activity of diverse species of *Ocimum* genus as well as the same *micranthum* species may be attributed to the biochemical properties of the plants that have been influenced by several factors such as the geographical origin, soil, environmental conditions, crop conditions, and seasonal variations, this may also be linked to the difference in the chemical composition, especially the presence of eugenol since aromatic alcohols are mainly responsible for the antimicrobial activity of essential oils [47, 48]. Some authors have mentioned that the antimicrobial action of essential oil is due to the lipophilic character of its hydrocarbon skeleton and the hydrophilic character of its functional groups; the chemical group with higher antimicrobial activity is phenol, followed by aldehydes, ketones, alcohols, ethers, and hydrocarbons [47]. A higher antimicrobial activity has been reported for phenolic compounds such as thymol, carvacrol, and eugenol, which are associated with the acidic nature of the hydroxyl group, forming a hydrogen bond with an active enzyme centre [49]. Concerning the volatile compounds in the essential oil from the *micranthum* species, some authors [12] used the GC/MS analysis to identify majority compounds such as β-caryophyllene (27%), methyl eugenol (14%), eugenol (12%) and in lower percentages, spathulenol (3%) and caryophyllene oxide (3%). Also, the authors identified compounds with antimicrobial activity in the ethanolic extract such as eugenol (18%), β-caryophyllene (6%), benzoic acid (3%), methyl eugenol (2%), dodecanoic acid (2%) and spathulenol (1%). Finally, in the aqueous extract eugenol (59%), 2,2-dimethyl-4-(methylethyl)-2H-imidazole, (4%), phenethyl alcohol (2%), methyl eugenol (2%) and catechol (1%) were identified, compounds that have shown antimicrobial activity [50, 51]. In the present study, the ethanolic extract showed a bacteriostatic effect and a fungistatic effect at lower concentrations than aqueous extract, despite having the lowest content of eugenol; thus it is possible that the antimicrobial properties of the ethanolic extract may be attributed to a synergic effect between its compounds.

Hydro-alcoholic extracts of *Calendula officinalis* L. flowers and *Mimosae tenuiflorae* bark

The results of the MIC tests (**Table 2.2)** suggest that the fungi, *Candida albicans* were most susceptible to both hydro-alcoholic extracts since it displayed the lower MIC values (10 and 80 µL/mL**)**. Both extracts had the same value of MIC against *S. aureus*, *B. subtilis* and *P. aeruginosa*, despite of being bacteria with a different kind of Gram stain (gram-positive and gram-negative) and therefore with a different chemical composition of its cell wall. The positive controls, amikacin,

and nystatin showed an antimicrobial effect at 4 mg/L and 2 mg/L, respectively, because the wells of the plate, where the antibiotics were deposited with the different tested microorganisms, did not present a color change when the solution of iodonitrotetrazolium chloride was added during the MIC assay.

Table 2.2. MIC of hydro-alcoholics extracts of *Calendula officinalis* L. flowers and *Mimosae tenuiflorae* bark.

Plant	Extract	Minimal Inhibitory Concentration (µL/mL)			
		Staphylococcus aureus	***Bacillus subtilis***	***Pseudomonas aeruginosa***	***Candida albicans***
Mimosa tenuiflora	**Hydro-alcoholic**	125	125	125	10
Calendula officinalis	**Hydro-alcoholic**	125	125	125	80

The hydro-alcoholic extracts of *C. officinalis* L. flowers and *M. tenuiflora* bark showed a bacteriostatic effect against *S. aureus, B. subtilis,* and *P. aeruginosa*. The bacteriostatic effect against Gram-positive and Gram-negative bacteria, at the same concentration, suggests that the chemical composition of the extracts and its mechanism of action had a bacteriostatic effect that was independent of the chemistry of the cell wall of the microorganisms, which in other study has been reported to be an essential factor in the mechanism of inhibition [44].

Moreover, both extracts had a fungistatic effect against *C. albicans* to minor concentration. These results suggest that the bacterias *S. aureus, B. subtilis and P. aeruginosa* were more resistant to the action of hydro-alcoholic extract of *C. officinalis* L. flowers and *M. tenuiflora* than the fungi *C. albicans*.

Previous study **[**52**]** reported the antimicrobial activity of chloroform, petroleum ether, ethanol and water extracts from *C. officinalis* leaves against *S. aureus, B. subtilis, E. coli, Klebsiella pneumonia, C. albicans and Aspergillus niger* using agar-well diffusion method. The ethanol, chloroform, and water extracts showed antimicrobial activity against Gram-positive and Gram-negative microorganisms but did not present activity against fungi *C. albicans* and *A. niger*. While that petroleum ether extract only showed activity against *S. aureus* and *Klebsiella pneumonia*. Preliminary phytochemical screening of the extracts indicated the presence of alkaloids, carbohydrates, flavonoids, terpenoids, sterols, and tannins **[**52**].**

Other authors [53] have researched the antimicrobial activity of aqueous-methanolic leaf and flower extracts from *C. officinalis* using the modified cellulosic disc method. In this study, aqueous-methanolic leaf extract was more effective against *E. coli* and *S. aureus* than aqueous-methanolic flower extract having strong activity against *Salmonella typhimurium* at lower quantities (27-54 μg). Both extracts showed activity against the fungi *C. albicans* and *Aspergillus niger*. The phenolic compounds and flavonoids founded in the extracts of *C. officinalis* could be responsible for its antimicrobial activity against all microorganisms tested [53].

Studies of antimicrobial activity in methanol and ethanol extracts from *C. officinalis* petals using disc diffusion method had carried out [54]. The results showed that the methanol extract had higher inhibition against *B. subtilis*, *P. aeruginosa*, *Bacillus cereus*, *E. coli*, *Klebsiella aerogenes*, *Bacillus pumilis* and *Klebsiella pneumoniae* than the ethanol extract. However, against *S. aureus* and *Enterococcus faecalis*, the ethanol extract had better activity than methanol extract. Both methanol and ethanol extract of *C. officinalis* petals showed antifungal activity against *C. albicans* and *Aspergillus niger*, the results were comparable with fluconazole, a standard drug [54].

The antimicrobial activity showed by the commercial hydro-alcoholic extract of *C. officinalis* flowers, may be attributed in part to the presence of some volatile compounds researched in previous studies [55]. Between those compounds are eucalyptol, 4-terpineol, bornyl acetate, 2-methoxy-3-methylhydroquinone, which have shown antibacterial and antifungal activity [56, 57, 58, 59, 60].

In a previous study with an ethanolic extract from the bark of *M. tenuiflora* [61] was observed antibacterial activity against *S. aureus*, *E. coli*, *P. aeruginosa*, and antifungal activity against *C. albicans*. Interestingly the authors found that Gram-positive bacteria were more sensitive (MIC 10 μg/mL) to the extract in comparison with Gram-negative bacteria (MIC 20-40 μg/mL); however, major concentrations of the extract was required to produce antifungal activity (MIC 70 μg/mL). While in the present study, the same concentration of the hydro-alcoholic extract was sufficient to exert antibacterial effects in both Gram-positive and Gram-negative bacteria (**Table 2.2**) and a low concentration was required to produce antifungal activity against *C. albicans*.

Another study [62] with ethanolic extract reported antibacterial activity against *B. subtilis* and *E. coli*, and antifungal activity against *Penicillium oxalicum*; these authors also observed a tendency of Gram-positive bacteria to be more sensitive to the ethanolic extract. This study also showed that a higher concentration of the extract was required to exert antibacterial activity against Gram-negative bacteria in comparison with the concentration necessary to exert antifungal activity against *Penicillium oxalicum*, behaviour similar observed in the present study.

Other researches that have been carried out with an ethanolic extract from *M. tenuiflora* using a broth microdilution method [63] or agar diffusion method [64] were demonstrated the antibacterial activity of this extract against *S. aureus, E. coli* and *P. aeruginosa.* Nevertheless, the antibacterial activity of hydro-alcoholic extracts from *M. tenuiflora* bark against pathogenic microorganisms has not been investigated until now.

A previous study has been carried out about the content of the volatile compounds in the hydro-alcoholic extract of *M. tenuiflora* bark [55]. In this study was identified the presence of eucalyptol, 4-terpineol, 2-Methoxyphenol, camphor, resorcinol, 2-(5 acetyl-2furyl)-1,4 naphthoquinone; these volatile compounds are known to have a demonstrable antimicrobial activity which has been corroborated by other studies (65, 66, 67, 68, 69, 70). Therefore, the antimicrobial activity shown by the hydro-alcoholic extract may be attributed at least in part to the presence of these compounds.

Azadirachta indica A. Juss oil

The results of the MIC test (**Table 2.3**) suggested that the oil exerted lowest antimicrobial effect which was indicated through displaying the high value of MIC in all tested microorganisms, only *Candida albicans* showed at least value of MIC.

Table 2.3. MIC of oil from *Azadirachta indica* A. Juss seeds.

Minimal Inhibitory Concentration (µL/mL)			
Staphylococcus aureus	***Bacillus subtilis***	***Pseudomonas aeruginosa***	***Candida albicans***
500	250	500	125

The oil from *A. indica* seeds showed a bacteriostatic effect against *S. aureus*, *B. subtilis* and *P. aeruginosa*. The bacteriostatic effect against Gram-positive and Gram-negative bacteria, at the same concentration, suggests that the chemical composition of the oil and its mechanism of action are responsible for this effect, which was independent of the chemistry of the cell wall of the microorganisms. On the other hand, the oil exerted a fungicide effect against *C. albicans*, since its growth was not observed in the petri dishes. These results suggest that the oil of this plant may produce a fungicide effect at a less concentration in comparison with the levels that are necessary to cause bacteriostatic effect against the microorganisms tested.

The behaviour fungicide of the oil obtained in the present study may be associated with the kind of compounds present. Among the compounds identified previously by GC/MS is the γ-sitosterol which has shown antifungal activity against some *Candida* strains such as *albicans*, *virusei* and *tropicalis* [71, 72]; the mechanism that this kind of compounds uses for this effect is interfering or disintegrating the cell wall or spore wall of the pathogenic fungus leading to the arrest of the germination or growth. By the other hand, the activity of the oil against bacterias may be linked to the presence of compounds such as squalene [73], octadecanoic acid **[**74**],** and fatty acid ethyl esters (ethyl palmitate, ethyl-9,12-octadecadienoate, ethyl cis-9-octadecenoate) compounds identified previously by GC/MS and some of these with activity previously showed in other studies. In the most of these studies, it had observed that the unsaturated fatty acids have more antimicrobial activity than the saturated fatty acids [75, 76].

There are few previous studies on the antimicrobial activity of oil from *Azadirachta indica* seeds. In one of these [77], the oil was obtained using CO_2 supercritical fluid extraction and this showed activity against *S. aureus, E. coli* and *Salmonella enteritidis,* in the broth microdilution essay. Among these microorganisms, *Escherichia coli* had the least value of MIC (1.25 mg/mL), which indicates that was more susceptible to the oil. In another study [78], the oil was obtained by extraction with petroleum ether and showed the effect against *Staphylococcus aureus, Salmonella typhi, E. coli,* and *P. aeuruginosa* to different dilutions (1:32, 1:16, 1:32 and 1:8 respectively). In this case, the MIC was determined using broth dilution method and the bacterial susceptibility by agar diffusion method. Other authors [79] analyzed a commercial oil of this plant by broth macrodilution test and reported the bactericidal effect against *S. aureus, E. coli*, and *P. aeuruginosa* at a concentration of 500 μL/mL (CMI), but among these microorganisms, *S. aureus* was more susceptible. Finally, another study [80] reported that the oil obtained by soxhlet method using hexane as solvent had activity against *E. coli,* and *S. aureus*. In in the GC/MS profile of this oil were majority compounds the unsaturated fatty acids linoleic acid and oleic acid. The different antimicrobial activity of the oil obtained in the present study compared with other researchers may attribute mainly to the origin and growth conditions of the plant and the extraction method used, as well as solvent employed.

2.3.2 MTT assay

Essential oil, ethanolic and aqueous extracts of *Ocimum micranthum* Willd leaves

The results of the MTT test suggest that the essential oil (EOA) produced a significant ($p < 0.05$) antiproliferative effect at concentrations over 0.06% on the CHO-K1 cell line with relative cell proliferation percentage values from 69.78% to 87.38% (**Figure 2.1**), while its effect on the fibroblast cell line did not significant ($p > 0.05$) in comparison with the control.

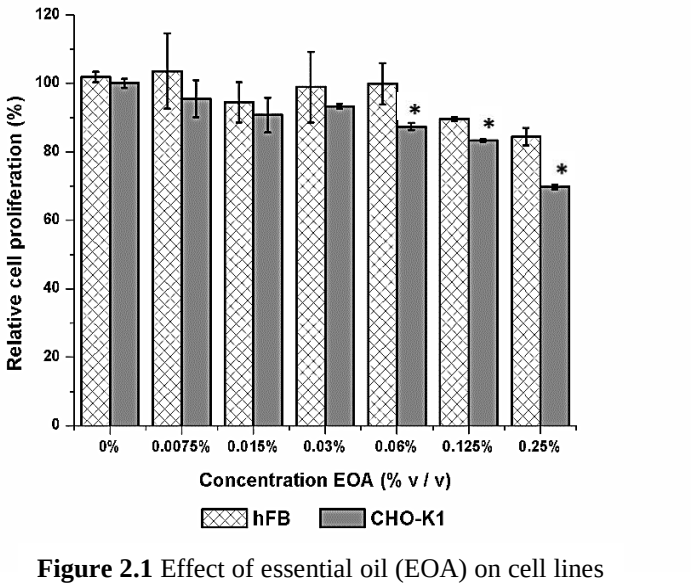

Figure 2.1 Effect of essential oil (EOA) on cell lines CHO-K1 and hFB by the MTT test. Error bars represent standard deviation and * represent statistically significant difference.

The aqueous extract of *O. micranthum* (AAE) caused a decrease in the cell proliferation in both cell lines assessed (**Figure 2.2**). At concentrations of 4% and 8%, the human fibroblast cell line displayed relative cell proliferation percentage values of 73.56% and 46.93% respectively. The same effect was observed in the CHO-K1 cell line, but at a concentration of 8% with a relative cell proliferation percentage value of 50.82%.

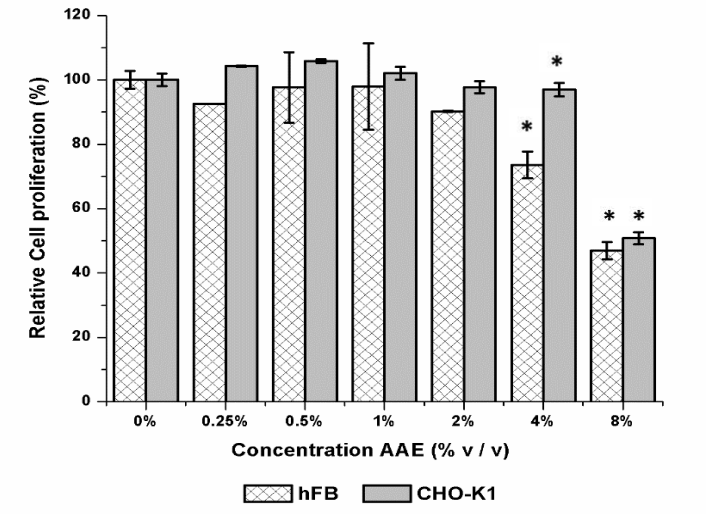

Figure 2.2 Effect of aqueous extract (AAE) on cell lines CHO-K1 and hFB by the MTT test. Error bars represent standard deviation and ***** represent statistically significant difference.

The ethanolic extract from *O. micranthum* (EAE) caused a decrement of cell proliferation in both cell lines at low concentrations (**Figure 2.3**). In the case of the human fibroblast cell line, this decrease was observed at concentrations of 0.06%, 0.125% and 0.25% with relative cell proliferation percentage values of 80.82%, 82.35%, and 77.80%, respectively. The CHO-K1 cell line displayed this effect at the same concentrations of extract, but with values of 77.12%, 80.08%, and 57.12% respectively.

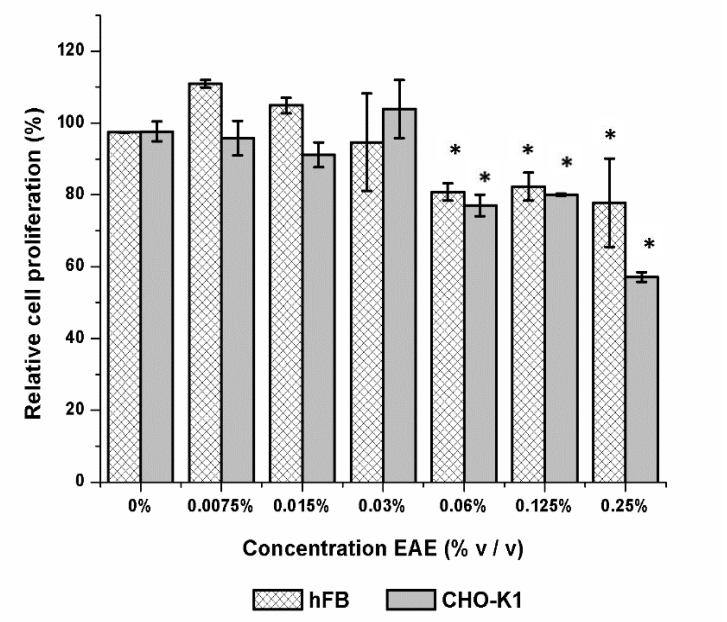

Figure 2.3 Effect of ethanolic extract (EAE) on cell lines CHO-K1 and hFB by the MTT test. Error bars represent standard deviation and ***** represent statistically significant difference.

When the values of relative cell proliferation percentage were compared between the essential oil, aqueous and ethanolic extracts of *O. micranthum* Willd, the aqueous extract demonstrated a significant ($p < 0.05$) antiproliferative effect on both cell lines at higher concentrations (at 4% on human fibroblast cell line and at 8% on the CHO-K1 cell line) than the other extracts; while the ethanolic extract displayed the same effect at lower concentrations (above 0.06% v/v) in both cell lines.

The behavior of the ethanolic extract in the MTT assay can be predicted from the MIC test where a fungistatic effect on *C. albicans* at a low concentration (5 µL/mL) was observed; this fungus is a microorganism of eukaryote origin as the cell lines that were used in MTT assay. This behavior may be associated with the chemical nature of the extract, specifically a possible synergic effect of its compounds, because this extract has a lower percentage of eugenol, a phenolic compound with high antimicrobial activity and anti-proliferative activity in cancer cells. Eugenol has been shown to be a molecule capable of exerting an antiproliferative effect on diverse cancer cells [81], however, it does not seem to be the determinant compound in the antiproliferative behavior of *O. micranthum* extracts, from the aqueous extract exerted this effect at higher concentrations, despite containing a higher content of eugenol than the essential oil and the ethanolic extract [12].

Hydro-alcoholic extracts of *Calendula officinalis* L. flowers and *Mimosa tenuiflora* bark.

The results of the MTT test suggested that the hydro-alcoholic extract of *C. officinalis* (HAECa) exerts a significant ($p<0.05$) proliferative effect on CHOK-1 cell line using all concentrations (from 0.25% to 8%) with relative cell proliferation percentage values of 155.61%, 152.2%, 161.72%, 161.41%, 180.25% and 152.66% respectively (**Figure 2.4**). Whereas that on hFB cell line did not observe a significant effect ($p > 0.05$) when was used the concentrations from 0.5% to 8% v/v.

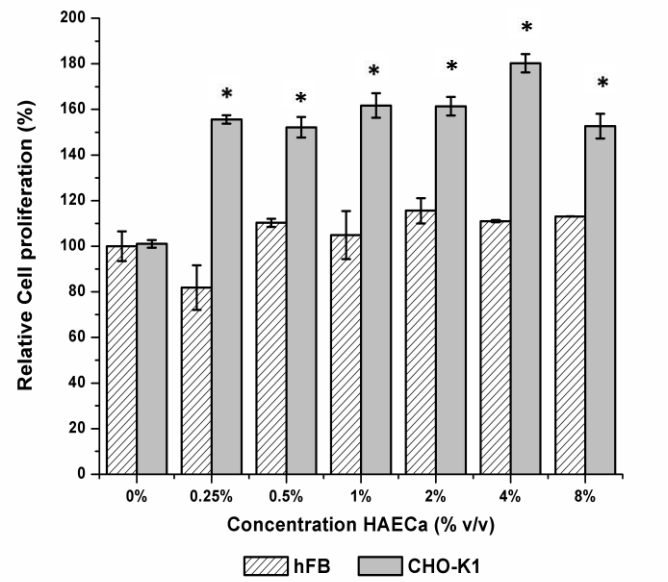

Figure 2.4 Effect of hydro-alcoholic extract of *Calendula* (HAECa) on cell lines CHO-K1 and hFB by the MTT test. Error bars represent standard deviation and ***** represent statistically significant difference.

The results of the MTT assay showed that hydro-alcoholic extract from *M. tenuiflora* bark (HAEMT) caused slight proliferative effect and antiproliferative effect on hFB cell line (**Figure 2.5**). The slight proliferative effect was observed at concentrations of 0.015%, 0.03% and 0.06% with relative cell proliferation percentage values of 102.67%, 103.68%, and 105.74%, respectively. The antiproliferative effect was observed at extract concentrations of 0.25% and 0.5% v/v with relative cell proliferation percentage values of 79.31% and 67.53%, respectively.

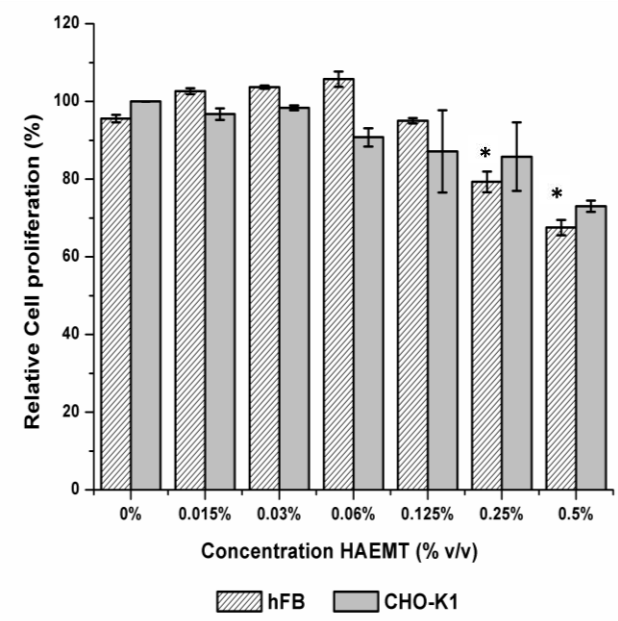

Figure 2.5 Effect of hydro-alcoholic extract of *Mimosa tenuiflora* (HAEMT) on cell lines CHO-K1 and hFB by the MTT test. Error bars represent standard deviation and * represent statistically significant difference

In contrast with the results of MTT assay, the visual observation with an inverted microscope showed low cell density of hFB at all concentrations of this extract tested in comparison with the untreated cells (control). In the concentration of 0.5% was observed cell lysis with the presence of cell debris (**Figure 2.6).**

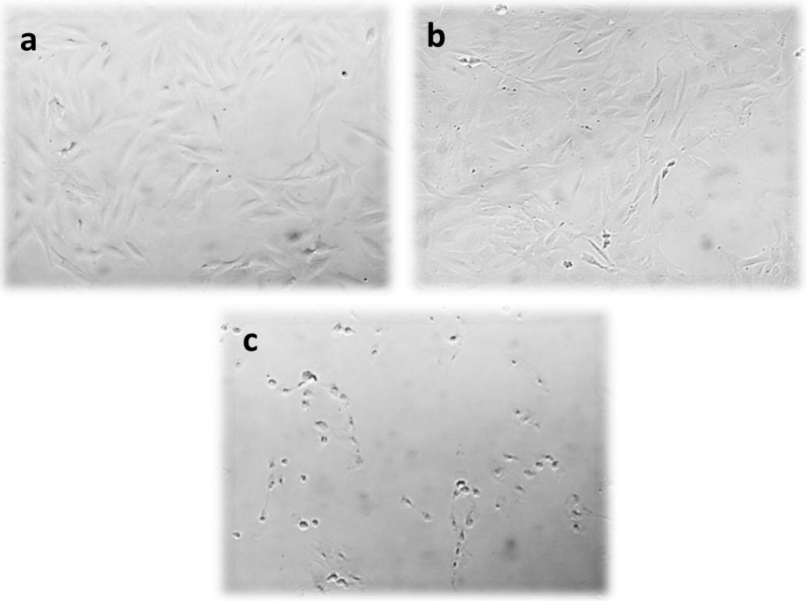

Figure 2.6: Effect of the hydro-alcoholic extract of *Mimosa tenuiflora* bark (HAEMT) on hFB cell line. **(a)** hFB Cell line control **(b)** HAEMT 0.015% **(c)** HAEMT 0.50%. Magnification 10x.

The hydro-alcoholic extract (HAEMT) produced a significant ($P<0.05$) antiproliferative effect on the CHOK-1 cell line at extract concentrations of 0.25% and 0.5% v/v with relative cell proliferation percentage values of 85.80% and 73.04%, respectively**.** These effects were confirmed visually (**Figure 2.7**.).

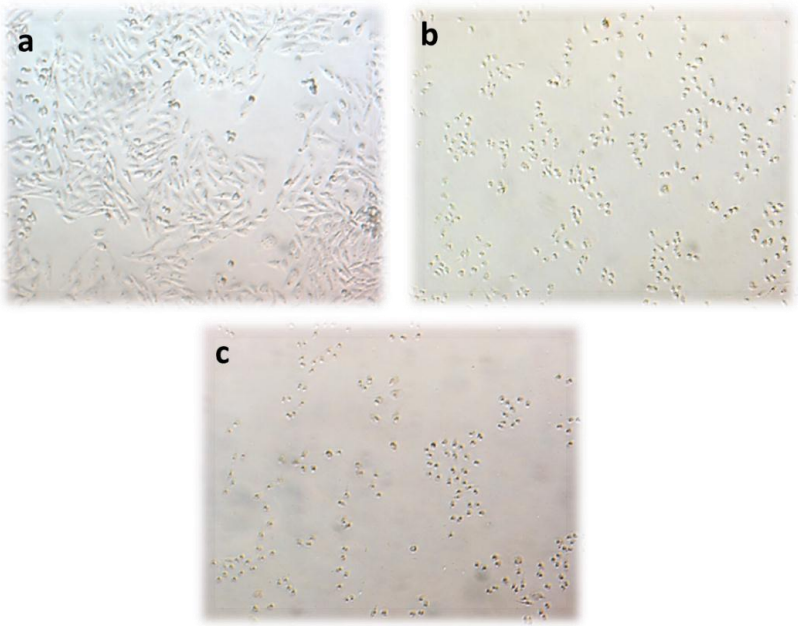

Figure 2.7: Effect of the hydro-alcoholic extract of *Mimosa tenuiflora* bark (HAEMT) on CHO-K1 cell line. **(a)** CHO-K1 cell line control **(b)** HAEMT 0.25% **(c)** HAEMT 0.50%. Magnification 10x.

The behaviour of the hydro-alcoholic extract from *C. officinalis* and *M. tenuiflora* observed in the MTT assay was similar to the MIC test, where high antifungal activity was observed at a low concentration of the extracts (80 and 10 μL/mL, respectively). These results suggest that these extracts have a higher selectivity and effect on eukaryote cells than on prokaryote cells, such as the microorganisms, which were affected using a higher concentration of the extracts.

Some authors [82, 83, 84] have been observed, that the effect of the extracts and/or isolated compounds from *C. officinalis* and *M.tenuiflora* on cell growth during *in vitro* cell proliferation, depended on the type of cell line used; also proposed that may exist a synergic effect between the extract and/or isolated compounds from this plant and other ingredients used in treatments employed in the test of cell growth or cell inhibition.

By the other hand, authors observed that the presence of alkaloids might cause cell growth or cell inhibition; therefore the cell behaviour depends on the presence of alkaloid and the cell line

used [85, 86]. In this sense, a study about volatile compounds in hydro-alcoholic extracts from *M. tenuiflora* identified the presence of the alkaloid N-N dimethyltryptamine using Gas chromatography–mass spectrometry (GC/MS) [55], a compound that may be associated with the effect observed on the hFB and CHO-K1 cells lines in the present study.

***Azadirachta indica A.* Juss oil**

In the MTT assay, the oil from *A. indica* (Neem) seeds exerted a significant ($P<0.05$) anti-proliferative effect on hFB cell line at concentrations of 0.03%, 0.06%, 0.125%, and 0.25% with relative cell proliferation percentage values of 89.47%, 86.27%, 81.62%, and 69.46% respectively (**Figure 2.8**). While, that this same effect was observed in the CHO-K1 cell line at concentrations of 0.06%, 0.125% and 0.25% with values of relative cell proliferation of 90.03%, 88.30% and 69.27 respectively. These results suggest that hFB cell line was more susceptible to the oil.

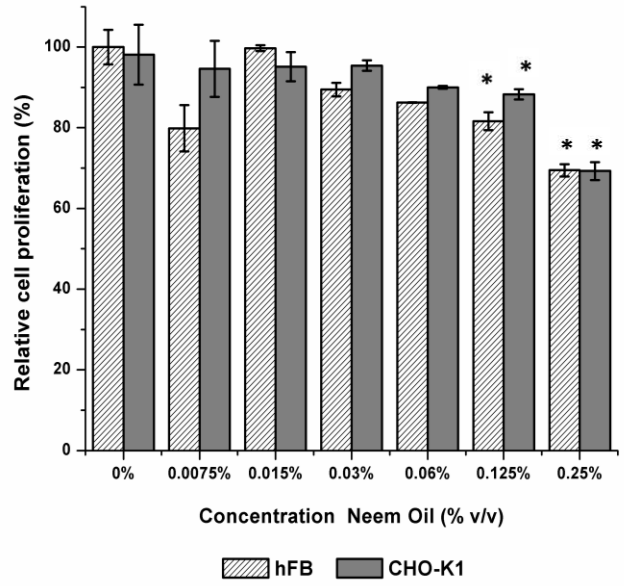

Figure 2.8 Effect of Neem oil on CHO-K1 and hFB cell lines by the MTT test. Error bars represent standard deviation and * represent statistically significant difference.

The MTT assay results at 0.25% coincided with the cell density observed in the inverted microscope during the test, where the anti-proliferative effect was confirmed visually (**Figure 2.9 and Figure 2.10**).

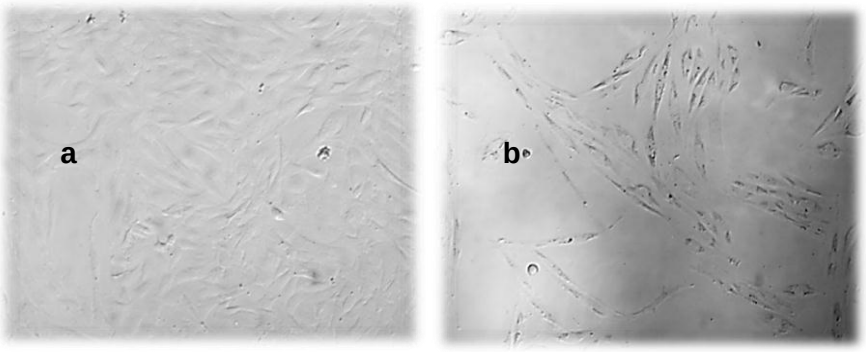

Figure 2.9 Effect of oil from *Azadirachta indica* A. Juss (Neem) on hFB Cell line control. **(a)** hFB Cell line control (**b)** Neem oil 0.25%. Magnification 10x.

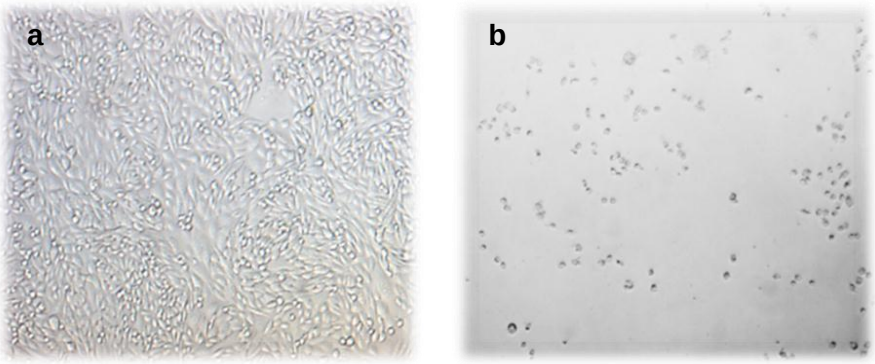

Figure 2.10 Effect of oil from *Azadirachta indica* A. Juss (Neem) on CHO-K1 Cell line control. **(a)** CHO-K1 Cell line control (**b)** Neem oil 0.25%. Magnification 10x.

The antiproliferative effect of extracts from *A. indica* leaves on diverse cell lines mainly malignant was observed in other studies [87, 88], that which has been attributed to the presence of the limonoids such as azadirachtin, and nimbolide [89].

2.3.3 Trypan Blue assay

Essential oil, ethanolic and aqueous extracts of *Ocimum micranthum* Willd leaves

The effect of the extracts on hFB cell line was also evaluated using Trypan Blue assay. This technique permits the direct count of viable cells through the staining of the cells and microscopic observation. The results of this assay showed a notable difference concerning the MTT test. For example, the essential oil in the Trypan blue test (**Figure 2.11**) showed a relative cell proliferation less than 80% at all concentrations evaluated, in contrast to the results obtained in the MTT test, where the cell line presented values higher than 80% at all concentrations assayed. In the trypan blue test, all concentrations suggested a significant difference with a notable effect starting from a concentration of 0.0075%.

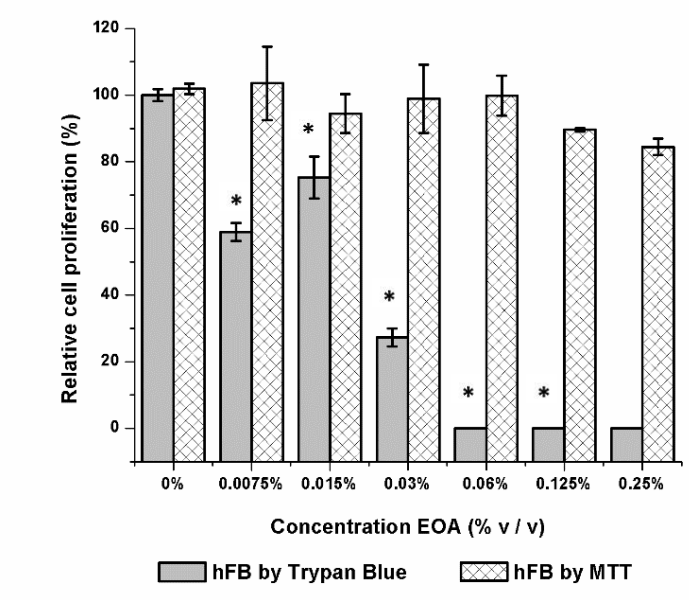

Figure 2.11 Comparative of relative cell proliferation percentage of hFB cell line in essential oil (EOA) by MTT and Trypan blue test. Error bars represent standard deviation * represent statistically significant difference.

The relative cell proliferation percentage values of the aqueous extract (**Figure 2.12**) showed a proliferative effect at concentrations of 0.25% and 0.50% v/v in the Trypan blue test, although the MTT test did not show a significant difference compared to the control. However, in these tests, there was a tendency of the relative cell proliferation percentage to decrease, starting at a concentration of 2% v/v of the extract. The decrease of the relative cell proliferation percentage values in the trypan blue assay was higher than in the MTT test.

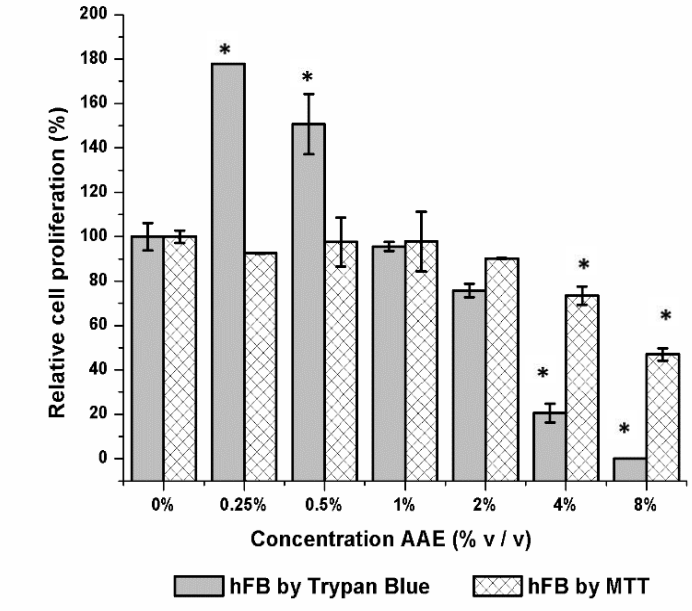

Figure 2.12 Comparative of relative cell proliferation percentage of hFB cell line in aqueous extract (AAE) by MTT and Trypan blue test. Error bars represent standard deviation and * represent statistically significant difference.

The values of relative cell proliferation percentage of the ethanolic extract at low concentrations (**Figure 2.13**) showed similar behaviour in both tests (Trypan blue and MTT). A slight significant ($p<0.05$) proliferative effect concerning the control was observed in the Trypan Blue and MTT tests at concentrations of 0.0075% and 0.015% v/v. However, in the Trypan Blue assay, the proliferative effect remained at a concentration of 0.06% v/v, while in MTT test a decrease in cell proliferation was observed from this concentration. Finally, when extract concentrations of 0.125% and 0.25% v/v were tested using the trypan blue assay, relative cell proliferation percentage values of 58.71% and 12.26% respectively were obtained, while in the MTT test the values of relative cell proliferation percentage were 82.35% and 77.80%, respectively.

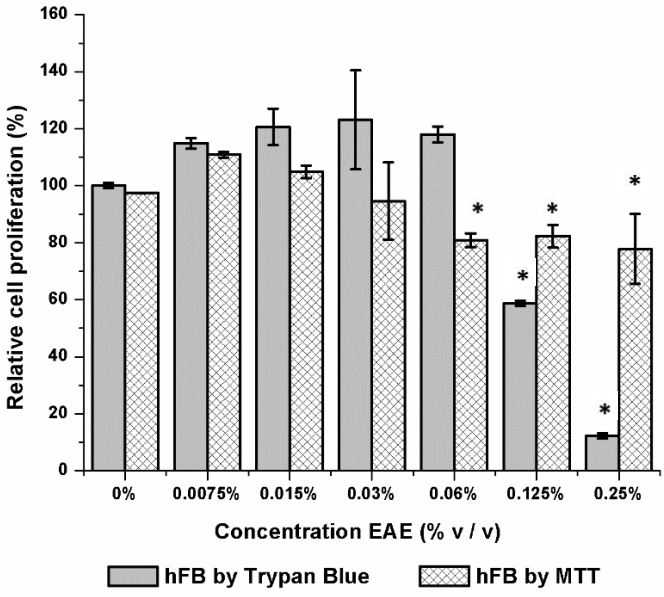

Figure 2.13 Comparative of relative cell proliferation percentage of hFB cell line in ethanolic extract (EAE) by MTT and Trypan blue test. Error bars represent standard deviation and * represent statistically significant difference.

All results o the Trypan blue assay were coherent with the visual observations made under the inver cope, while this did not occur with the results of the MTT test. Also, through visual inspection, the cytotoxic effect of the extracts on hFB cells was observed.

In general, in the MTT assay, the antiproliferative effect on the hFB cell line was underestimated when high concentrations of the extracts from *O. micranthum* Willd were tested. The results also suggest that the measurement of the antiproliferative or proliferative effects of the phytochemicals contained in the extracts may vary between a colorimetric method (MTT assay) and a method that involves the direct counting of viable cells such as the Trypan blue assay. This difference is probably associated with the interaction of diverse chemical components in the

extracts (such as the phenolic compounds) with the MTT reagent [90]; it is possible that these types of compounds may interfere with critical formazan formation in the MTT method.

In a previous study [91], it was observed that natural compounds with intrinsic reductive potential such as some flavonoids, phytoestrogens and ascorbic acid might lead to false positives in the MTT assay, due to a mechanism of non-enzymatic reduction of the MTT to formazan. Other authors have reported that changes in the metabolism of the cells may induce an increase in the reduction of the MTT to formazan, which has been observed as an increase in the coloration of the reaction, hence in the values of absorbance [92].

In the comparison of the three extracts, it was observed that the underestimation of the antiproliferative effect was most notable in the essential oil, which may be related to a synergic effect of some volatile compounds with antioxidant characteristics present in the extract such as eugenol, methyl-eugenol and other compounds including isoborneol, eucalyptol, spathulenol, a profile of volatile compounds that have been previously identified [12]. The isolation of the active compounds from these extracts, as well as *in vivo* studies are necessary, and that can improve understanding of the mechanisms underlying these bioactivities.

Hydro-alcoholic extracts of *Calendula officinalis* L. flowers and *Mimosa tenuiflora* bark

The effect of the hydro-alcoholic extract of *C. officinalis* on hFB cell line was also evaluated using Trypan Blue assay. The results of this assay showed an evident difference with respect to the MTT test, because was obtained a relative cell proliferation less of the 100% at all concentrations evaluated, in contrast to the results obtained in the MTT test where the cell line presented values higher than 100% when concentrations from 0.50% to 8% was assayed (**Figure 2.14**). Trypan blue test suggested a notable antiproliferative effect of the hydro-alcoholic extract of *C. officinalis* on hFB cell line.

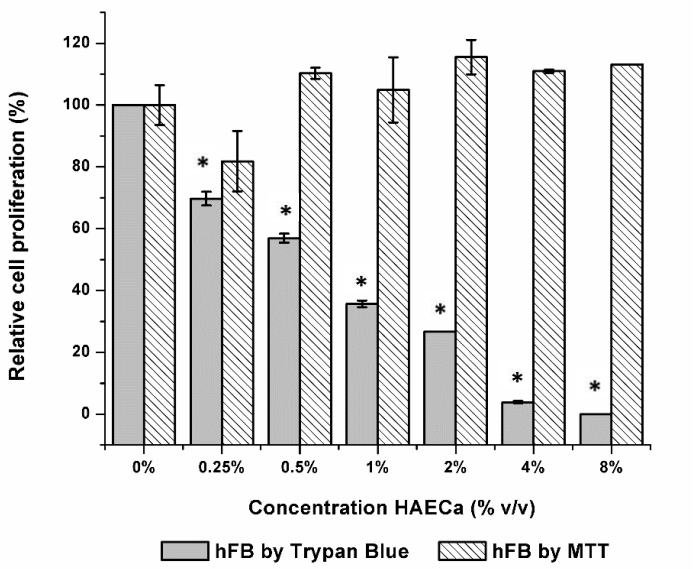

Figure 2.14 Comparative of relative cell proliferation percentage of hFB cell line in hydro-alcoholic extract of *Calendula officinalis* (HAECa) by MTT and Trypan blue test. Error bars represent standard deviation and * represent statistically significant difference.

The values of relative cell proliferation percentage values indicated a notable antiproliferative effect when extract concentrations from 0.125% to 0.50% v/v of the hydro-alcoholic extract of *Mimosa tenuiflora* were applied on hFB cell line (**Figure 2.15**). In general, the values of relative cell proliferation percentage obtained for all concentrations of this extract were contrasted with the values obtained by MTT test; the rate of diminution of these values in trypan blue assay was higher than the MTT test. In general, the MTT assay underestimated the antiproliferative effect of the hydro-alcoholic extract of *Mimosa tenuiflora* bark on the hFB cell line.

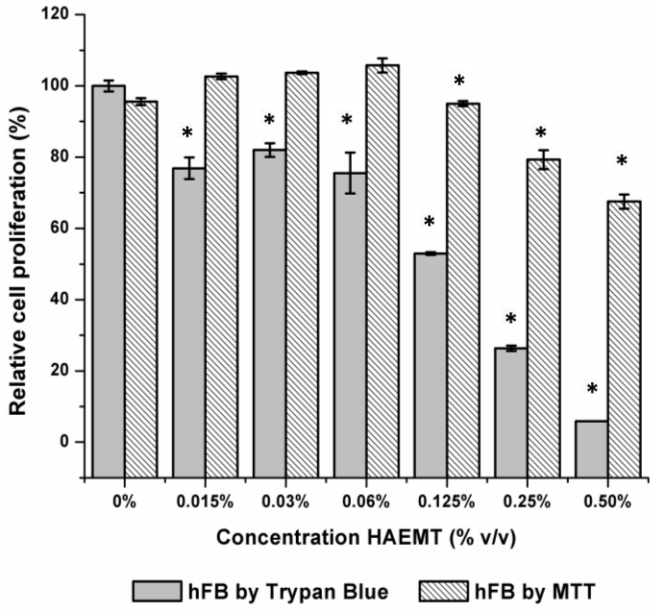

Figure 2.15 Comparative of relative cell proliferation percentage of hFB cell line in hydro-alcoholic extract of *Mimosa tenuiflora* (HAEMT) by MTT and Trypan blue test. Error bars represent standard deviation * represent statistically significant difference.

In general, the MTT assay underestimated the antiproliferative effect of the hydro-alcoholic extract of *M. tenuiflora* bark on the hFB cell line. Some authors have been indicated this underestimated may be attributed to interactions between some chemical components of the extracts (such as the phenolic compounds) with the MTT reagent which can produce an increase in the conversion to formazan, a critical compound in this colorimetric method [90]. The above has been supported by other studies where were observed that natural compounds with intrinsic reductive potential might lead to false positives in the MTT assay, through the mechanism of non-enzymatic reduction of MTT to formazan [91]. While, others authors have reported that changes in the metabolism of the cells may induce an increase in the reduction of MTT to formazan, which was observed as an increase in the coloration of the reaction, and hence contributes to the values of absorbance [92].

2.4 Conclusions

These assays showed that low concentrations of essential oil and extracts of *O. micranthum* leaves are sufficient to cause an antiproliferative effect on the hFB cell line, but do not produce an antimicrobial effect against the microorganisms evaluated in this study, whereby neither of the extracts demonstrated both bioactivities at the same time. However, the ethanolic extract showed potential as a fungistatic agent at low concentrations.

With respect to commercial fluid hydro-alcoholic extracts from *Calendula officinalis* flowers and *Mimosa tenuiflora* bark, the results of the study showed that low concentrations are sufficient to exert an antiproliferative effect on the hFB cell line and a fungistatic effect against *Candida albicans*, but no to produce a bacteriostatic effect against *Staphylococcus aureus, Bacillus subtilis, Pseudomonas aeruginosa*, which suggest that eukaryote cells are most sensitive to these extracts than the prokaryote cells.

These results have also indicated the importance of conducting studies on the effects of natural extracts that are used in traditional herbal medicine as well as in the formulations of products topical use such as creams, ointments, gels, and soaps, through *in vitro* tests using healthy cell lines. More studies are necessary to improve understanding of the mechanism of action of the compounds implicated in the bioactivities shown by the crude extracts.

2.5 References

1. González-Elizondo M, López-Enríquez L, González-Elizondo S, Tena-Flores J. Plantas Medicinales del Estado de Durango y Zonas Aledañas. Centro Interdisciplinario de Investigación para el Desarrollo Integral Regional (CIIDIR) Unidad Durango. Instituto Politécnico Nacional. México, D.F. 2004.p. 12–13.
2. Sánchez-Medina A, García-Sosa K, May-Pat F, Peña-Rodríguez LM. Evaluation of biological activity of crude extracts from plants used in Yucatecan Traditional Medicine. Part1. Antioxidant, antimicrobial and ß-glucosidase inhibition activities. Phytomedicine. 2001; 8: 144–151.
3. De Pinho JPM, Silva ASB, Pinheiro BG, Sombra I, De Carvalho-Bayma J, Lauhlou S. et al. Antinociceptive and antispasmodic effects of the essential oil of *Ocimum micranthum*: Potential anti-inflammatory properties. Planta Med. 2012; 78: 681-685.
4. Priyanka M, Patidar A, Gupta A, Agrawal S. Treatment of acne with herbal remedy *Calendula officinalis*: An overview. Int J Pharm Biol Arch. 2011; 2(4): 1020–1023.
5. Zippel J, Deters A, Hensel A. Arabinogalactans from *Mimosa tenuiflora* (Willd) Poiret bark as active principles for wound-healing properties: Specific enhancement of dermal fibroblast activity and minor influence on HaCaT keratinocytes. J. Ethnopharmacol. 2009; 124: 391–396.
6. Singh A, Singh AK, Narayan G, Singh TB, Shukla VK. Effect of Neem oil and *Haridra* on non-healing wounds. Effect of *Neem* oil and *Haridra* on non-healing wounds. Ayu. 2014; 35(4): 398–403.

7. Agyare C, Dwobeng AS, Agyepong N, Boakye YD, Mensah KB, Patrick George Ayande PG, Adarkwa-Yiadom M. Antimicrobial, Antioxidant, and Wound Healing Properties of *Kigelia africana* (Lam.) Beneth. and *Strophanthus hispidus* DC. Adv Pharmacol Sci. 2013;692613.

8. Lino CS, Gomes PB, Lucetti DL, Diógenes JPL, Sousa FCF, Silva MGV, et al. Evaluation of Antinociceptive and antiinflammatory activities of the essential oil (EO) of *Ocimum micranthum* Willd from Northeastern Brazil. Phytother Res. 2005; 19: 708-712.

9. Villaseñor JL, Espinosa FJ. Catálogo de malezas de México. Universidad Nacional Autónoma de México. Consejo Nacional Consultivo Fitosanitario. Fondo de Cultura Económica. México, D. F. 1998. p.449.

10. Jaramillo BE, Duarte E, Delgado W. Bioactividad del aceite esencial de *Ocimum micranthum* Willd recolectado en el departamento de Bolívar, Colombia. Rev Cubana Plant Med. 2014; 19(2): 185-196.

11. Silva MGV, Craveiro AA, Matos FJA, Machado MIL, Alencar JW, Aurelio FKF. Essential Oils from Leaves and Inflorescences of *Ocimum micranthum* Willd from Northeastern Brazil. J. Essent Oil Res. 1998; 10: 77-78.

12. Caamal-Herrera IO, Muñoz-Rodríguez D, Madera-Santana T, Azamar-Barrios JA. Identification of volatile compounds in essential oil and extracts of *Ocimum micranthum* Willd leaves using GC/MS. Int J Appl Res Nat Prod.2016; 9(1): 31-40.

13. Ghosh R, Nadiminty N, Fitzpatrick JE, Alworth WL, Slaga TJ, Kumar AP. Eugenol causes melanoma growth suppression through inhibition of E2F1 transcriptional activity. J Biol Chem. 2005; 280: 5812-9.

14. Kalmes M, Blömeke B. Impact of Eugenol and Isoeugenol on AhR Translocation, Target Gene Expression and Proliferation in Human HaCaT Keratinocytes. J Toxicol Environ Health A.2012; 75: 478-491.

15. Shetty S, Udupa S, Udupa L. Evaluation of antioxidant and wound healing effects of alcoholic and aqueous extract of *Ocimum sanctum linn* in rats. Evid Based Complement Alternat Med (*e* Cam). 2008; 5(1): 95-101.

16. Orafidiya LO, Agbani EO, Abereoje OA, Awe T, Abudu A, Fakoya FA. An investigation into the wound-healing properties of essential oil of *Ocimum gratissimum linn*. J Wound Care. 2003; 12(9): 331-334.

17. Paschapur M, Patil MB, Kumar R, Patil SR. Evaluation of aqueous extract of leaves of *Ocimum kilimandscharicum* on wound healing activity in albino wistar. Int J PharmTech Res. 2009; 1(3): 544-550.

18. Chakraborthy GS. Antimicrobial activity of leaf extract of Calendula officinalis Linn. J Herb Med Toxicol. 2008; 2:65–66.
19. Dumenil G, Chemli R, Balasaurd G. Evaluation of antibacterial properties of *Calendula officinalis* flowers and mother homeopathic tincture of calendula. AnnPharm Fran. 1980; 38:493–499.
20. Domínguez-Marín L. Efecto de la aplicación del extracto hidroalcohólico de flores de caléndula (*Calendula officinalis*) en la estabilización del color y vida útil en pulpa de frutas. Universidad Nacional de Colombia. Maestría en Ciencia y Tecnología de Alimentos. Programa Interfacultades. Bogota, Colombia. 2012; 22–41.
21. Patrick KFM, Kumar S, Edwarson PAD, Hutchinson JJ. Induction of vascularization by an aqueous extract of the flowers of *Calendula officinalis* L. The European Marigold. *Phytomedicine*. 1996; 3(1): 11–18.
22. Priyanka M, Patidar A, Gupta A, Agrawal S. Treatment of acne with herbal remedy *Calendula officinalis*: An overview. *Int J Pharm Biol Arch*. 2011; 2(4): 1020–1023.
23. Camargo S. Descripción, distribución, anatomía, composición química y usos de *Mimosa tenuiflora* (*Fabaceae–Mimosoideae*) en México. Rev Biol Trop. 2000; 48: 939–954.
24. Camargo-Ricalde S, Grether R, Martínez-Bernal A. Uso medicinal del "tepescohuite", *Mimosa tenuiflora* (Leguminosae) en Mexico. Contacto. 1994; 5: 29–34.
25. Grether R. Nota sobre la identidad del tepescohuite en Mexico. Bol Soc Bot Méx. 1988. 48: 151–152
26. Rivera-Arce E, Chávez-Soto MA, Herrera-Arellano A, Arzate S, Agüero J, Feria-Romero I, et al. Therapeutic effectiveness of a *Mimosae tenuiflorae* cortex extract in venous leg ulceration treatment. *J Ethnopharmacol*. 2007; 109: 523–528.
27. Galeane MC, Martins CHG, Massuco J, Bauab TM, Sacramento LVS. Phytochemical screening of *Azadirachta indica* A. Juss for antimicrobial activity. African J Microbiol Res. 2017; 11 (4): 117-122.
28. Alzohairy MA. Therapeutics Role of *Azadirachta indica* (Neem) and Their Active Constituents in Diseases. Prevention and Treatment. J Evid Based Complementary Altern. 2016.
29. Singh N, Sastry MS. Antimicrobial activity of Neem oil. Indian J Pharmacol. 1997; 13: 102–106.
30. Raja Ratna RY, Krishna Kumari C, Lokanatha O, Mamatha S, Damodar RC. Antimicrobial activity of *Azadirachta Indica* (neem) leaf, bark, and seed. Int. J. Res. Phytochem Pharmacol. 2013; 3(1): 1-4.

31. Govindachari TR, Suresh G, Gopalakrishnan, G, Banumathy B, Masilamani S. Identification of antifungal compounds from the seed oil of Azadirachta indica. Phytoparasitica. 1998; 26 (2): 109–116.

32. Biswas K, Chattopadhyay J, Barnejee RK, Bandyopadhyay U. Biological activities and medicinal properties of Neem (*Azadirachta indica*). Curr. Sci. 2002; 82: 1336-1345.

33. Bwala DG, Elisha IL, Habu KA, Dogonyaro BB, Kaikabo AA. Management of surgical wounds using crude neem oil in one year old ram: A successful report. J. Vet. Med. Anim. Health. 2011; 3(6): 75-78

34. Charles DJ, Simon JE, Wood KV. Oil constituents of *Ocimum micranthum* Willd. J Agric Food Chem. 1990; 38: 120–122.

35. Rodríguez-Álvarez M, Alcaraz-Meléndez L, Real-Cosío SM. Procedimientos para la extracción de aceites esenciales en plantas aromáticas. Edit. Centro de Investigaciones Biológicas del Noroeste, S.C. La Paz, Baja California Sur, México. 2012; p.24-29

36. Joshi B, Sah GP, Basnet BB, Bhat MR, Sharma D, et al. Phytochemical extraction and antimicrobial properties of different medicinal plants: *Ocimum sanctum* (Tulsi), *Eugenia caryophyllata* (Clove), *Achyranthes bidentata* (Datiwan) and *Azadirachta indica* (Neem). J. Microbiol. Antimicrob. 2011; 3(1):1-7.

37. McFarland J. The Nephelometer: an instrument for estimating the number of bacteria in suspensions used for calculating the opsonic index and for vaccines. J Am Med Assoc. 1907; 14: 1176–8.

38. Eloff JN. A sensitive and quick microplate method to determine the minimal inhibitory concentration of plant extracts for bacteria. Planta Med. 1998; 64: 711–13.

39. Goswami M, Chaitra T, Chaudhary S, Manuja N, Sinha A. Strategies for periodontal ligament cell viability: An overview", J Conserv Dent. 2011; 14 (3): 215-220.

40. Sestili P, Cantoni O, Cattabeni F, Murray D. Evidence for separate mechanisms of cytotoxicity in mammalian cells treated with hydrogen peroxide in the absence or presence of L-histidine. Biochim Biophys Act. 1995; 1268(2): 130-136.

41. Mosmann T. Rapid colorimetric assay for cellular growth and survival: application to proliferation and cytotoxicity assays. J Immunol Methods.1983; 65: 55-63.

42. Sacchetti G, Medici A, Maletti S, Radice M, Muzzoli MV. Composition and functional properties of the essential oil of Amazonian Basil, *Ocimum micranthum* Willd Labiatae in comparison with commercial essential oils. J Agric Food Chem. 2004; 52: 3486–3491.

43. Adigüzel A, Güllüce M, Sengüil M, Ögütcü H, Sahin T, Karaman I. Antimicrobial effects of *Ocimum basilicum* (Labiatae) extract. Turk J Biol. 2005; 29: 155–160.

44. Oboh, G. Antioxidant and antimicrobial properties of ethanolic extracts of *Ocimum gratissimum* leaves. J Pharmacol Toxicol. 2010; 5: 396–402.

45. Joshi B, Sah GP, Basnet BB, Bhat MR, Sharma D, et al. Phytochemical extraction and antimicrobial properties of different medicinal plants: *Ocimum sanctum* (Tulsi), *Eugenia caryophyllata* (Clove), *Achyranthes bidentata* (Datiwan) and *Azadirachta indica* (Neem). J. Microbiol Antimicrob. 2011; 3(1):1-7.

46. Khalil A. Antimicrobial Activity of Ethanolic Extracts of *Ocimum basilicum* leaf from Saudi Arabia. Biotechnology. 2013; 12 (1): 61-74.

47. Vieira P, M de Morais S, Bezerra HQF, Travassos-Ferreira PA, Oliveira IR, Silva MGV. Chemical composition and antifungal activity of essential oils from *Ocimum* species. Ind. Crop. Prod. 2014; 55: 267–271.

48. Fontenelle RO, Morais SM, Brito EH, Brilhante RS, Cordeiro RA, Lima YC, et al. Alkylphenol activity against *Candida* spp. and *Microsporum canis*: a focus on the antifungal activity of thymol, eugenol and O-methyl derivatives. Molecules. 2011; 16: 6422–31.

49. Kalemba D, Kunicka A. Antibacterial and fungi properties of essential oils. Curr Med Chem. 2003; 10(10): 813-29.

50. Gutierrez J, Barry-Ryan C, Bourke P. Antimicrobial activity of plant essential oils using food model media: Efficacy, synergistic potential and interactions with food components Food Microbiol. 2009; 26: 142–50.

51. Rahman A, Shanta ZS, Rashid MA, Parvid T, Afrin S, Khatun MK et al. *In vitro* antibacterial properties of essential oil and organic extracts of *Premna integrifolia* Linn. Arabian J Chem.2011; doi:10.1016/j.arabjc.2011.06.003.

52. Chakraborthy GS. Antimicrobial activity of leaf extract of *Calendula officinalis* Linn. J Herb Med Toxicol. 2008; 2:65–66.

53. Rigane G, Ben Younes S, Ghazghazi H, Ben Salem R. Investigation into the biological activities and chemical composition of *Calendula officinalis* L. growing in Tunisia. Int Food Res J. 2013; 20(6): 3001-3007.

54. Efstratiou E, Hussain AI, Nigam PS, Moore JE, Ayub MA, Rao JR. Antimicrobial activity of *Calendula officinalis* petal extracts against fungi, as well as Gram-negative and Gram-positive clinical pathogens. Complement Ther Clin Pract. 2012; 18:173-176.

55. Caamal-Herrera IO, Muñoz-Rodríguez D, Madera-Santana T, Azamar-Barrios J.A. Identification of volatile compounds in hydro-alcoholic extracts of *Calendula officinalis* L. flowers and *Mimosae tenuiflorae* bark using GC/MS. 2016. IJARNP. Vol. 9 (1), pp. 20-30.

56. Pattnaik S, Subramanyam V.R, Bapaji M, Kole CR. Antibacterial and antifungal activity of aromatic constituents of essential oils. Microbios. 1997; 89: 39-46.

57. Carson CF, Riley TV. Antimicrobial activity of the major components of the essential oil of *Melaleuca alternifolia*. J Appl Bacterial. 1995; 78(3):264-269.

58. Wang P, Kong CH, Zhang CX. Chemical Composition and Antimicrobial Activity of the Essential Oil from *Ambrosia trifida* L. Molecules 2006; 11:549-555.

59. Pintore G, Chessa M, Usai M, Cerri R, Bradesi P, Casanova J, Juliano C, Boatto G, Tomi F. Chemical composition and antimicrobial activity of *Rosmarinus officinalis* L. oils from *Sardinia* and *Corsica*. Flavour Fragr. J. 2002; 17: 15–19.

60. Bone K, Mills S. Materia Medica. Principle and Practice of Phytotherapy. 2nd edition. Elsevier. 2012; pp. 394.

61. Lozoya X, Navarro V, Arnason JT, Kourany E. Experimental evaluation of *Mimosa tenuiflora* (Willd.) Poir. (Tepescohuite) I. screening of the antimicrobial properties of bark extracts. Arch Invest Med (Mex). 1989; 20 (1): 87-93.

62. Heinrich M, Kuhnta M, Wright CW, Rimpler H, Phillipson JD, Schandelmaier A, Warhurst DC. Parasitologica and microbiological evaluation of Mixe Indian medicinal plants (Mexico). J Ethnopharmacol. 1992; 36: 81-85.

63. Padilha IQM, Pereira AV, Rodrigues OG, Siqueira-Junior JP, Pereira MSV. Antimicrobial activity of *Mimosa tenuiflora* (Willd) Poir from Northeast Brazil against clinical isolates of Staphylococcus aureus. Braz J Pharmacog. 2010; 20 (1): 45-47.

64. Morais Leite SC, Soares Medeiros CLL, Gomes PC, Souto Maia G, Silva Magalhães MI, Freitas FOR, Freire Pessôa HL, Sousa Nogueira TBS, Batista de Morais AM, Medeiros Mazzaro VD, Passos Brustein V, Almeida Filho GG. Antibacterial and Hemolytic Activities of *Mimosa tenuiflora* (Willd) Poir. (Mimosoidea). Afr. J. Microbiol. Res. 2015; 9 (42): 2166-2177.

65. Carson CF, Riley TV. Antimicrobial activity of the major components of the essential oil of *Melaleuca alternifolia*. J Appl Bacteriol. 1995; 78 (3): 264-269.

66. Durairaj RB. Resorcinol Chemistry in Pharmaceuticals Applications. Resorcinol Chemistry, Technology and Applications", Springer-Verlag Berlin Heidelberg, New York, pp. 641, 2005.

67. Pattnaik S, Subramanyam VR, Bapaji M, Kole CR. Antibacterial and antifungal activity of aromatic constituents of essential oils. Microbios. 1997; 89:39-46.

68. Rodríguez-Flores C, Pennec A, Nugier-Chauvin C, Daniellou R, Herrera-Estrella L, Chauvina AL. Chemical Composition and Antibacterial Activity of Essential Oils Extracted from Plants Cultivated in Mexico. J Mex Chem Soc. 2014; 58 (4): 452-455.

69. Sanchez-Calvo JM, Macias M, Barbero GR, Rodriguez-Iglesias MA, Guerrero-Vasquez G, Molinillo MG, Duran AG, Macias F**.** Synthesis, antibacterial and antifungal activities of naphthoquinone derivatives: a structure–activity relationship study. Med Chem Res. 2016; 25: 1274–1285.

70. Yang JF, Yang CH, Liang MT, Gao ZJ, Wu YW, Chuang LY. Chemical Composition, Antioxidant, and Antibacterial Activity of Wood Vinegar from *Litchi* chinensis Molecules. 2016; 21:1150.

71. Venkata Raman B, Samuel L, Pardha Saradhi M, Narashimha Rao B, Naga Vamsi Krishna A, Sudhakar M, Radhakrishnan TM. Antibacterial, antioxidant activity and GC-MS analysis of *Eupatorium odoratum.* Asian J Pharm Clin Res. 2012; 5(2): 99-106.

72. Karthikeyan SC, Velmurugan S, Donio MBS, Michaelbabu M, Citarasu T. Studies on the antimicrobial potential and structural characterization of fatty acids extracted from Sydney rock oyster *Saccostrea glomerata*. Ann Clin Microbiol Antimicrob. 2014;13:332.

73. Gomathi D, Kalaiselvi M, Ravikumar G, Devaki K, Uma C. GC-MS analysis of bioactive compounds from the whole plant ethanolic extract of *Evolvulus alsinoides* (L.). J Food Sci Technol. 2015; 52(2):1212–1217.

74. Abubakar MN, Majinda RRT. GC-MS Analysis and Preliminary Antimicrobial Activity of *Albizia adianthifolia* (Schumach) and *Pterocarpus angolensis* (DC). *Medicines*. 2016; 3(1):3.

75. Choi JS, Park NH, Hwang SY, Sohn JH, Kwak I, Cho KK, Choi IS. The antibacterial activity of various saturated and unsaturated fatty acids against several oral pathogens. J Environ Biol. 2013; 34: 673-676.

76. Zheng CJ, Yoo JS, Lee TG, Cho HY, Kim YH, Kim WG. Fatty acid synthesis is a target for antibacterial activity of unsaturated fatty acids. FEBS Letters. 2005; 579:5157–5162.

77. Zhang YQ, Xu J, Yin ZQ, Jia RY, Lu Y, Yang F, Du YH, Zou P, Cheng LV, Hu TX, Liu SL, Shu G, Yi G. Isolation and identification of the antibacterial active compound from petroleum ether extract of neem oil. Fitoterapia. 2010; 81:747–750.

78. Jahan T, Begum ZA, Sultana S. Effect of neem oil on some pathogenic bacteria. Bangladesh J Pharmacol. 2007; 2: 71-72.

79. Divya J, Lakshmi J, Venkatraya Prabhu M, Gopalkrishna Bhat K. Antibacterial effect of neem (*Azadirachta indica*) oil on multidrug resistant bacteria isolated from human infections. Int J Biol Med Res. 2013; 4(4):3544-3546.

80. Sandanasamy JDO, Nour AH, Tajuddin SNB, Nour AH. Fatty Acid Composition and Antibacterial Activity of Neem (*Azadirachta indica*) Seed Oil Open Conf Proc J. 2013; 4 (2): 43-48.

81. Jaganathan SK, Supriyanto E. Antiproliferative and molecular mechanism of Eugenol-induced apoptosis in cancer cells. Molecules. 2012; 17: 6290-304.

82. Jiménez-Medina E, Garcia-Lora A, Paco L, Algarra I, Collado A, Garrido F. A new extract of the plant *calendula officinalis* produces a dual *in vitro* effect: cytotoxic anti-tumor activity and lymphocyte activation. BMC Cancer. 2006. 6:119.

83. Villarreal ML, Nicasio P, Alonso-Cortes D. Effects of *Mimosa tenuiflora* bark extracts on WI38 and KB human cells in culture. Arch Invest Med (Mex).1991; 22 (2):, 163-169.

84. Jiang Y, Weniger B, Haag-Berrurier M, Anton R et al. Effects of saponins from *Mimosa tenuiflora* on lymphoma cells and lymphocytes. Phytother Res. 1992; 6 (6):310-313.

85. Porras-Reyes BH, Lewis WH, Roman J, Simchowitz L, Mustoe TA. Enhancement of wound healing by the alkaloid taspine defining mechanism of action. Proc. Soc. Exp. Biol. Med. 1993; 203 (1): 18-25.

86. Weniger B, Italiano L, Beck JP, Bastida J, et al. Cytotoxic activity of *Amaryllidaceae alkaloids*. Planta Med. 1995; 61(1) 1:77-79.

87. Kumar GH, Chandra Mohan KVP, Rao AJ, and Nagini S. Nimbolide a limonoid from *Azadirachta indica* inhibits proliferation and induces apoptosis of human choriocarcinoma (BeWo) cells. Invest New Drugs. 2009; 27 (3): 246–252.

88. Arumugam A, Agullo P, Boopalan T, et al. Neem leaf extract inhibits mammary carcinogenesis by altering cell proliferation, apoptosis, and angiogenesis. Cancer Biol Ther. 2014; 15 (1): 26–34.

89. Alzohairy M.A. Therapeutics Role of Azadirachta indica (Neem) and Their Active Constituents in Diseases Prevention and Treatment. 2016. eCAM.

90. Wang P, Henning SM, Heber D. Limitations of MTT and MTS-Based Assays for Measurement of Antiproliferative Activity of Green Tea Polyphenols. PLoS ONE. 2010; 5(4): e10202. doi:10.1371/journal.pone.0010202.

91. Bruggisser R, von Daeniken K, Jundt G, Schaffner W, Tullberg-Reinert H. Interference of plant extracts, phytoestrogens, and antioxidants with MTT tetrazolium assay. Planta Med. 2002; 68: 445-448.

92. van Tonder A, Joubert AM, Cromarty AD. Limitations of the 3-(4,5-dimethylthiazol-2-yl)- 2,5-diphenyl-2H-tetrazolium bromide (MTT) assay when compared to three commonly used cell enumeration assays. BMC Res Notes. 2015; 8:47.

Chapter 3

Material based on chitosan, aqueous extract of *Ocimum micranthum* Willd leaves and hydro-alcoholic extract of *Calendula officinalis* L. flowers for biomedical applications

3.1 Introduction

Chitosan is a natural biopolymer obtained by deacetylation of chitin and consisting of N-acetyl-D-glucosamine and D-glucosamine units linked by β-(1–4) bonds. For its particular characteristics, such as biodegradability, biocompatibility, non-toxicity and antimicrobial properties, it has been used in wound healing, tissue repair, cell adhesion, drug delivery, and food packaging [1,2]. Due to the cationic property of chitosan and to its film-forming ability, it has been used to develop active films and membranes adding essential oils, silver nanoparticles, and pharmaceutical products [3-5]. These compounds are incorporated with the aim to impart functional properties to chitosan films, and these can use in diverse areas, such as food and biomedical. However, these compounds can modify the properties of chitosan films.

Recently, it has been developed a tendency to incorporate extracts from plants in chitosan films and nanoparticles [6, 7], the goal is to take the advantages of medicinal benefits that these natural extracts possess due to the presence of diverse metabolites. In México, *O. micranthum* and *C. officinalis* are plants used in the folk medicine by its varied biological activities, such as antimicrobial, antioxidant, anti-inflammatory properties, with a positive effect on the healing process of wounds [8, 9]. Therefore, the principal objective of this work was to study the effect of the presence of the aqueous extract of *O. micranthum* leaves and the hydro-alcoholic extract of *C. officinalis* flowers on the physical, chemical, thermal and mechanical behavior of chitosan films. Moreover, the antimicrobial and proliferative properties of these extracts were evaluated after their incorporation into chitosan matrix.

3.2 Elaboration and physicochemical characterization of films based on chitosan, aqueous extract of *Ocimum micranthum* Willd leaves and hydro-alcoholic extract of *Calendula officinalis* L. flowers.

3.2.1. Experimental Methods

Materials

Chitosan of medium molecular weight with 75-85% deacetylated degree (batch SLBH2747V) an a viscosity 200-800 cP, 1% w/v in 1% v/v acetic acid at 25° C, Brookfield. Acetic acid (ACS reagent 99.70%) batch SHBB8524V was purchased from Sigma-Aldrich.

Preparation of films

The chitosan films were prepared by the casting method, with a film-forming solution 1% w/v in acetic acid 1% v/v. The chitosan solution was heated at 50°C and stirred for 2 h using a water bath. Afterwards, the solution was filtered through a filtration system comprising a stainless-steel base and a Millipore filter (Durapore 0.45 μm HV), the next step was to degas the solution using an ultrasonic bath (Branson model 2510) for 10 min. The hydro-alcoholic extract of *Calendula officinalis* flowers (HAECa) and the aqueous extract of *Ocimum micranthum* Willd leaves (AAE) was added in concentrations of 8, 10, 12% v/v and 2, 4, 6% v/v, respectively. The solution of chitosan with extracts was stirred for 1 h. Subsequently, these solutions were degassed with the application of an ultrasonic bath and vacuum. The chitosan solution with extracts was poured into polypropylene containers and placed into an oven (Lindberg Blue model MO144OA) at 50°C for 16 h. After drying time, the films obtained were carefully released from the container and stored in plastic bags and the films separated by wax paper.

Thickness

The thickness of each film was measured using a digital micrometre (Mitutoyo model 293-330-30). At least seven representative samples of each film formulated were tested at 6 random points. Each mean and standard deviation of each film formulation were reported. Similarly, the thickness of the films used for determining water vapor transmission rate, elongation, and tensile strength was also measured.

Optical microscopy

The surface of chitosan films with extracts was observed using an optical microscope Zeiss model STEMI 2000 coupled to Axio cam ERC5S. The images of the samples were taken at different magnifications (0.65x, 1.25x, 2.5x, 5x).

Mechanical and dynamic-mechanical test

The mechanical test of the films with the aqueous extract of *O. micranthum* leaves was performed using a universal testing machine (United model SSTM-5kN, Huntington Beach, CA). In the case of the films with hydro-alcoholic extract of *C. officinalis* flowers was realized using a texturometer (Texture Technologies Corp., New York, USA) at 25°C, in both types of films the gauge length and the crosshead speed was 30 mm and 1 mm/min respectively. The tensile strength, elongation at break, and Young´s modulus were determined, and at least six specimens of each formulation were tested. The relaxation modulus was measured with a TA Instrument DMA Q800, using a temperature sweeping from 30 to 120°C and a heating rate of 5.00 °C/min.

Color

The color test in the chitosan films was carried out using a colorimeter (CR-300 Konica-Minolta Co., Ltd., Osaka, Japan) with a white plate of calibration. Seven samples of chitosan film with each extract were evaluated, and as control, chitosan film without extracts was used.

The CIE Lab color scale was used for measuring color values: L*, is the lightness variable; a*, from green to blue and b*, from yellow to red. The total color difference (ΔE*), chroma (C*) and angle tone (h*) were calculated as follows:

$$\mathbf{\Delta E^* = [\Delta L^{*2} + \Delta a^{*2} + \Delta b^{*2}]^{1/2}}$$

Where:

$\Delta L^* = L^*$ standard $- L^*$ sample, $\Delta^* a = a^*$ standard $- a^*$ sample, $\Delta^* b = b^*$ standard $- b^*$ sample.

$$\mathbf{C^* = [a^{*2} + b^{*2}]^{1/2}}$$

$$\mathbf{h^* = arctg\ [b^{*2}/\ a^{*2}]}$$

Transparency

The transparency was determined using a spectrophotometer (Evolution 300 Thermo Scientific) and the Vision Pro Software [10, 11]. A range of wavelength from 200 nm to 800 nm was evaluated in three samples of each formulation with the goal of to determine the percentages of light transmission in the barrier properties of the film with extracts against ultraviolet (UV) and visible light. The parameter of transparency was calculated with the next equation [12]:

Transparency (T) = $\mathbf{A_{600}/s}$

Where:

A: absorbance at 600 nm

s: Thickness (mm)

According to this equation; the high values of T indicate lower transparency and a higher degree of opacity.

Contact angle

The surface free energy of chitosan films with extracts was performed by static contact angle measurements carried out by the sessile drop method. A small drop of deionized water was placed on the film surface by a syringe, at 25°C. A camera connected to a computer was used to take snapshots of the liquid drop and the software (AmScope 3.7) fitted a curve to the shape to determine the contact angle, which may be defined as the angle between the film surface and the tangent line at the point of contact of the water droplet with the surface. At least three measurements were carried out for each film type and the average value was calculated.

Water Vapor transmission rate

The WVTR was carried out by the ASTM-E96-95 method. In this method, the test film covered a container filled with distilled water (to maintain a relative humidity gradient across the film), and each film was stored at 25°C in a desiccator (with a dry silica gel). The mass of water lost from the container was monitored as a function of time (approximately 2 h), and the WVTR was calculated from the slope of each line by linear regression ($r > 0.98$) following the equation:

$WVTR = w/(t)$ (A)

Where: w is the mass H_2O lost in g.

t is the time in h, and A is the permeation area in cm^2. The test of each film was performed in triplicate.

FTIR

The structural changes in the chitosan matrix when HAECa and AAE were added have been determined using a FTIR spectrophotometer model NEXUS 670 from Thermo Nicolet. All spectra were taken with a resolution of 4 cm-1 and were averaged over 64 scans in the range of 4000-650 cm-1. The thicknesses of the assayed films in the infrared test were between 0.03-0.06 mm and spectra of films were determined using an ATR accessory. The spectrum of the HAECa, and AAE extracts were obtained by ATR analysis.

Differential Scanning Calorimetry (DSC)

DSC analysis was performed in chitosan films with three different concentrations of each extract (HAECa and AAE). The specimens were mounted in aluminium pans and heated from 25°C to 400°C using a heating rate of 10°C/min under a nitrogen atmosphere on a DSC equipment Discovery series (TA Instruments).

Termogravimetric Analysis (TGA)

The thermogravimetric analysis was carried out on a TGA equipment Discovery series (TA Instruments) under a nitrogen atmosphere using a rate of 20°C/min from 50°C to 800°C.

Water content by isotherm in TGA equipment

The moisture content was measured by heating the samples to 120 °C under a nitrogen atmosphere using a heating rate of 5 °C/min on a TGA equipment Discovery series (TA instruments). At this temperature (120 °C), an isotherm was kept for 60 min^{1}. The percentage of moisture was calculated from the weight loss at the end of the isotherm.

Scanning Electron Microscopy (SEM) with Chemical Analysis by Energy Dispersive Spectroscopy (EDS).

The morphology and the elemental composition of the control and chitosan films with AAE and HAECa were analyzed using a Field Emission Scanning Electron Microscope JEOL JSM-6390LV model (Tokyo, Japan) coupled to an energy dispersive spectrometer Oxford Instrument. Pieces of the film were mounted on nickel stubs using double-sided tape and then coated with a layer of gold to make them more conductive allowing the surface visualization. In the morphological analysis, all samples were examined with 5 kV accelerating voltage, while that in the elemental film composition analysis a voltage of 20 kV was used. The images were obtained by detector Electrons Secondary (SEI), under high vacuum, LM mode, with a working distance of 15 mm and a magnification of 1000X.

3.2.2 Results and discussion

Thickness

The mean and standard deviation of the film thickness for all formulations are shown in **Table 3.1**. The thickness of the control (chitosan film) and chitosan films with extracts (AAE and HAECa) showed significant difference among them ($p<0.05$). The standard deviation values were small, which suggested good film homogeneity, except for the formulation with HAECa at 10%.

The formulation with HAECa 12% had the highest thickness in comparison with the others film formulations. The above indicates that the presence of extracts affected the thickness of the chitosan films and contrast with the results observed in chitosan films with *Aloe vera*, where the film thickness decreased to higher concentrations of *Aloe vera* [6]. In a study with an aqueous extract from quinoa was observed the same behavior of the formulations with HAECa [13], which suggest that the film thickness depends on the film nature and composition (film-forming polymer and chemical nature of the compounds added).

Table 3.1 Thickness of chitosan films with AAE and HAECa.

Formulation	Thickness (µm)
Control	32.60 ± 5.80^{a}
AAE 2%	42.00 ± 6.30^{b}
AAE 4%	40.40 ± 4.70^{b}
AAE 6%	40.40 ± 3.60^{b}
HAECa 8%	45.00 ± 11.00^{b}
HAECa 10%	51.40 ± 17.80^{b}
HAECa 12%	63.30 ± 14.60^{c}

Different letters in the same column indicate significant difference ($p<0.05$). Mean +/- standard deviation.

Optical microscopy

The chitosan films with aqueous extract of *Ocimum micranthum* Willd (AAE) were semi-transparent (**Figure 3.1**) similar to the control (chitosan films without extracts), but with the presence of some loose threads, which appeared when the extract was added into the chitosan matrix. These threads could be attributed to the presence of some compounds in the extract such as lignin, cellulose, hemicellulose, pectic compound, suberin and protein from the cell wall of the plant leaves. These substances could also be released when cell walls are damaged during extract preparation.

While that the chitosan films with hydro-alcoholic extract of *Calendula officinalis* (HAECa) presented a yellow-orange color (**Figure 3.2**); this color was more intense when the extract concentration was increased. The change of coloration in the chitosan films with HAECa may be attributed to the presence of pigments in the extract such as carotenoids [14].

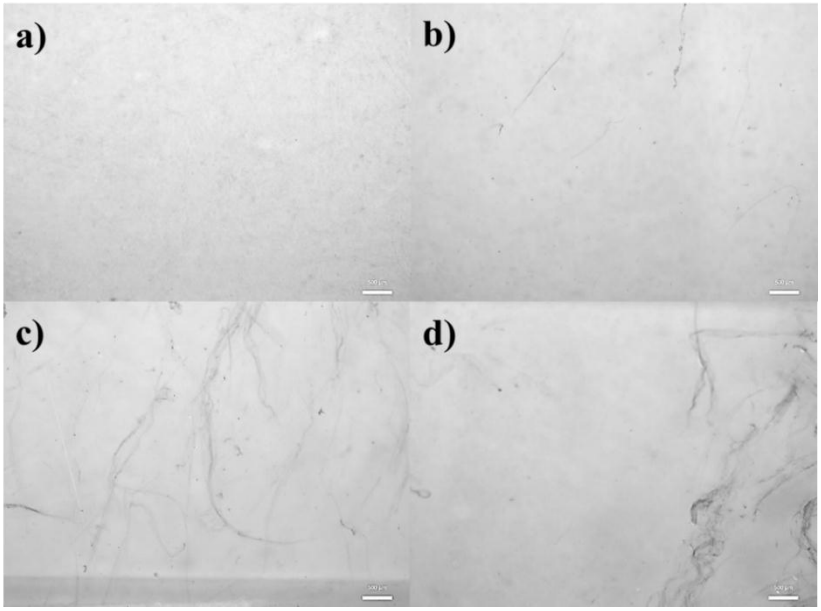

Figure 3.1 Surface of chitosan films with AAE extract to different concentrations **a)** Control (chitosan film) **b)** 2% AAE **c)** 4% AAE **d)** 6% AAE. Magnification 1.25x.

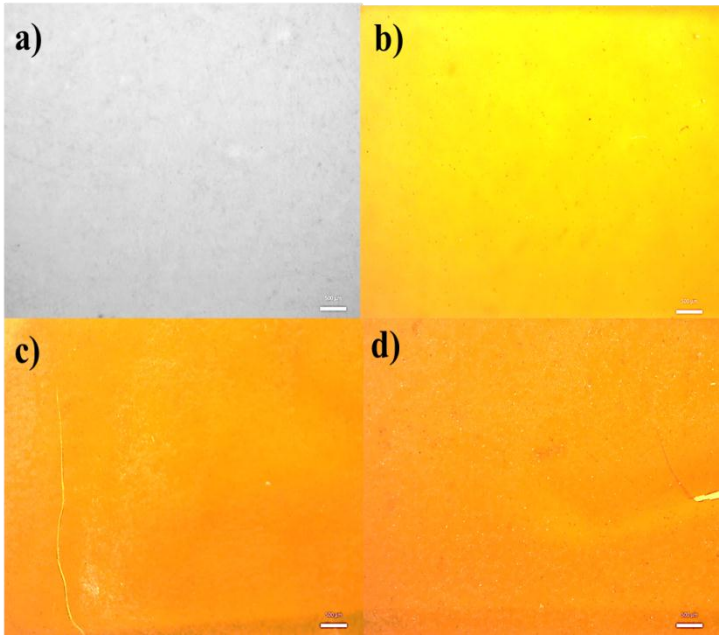

Figure 3.2 Surface of chitosan films with HAECa extract to different concentrations. **a)** Control (chitosan film) **b)** 8% HAECa **c)** 10% HAECa **d)** 12% HAECa. Magnification 1.25x

Mechanical and dynamic-mechanical test

Table 3.2 shows the mechanical properties of chitosan film prepared with different concentrations of extract. The tensile strength did not present a significant difference between control and films with AAE (except in the concentration 6% v/v). In contrast, chitosan films with HAECa decreased the tensile strength ($p < 0.05$) significantly in all concentrations with this extract. The elongation at break values showed a significant decrease ($p < 0.05$) in all the films formulated with both extracts. The Young's modulus of the films was not affected significantly ($p > 0.05$) by the incorporation of any extracts.

The mechanical behavior showed by chitosan films formulated with HAECa could be attributed to interaction among the extract and the chitosan matrix through hydrogen bonds, which may cause changes in the macromolecular network of the biopolymer. These changes affected the film structure and a decrease in the tensile strength values (since 61.16 to 30.40 MPa) and elongation at break (1.41 to 2.55%) was observed; this tendency was more evident when the concentration of the extract was incremented. These results coincided with other studies, where the addition of *Aloe vera* and *Lycium barbarum* fruit extract showed a decrease in mechanical properties of chitosan films [15, 16].

On the other hand, the values of the control of chitosan (85.82 MPa) and chitosan with AAE (from82.86 to 70.03 MPa) were higher than values reported previously by other authors [17-19], who reported values on the range from 51.2 to 60.7 MPa. The differences among the results may be attributed to the components of the formulations, the method used for film preparation, the chemical nature of the extracts incorporated and the interaction of these with the chitosan matrix.

Table 3.2 Mechanical properties of chitosan films with HAE Ca and AAE incorporated extracts.

FORMULATION	TENSILE STRENGTH (MPa)	ELONGATION AT BREAK (%)	YOUNG´S MODULUS (MPa)
CONTROL	$85.82 \pm 1.10^{a\,d}$	6.24 ± 0.37^{a}	4664.40 ± 40.59^{a}
HAE Ca 8%	61.16 ± 15.36^{cd}	1.41 ± 1.06^{b}	6450.90 ± 1007.34^{b}
HAE Ca 10%	24.18 ± 0.20^{b}	1.73 ± 0.88^{bc}	4806.05 ± 415.71^{ab}
HAE Ca 12%	30.40 ± 7.81^{b}	2.55 ± 0.53^{bc}	3611.90 ± 923.91^{a}
AAE 2%	$82.86 \pm 3.34^{a\,d}$	2.61 ± 0.83^{c}	4353.05 ± 858.92^{a}
AAE 4%	$84.16 \pm 10.06^{a\,d}$	2.56 ± 0.72^{bc}	4410.1 ± 750.45^{a}
AAE 6%	70.03 ± 4.41^{d}	2.09 ± 0.31^{bc}	4027.40 ± 345.07^{a}

Different letters in the same column indicate significant difference ($p<0.05$).
Mean +/- standard deviation.

In the DMA test, the value of the relaxation modulus of the control and all formulations with extract decreased when the temperature was increased. The values of this parameter for chitosan films with HAECa (concentrations of 8 and 12% v/v) were significantly ($p < 0.05$) higher than the control and films with AAE in a temperature range from 30 to 40°C. Moreover, the formulation with a concentration of 12% of HAECa maintained values significantly ($p<0.05$) higher than the control and films with AAE in a temperature range of 50 to 110°C. The decrease in the relaxation modulus may be associated to moisture loss of the films, due to increase of temperature, which causes a reordering of the polymer chains of the chitosan. The tendency of the chitosan film with a concentration of 12% EHACa could be attributed to the interaction between the extract and the biopolymer chains (amorphous portion) of the chitosan. It permits to maintain the relaxation modulus values higher than the control and the films with AAE. Some authors have indicated that the range of temperature analyzed in this study, the chitosan may experiment a β-relaxation [20], a type of secondary relaxation, which is associated to the rotational motion of glycosidic bonds [21].

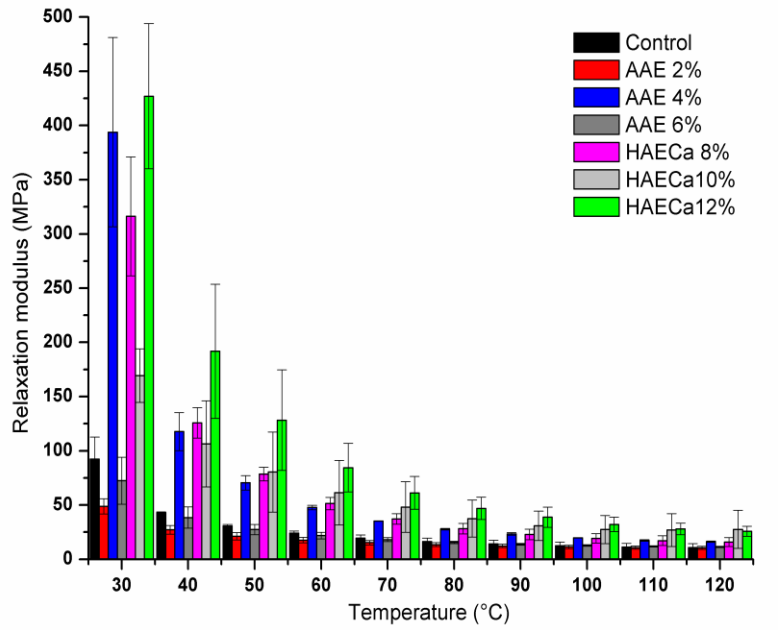

Figure 3.3 Relaxation modulus behavior of chitosan films incorporated with HAECa and AAE using a temperature sweeping.

Color

The incorporation of AAE and HAECa extracts into of the chitosan matrix caused a significant increment ($p < 0.05$) in the ΔE* values, when these are compared to the control film (**Figure 3.4**); this colorimetric parameter indicates the variation in color perception. The HAECa films presented the higher values of ΔE* (from 76.47 to 70.03), this increment was in relation to the increase of the values of a* (red-green) and b* (yellow-blue) parameters (**Table 3.3)**. This is associated with the presence of pigments or other compounds, contained in this extract, which may be bounded to the chitosan [22].

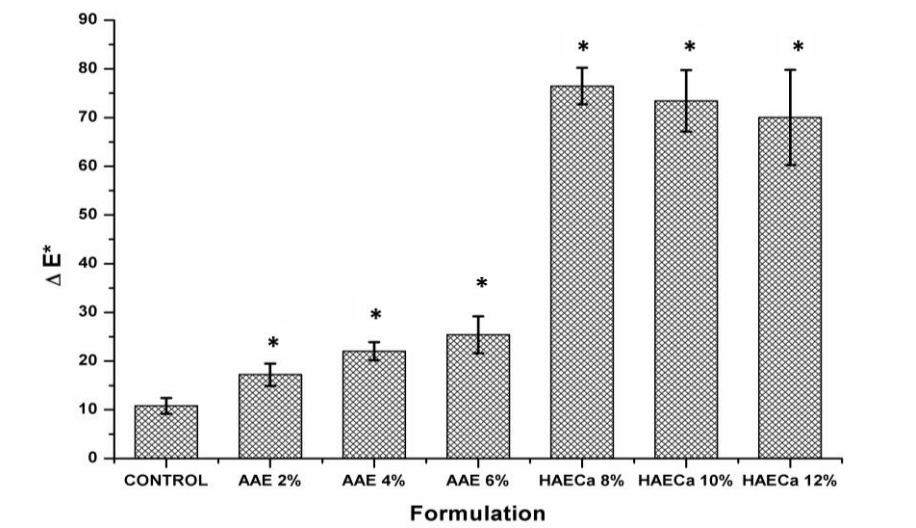

Figure 3.4. Comparative of the total color difference (ΔE*) in chitosan films with HAECa and AAE incorporated extracts. Error bars represent standard deviation and * represent statistically significant difference.

Table 3.3 Values of L* a* and b* in chitosan films with HAECa and AAE incorporated extracts.

Formulation	L*	a*	b*
Control	93.39 ± 0.55	-4.59 ± 0.42	7.33 ± 1.56
AAE 2%	91.37 ± 0.77	-5.23 ± 0.45	13.47 ± 2.20
AAE 4%	89.74 ± 0.81	-5.37 ± 0.26	18.07 ± 1.78
AAE 6%	89.24 ± 1.29	-5.76 ± 0.44	21.40 ± 3.63
HAECa 8%	64.03 ± 6.71	13.36 ± 6.40	64.03 ± 5.70
HAECa 10%	63.44 ± 8.71	12.86 ± 9.52	60.16 ± 4.31
HAECa 12%	55.28 ± 10.95	17.41 ± 9.24	47.23 ± 17.84

In relation to the chrome (C*) parameter (**Figure 3.5**), all films with HAECa showed values (from 65.53 to 51.65) significantly ($p < 0.05$) higher than the control (8.66) and the films with AAE (from 14.66 to 22.17); this parameter indicates the degree of saturation of color and is proportional to the strength of the color. This tendency may be attributed to the higher values of parameters a* and b*, due to that chrome depend on these parameters. However, in the hue angle (h*) parameter (**Figure 3.6**), the value of the film control (177.19) was significantly higher than the films with HAECa (from 78.06 to 66.49) and with AAE (from 111.44 to 105.34) extracts. The hue angle showed a tendency to reduce with an increase of the extract content in each film's formulation. The color parameters (C* and h*) indicates that the films formulated with AAE extract showed a yellow color, meanwhile films formulated with HAECa showed yellow orange color; although the samples showed transparent feature.

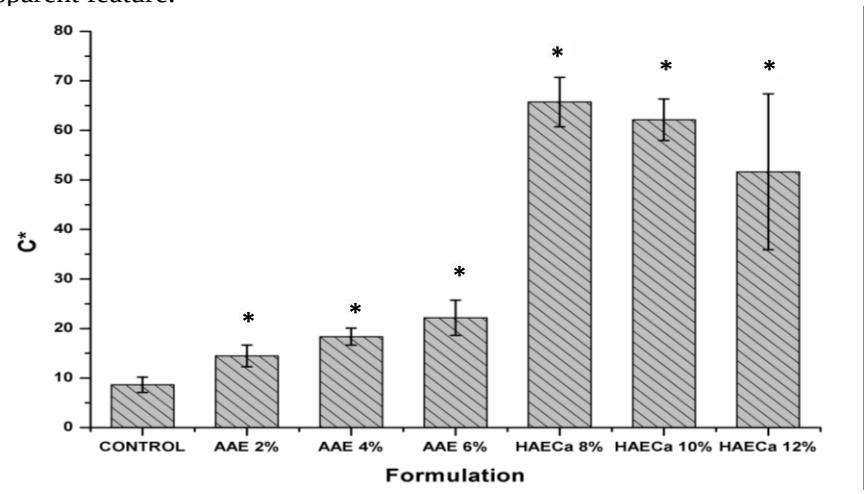

Figure 3.5 Comparative of chroma parameter (C*) in chitosan films with HAECa and AAE incorporated extracts. Error bars represent standard deviation and * represent statistically significant difference.

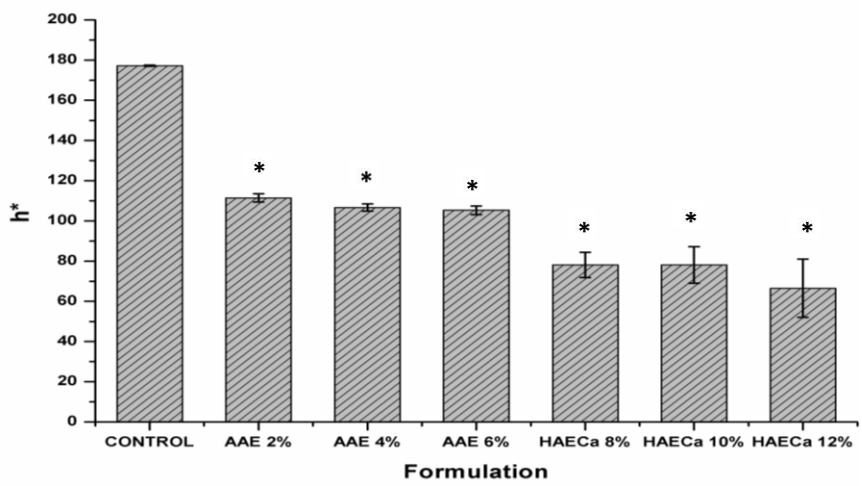

Figure 3.6 Comparative of hue angle (h*) in chitosan films with HAECa and AAE incorporated extracts. Error bars represent standard deviation and * represent statistically significant difference.

Similar changes in chitosan film color by adding of extracts were previously reported for others authors [23, 24], for example in chitosan films containing green tea extract or honeysuckle flower extract. The color of chitosan films was directly influenced by the type and concentration of added extract. The color parameter may be affected directly by other properties of chitosan films, such as the transparency or opacity.

Transparency

The tendency of the results of the transparency-opacity test can be observed in **Figure 3.7**. The chitosan films with HAECa showed higher significantly values (from 8.23 to 9.34) than the control (4.32) and the films with AAE (from 3.15 to 5.08). According to the equation used for the calculation, higher values indicate lower transparency and a higher degree of opacity. The opacity of these films increased significantly when the concentration of the HAECa was augmented; a similar behavior was observed in the films with AAE. These results are related to color test, where the films with HAECa showed higher values in C* and ΔE color parameters; the color development in chitosan films when the HAECa was added caused an opacity in the films at 600 nm which is the visible range. The changes in the color of chitosan films may be associated with diverse compounds that contain the extracts, such as pigments, antioxidants, etc.

The increase in the opacity of chitosan films is a consequence of the addition of extracts or compounds (antioxidants); it has been reported for chitosan films with green tea extract [23], honeysuckle flower extract [24], and α-tocopherol [25]. Nevertheless, the opacity is a desired characteristic in the development of packaging or biomedical material because it should protect from oxidative deterioration caused by visible and ultraviolet light.

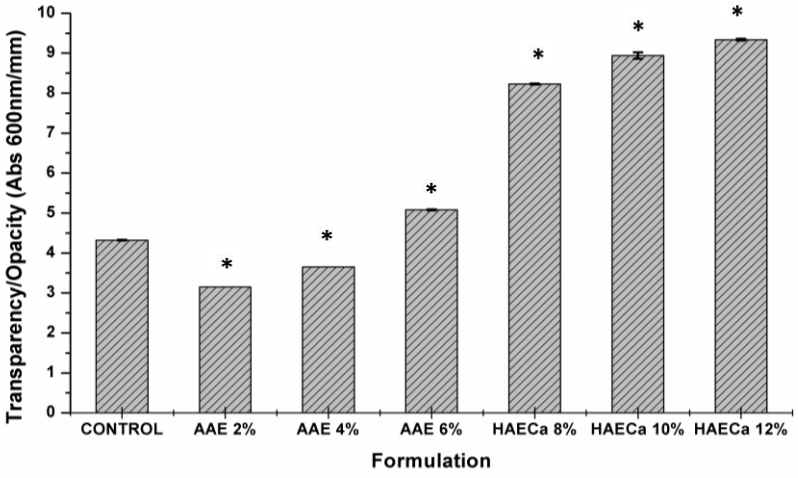

Figure 3.7 Transparency-opacity of chitosan films with HAECa and AAE incorporated extracts. Error bars represent standard deviation and * represent statistically significant difference.

Chitosan films formulated with the extracts showed higher absorbance in the UV range (200-350 nm) than the visible spectrum from 400 to 800 nm (**Figure 3.8**). The control (chitosan film without extract) showed absorption between 304 and 310 nm in the UV range, which agrees with results reported by other authors [26]. The chitosan films with HAECa did not show clearly this peak in the UV range, but showed a slight peak between at 650 to 700 nm in the visible spectrum, the absorbance increased lightly when the concentration of the extract incremented. In the case of the chitosan films with AAE, this peak displaced to minor wavelength and the absorbance increased when the concentration of the extract incremented and in the visible range was not observed any peak.

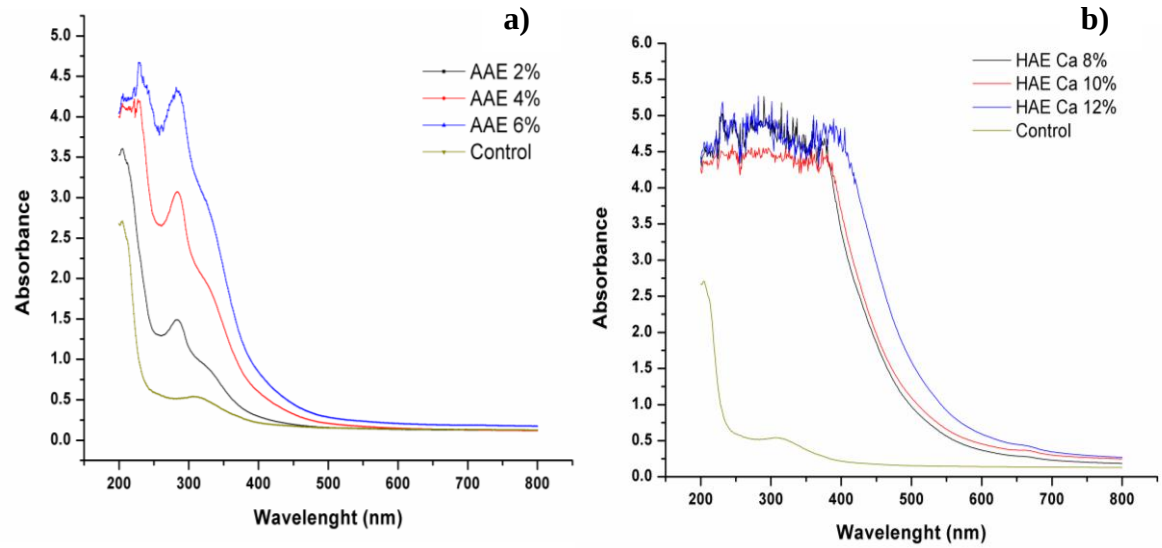

Figure 3.8 UV-Vis spectrum of chitosan films with extracts to different concentrations
(a) AAE **(b)** HAE Ca

Some authors [27] have indicated that the peak showed by the chitosan around 300 nm may be associated with the presence of carbonyl and amino groups in the chemical structure of the biopolymer. Otherwise, several authors [28] showed in UV-Vis study of *Calendula officinalis* extract that this has two peaks in the visible spectrum, the first one is present between 446-450 nm and the second is 2 T648-655 nm, it is associated to the presence of lutein and chlorophyll, respectively. Concerning to extracts of *Ocimum* genus, some authors [29] observed in previous UV-Vis study carried out on the *sanctum* variety, two peaks in the visible region, one between 644 and 661 nm, and other localized around 470 nm; these peaks appertain to chlorophyll a, chlorophyll b and carotenoids, respectively.

Contact angle

In the contact angle test by the drop method, the chitosan films with HAECa extract showed values below 50° and these films were significantly different ($p<0.05$) to the control and films with AAE extract, which showed values around of 90° (**Figure 3.9**). Some authors [30] have to the mentioned that contact angle value below 90° indicates a hydrophilic behavior of the material, although that contact angle value equal to above 90° indicates a hydrophobic behavior. The results suggest that the control and chitosan films with AAE incorporated extract were hydrophobic and that the addition of the HAECa extracts into chitosan matrix change the hydrophobic behavior to hydrophilic.

In a previous study [13], *Calendula officinalis* extract was used to produce nanofibers with PCL polymer, the same behavior was observed, the PCL films were hydrophobic with a contact angle of 130°; when the extract was added, the contact angle value decreased to 28.5°, with a concentration of 30%. This parameter also was measured in nano dressing based on chitosan, pectin and TiO_2 particles [30]; these nano dressings presented contact values of 86.2°, hence lightly hydrophilic materials. Some authors [31] indicated that the hydrophilic characteristic of the surface of the biomaterials might to stimulate the cytocompatibility.

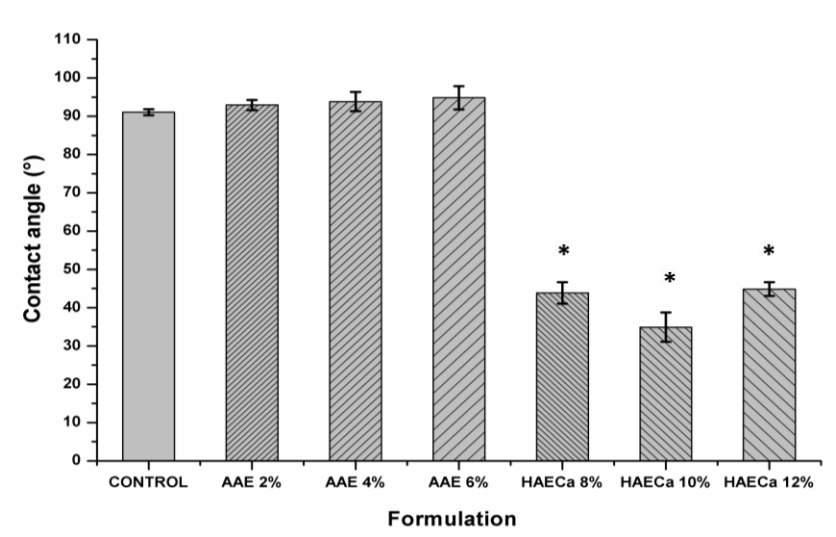

Figure 3.9 Contact angle of chitosan films with AAE and HAECa extracts to different concentrations. Error bars represent standard deviation and * represent statistically significant difference.

Water Vapor transmission rate (WVTR)

The chitosan films incorporated with HAECa at 8 and 12% were the formulations with a WVTR value significantly different (50.18 and 70 $gh^{-1}m^{-2}$, respectively) to the control (60 $gh^{-1}m^{-2}$) see **Figure 3.10.** The addition of AAE extract into chitosan matrix caused no significant effect on

the WVTR values. The higher WVTR value of the formulation with HAECa 12% may be attributed to the hydrophilic nature of the chitosan and the extract, as well as the concentration factor and the chemical interaction between these components.

Previous studies [32] have shown WVTR values of 47.5 g/m^2/h for chitosan films. Also, it have been developed composite films of chitosan with an inorganic material (Montmorillonite) [33] and with another biopolymer (*cassava* starch) [34]. The values reported for WVTR were from 45.08 to 83.33, and from 45.42 to 130.58 g h^{-1}m^{-2}, respectively. Other authors [35] suggest that the WVTR values between 83.33 to 104.17 g h^{-1}m^{-2} in materials or biomaterials have potential use in wound-dressing.

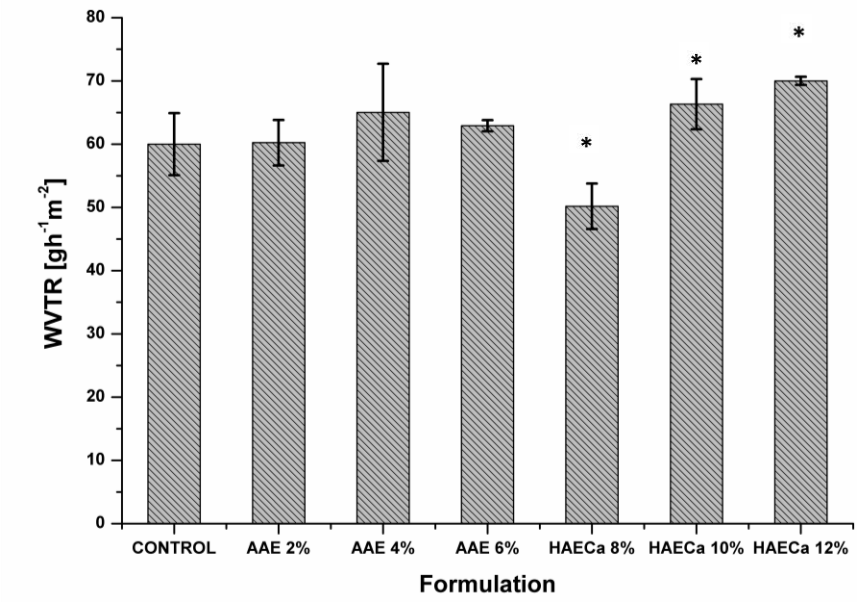

Figure 3.10 WVTR of chitosan films with AAE and HAECa extracts to different concentrations. Error bars represent standard deviation and * represent statistically significant difference.

FTIR analysis

The FTIR spectra of the chitosan control and with HAECa are described in **Figure 3.11**. In chitosan control, two important bands (**Table 3.4**) at 1639 and 1546 cm^{-1} were detected, the first due to the amide I (C=O) and the second corresponds to N-H bond (amine) vibration overlapping the amide II vibration [18, 36]. The band at 2881 cm^{-1} attributed to C-H stretching vibration [18], the band at 3212 cm^{-1} due to O-H stretching vibration that overlaps the N-H (amino group) stretching vibration [37], were also identified. Bands in the region between 1151 and 1020 cm^{-1} were localized; these may be assigned to skeletal vibration involving the bridge C-O stretch [37]. A

band due to CH_2 scissoring was observed at 1405 cm^{-1} [18, 36]. The peak localized at 896 cm^{-1} denotes the presence of C-N bond [37].

In the same **Figure 3.11** can be observed the spectra of HAECa extract, which shows a peak at 3008 cm^{-1} may be assigned to O-H bonds that overlaps the N-H stretching of the primary amide, which possibly arises from proteins [38, 39]. The band at 2981 cm^{-1} may be attributed to alkyl or CH groups [40]. The 1640 cm^{-1} band may be corresponding to some chlorophyll that overlaps amides of type I [40]. Moreover, the bands observed at 1453 and 1386 cm^{-1} are mentioned by some authors [40] to be associated with the presence of lycopene and β- carotene, respectively. Finally, the band at 1084 cm^{-1} could suggest the presence of terpenoids or flavonoids, compounds in the extract [39, 41].

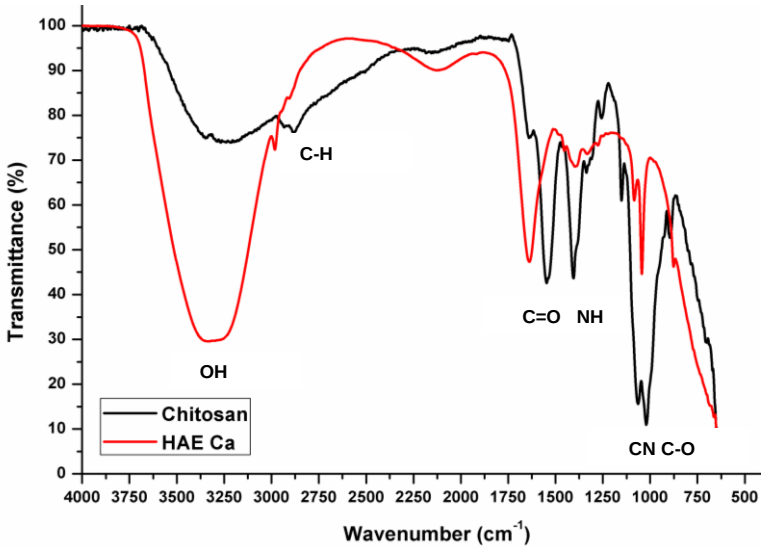

Figure 3.11 FTIR spectrums of chitosan control and HAECa extract.

Table 3.4 List of FTIR bands between 650 and 4000 cm^{-1} for chitosan films and chitosan films with HAECa extract incorporated at different concentrations.

Chitosan Control	Functional groups	HAE Ca extract	Ethanolic extract *Calendula officinalis*[5]	Chitosan film with HAECa 8% (v/v)	Chitosan film with HAECa 10% (v/v)	Chitosan film with HAECa 12% (v/v)
3212	OH NH_2	3296	3008	3291	3240	3274
2881	C-H	2981	2923, 2853	2967, 2867	2949, 2886	2934
1639	N-H C=O			1634		
1546	NH_2	1640	1463	1546	1572	1569
1405	CH_2	1453, 1386	1377			1399
1336	C-N			1373	1334	1335
1063	C-O	1084	1098	1092	1092	1057
896, 701	C-O-C	876		902, 751	752, 702	897

The **Figure 3.12** illustrates the FTIR spectra of chitosan films at different concentrations of HAECa. It can be observed a stretching band between 3100 and 3500 cm^{-1} in all concentrations. This band is related to the over tripping of O-H and N-H groups from the chitosan and the extract, that were overlapped, this signal becomes more intense and broader; it has shown a displacement with the increase of extract concentration **(Table 3.4).** It would indicate an interaction between chitosan and HAECa through this kind of bonds. All films also showed a band between 2800 and 3000 cm^{-1} associate with the C-H stretching vibrations of the chitosan and the extract; in the concentration of 12% HAE, an overlap of the individual band of each component of the film was observed. The chitosan films with 8 % of HAE showed an overlap of signals of functional groups of each component, such as the band to 1643 cm^{-1} (chlorophyll that overlaps to C=O signal of amide type I of the chitosan). However, the band to 1546 cm^{-1} (N-H of amide type II) from the chitosan, the band to 1373 cm^{-1} (β- carotene pigment) and the maximum band to 1092 cm^{-1} (terpenoid or flavonoids compounds) from the extract were conserved. The chitosan films with 10 % of HAECa incorporated also showed the characteristic bands of the extract, signals due to the presence of β-carotene pigment and terpenoids or flavonoids compounds, with a short displacement (**Table 3.4**). However, with a concentration of 12% of HAECa, the chitosan films showed a decrement in some bands, which were broader and less intense; this indicates an overlap of the signals from chitosan and HAECa, due to the extract concentration.

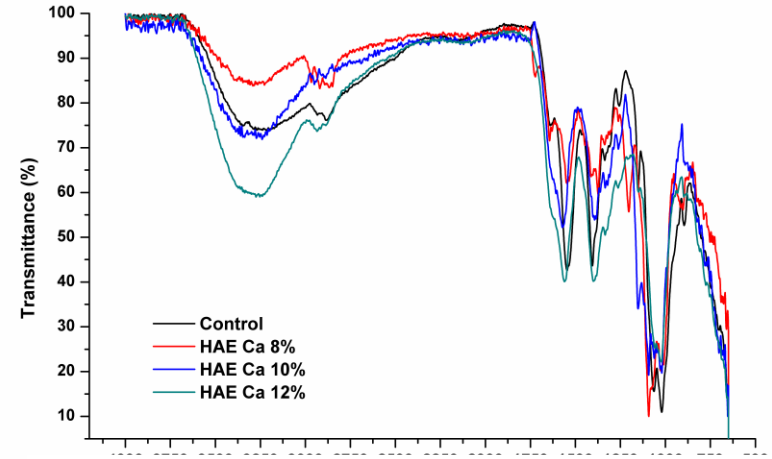

Figure 3.12 FTIR spectrum of chitosan films with HAECa extract at different concentrations.

The **Figure 3.13** shows the comparison of the FTIR spectrum of chitosan control and AAE extract. The characteristic bands present in chitosan control were previously described. With regard to the groups present in AAE extract, it can be observed a strong and broad peak at 3366 cm^{-1}

(**Table 3.5**), the asymmetric form indicates that this is composed of diverse compounds, which may be originated from the overlap of O-H and N-H stretching modes of vibration of water, phenolic compounds and amide group respectively [42-44]. The band at 2956 cm^{-1} may be associated with asymmetric C–H stretching of CH_3 [8], other authors associate it with O-H stretching of carboxylic acid [45, 46]. The peak around 2850 cm^{-1} is assigned due to the symmetric stretching C–H of the alkane group [42]. Also, it can be observed at 2121 cm^{-1} a marked peak attributed to asymmetrical stretching of C≡C of alkynes [8, 13]. The band around at 1752 cm^{-1} is assigned due to the C=O stretching of aromatic ester [42, 43].

The active band at about 1629 cm^{-1} is designated to C=O stretching vibrations of secondary amide [42, 47, 48]. Two bands around between 1516 and 1330 cm^{-1} denote the presence of the N–O asymmetric and symmetric stretching bands, respectively, of the aromatic NO_2 [42]. The peak at 1390 cm^{-1} may be attributed to C-N stretching of aromatic amine group [49, 50]. A weak band at around 1250 cm^{-1} was observed, this is assigned as the C–O stretching mode in the aromatic acetate group [42]. The band about 1046 cm^{-1} is assigned as the C–O stretching vibration of primary and secondary alcohols in cellulose [42, 51]. The group at 1021 cm^{-1} denotes the presence of C-C stretching of alcohols, carboxylic acids, ethers, esters [43, 49, 50]. A peak at 952 cm^{-1} is attributed to C=C-H [51]. An absorption band at about 712 cm^{-1} is present, which is probably due to the vibration bending vibrational mode of O–N–O of the NO group confirming the presence of nitro group [42]; other authors mentioned that this band might be associated to monounsaturated in the aromatic ring [51]. All the band assignments are summarized in **Table 3.5**.

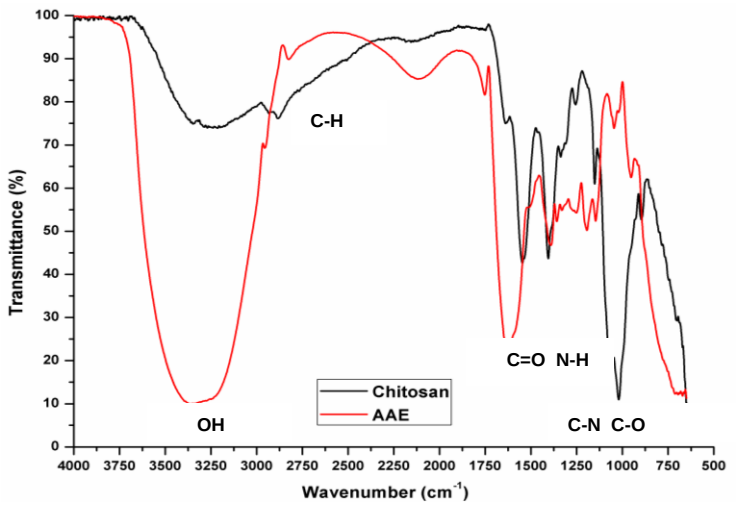

Figure 3.13 FTIR spectrum of chitosan control and AAE

Table 3.5 List of FTIR bands between 650 and 4000 cm^{-1} for chitosan films and chitosan films with AAE extract incorporated to different concentrations.

Chitosan Control	Functional Groups	AAE extract	*Ocimum sanctum* extract [5]	Chitosan film with AAE 2%	Chitosan film with AAE 4%	Chitosan film with AAE 6%
3212	OH NH_2	3366	3409	3371	3346	3336
2881	C-H	2956	2958	2880	2884	2886
1639	N-H C=O	1629	1622	1645	1641	1641
1546	NH_2	1516	1544	1551	1550	1549
1405	CH_2			1404	1404	1412
1336	C-N	1390	1319	1310	1379	1308
1063	C-O	1046	1066	1061	1061	1062
896, 701	C-O-C	952, 712	783	889, 787	898,787	888, 787

The FTIR spectrum for chitosan films embebed with AAE extract was illustrated in the **Figure 3.14**. It can be seen at 3400 cm^{-1} in all concentrations of extract, a peak of stretching originated by the overlapping of O–H, and N–H bonds of the chitosan and the extract; this signal decreased when the extract concentration was increased, which could indicates the interaction of the chitosan and the extract through of these bonds. The band at 2956 cm^{-1} associated with asymmetric C–H stretching of CH_3, the band at 1752 cm^{-1} due to the C=O stretching of aromatic ester and the band at 952 cm^{-1} attributed to C=C-H were not observed when the extract was incorporated into chitosan matrix. The characteristic bands of chitosan at 2881 cm^{-1}, 1639 cm^{-1}, and 1546 cm^{-1} associate to C-H stretching vibration, amide I (C=O) and N-H bond (amine) vibration overlapping the amide II, respectively were conserved with a minor displacement. Other bands of the characteristic spectrum of chitosan were conserved with a slight displacement after of the addition of the extract, such as 1405 cm^{-1}, 1336 cm^{-1}, 896 cm^{-1} and 701 cm^{-1}. The FTIR spectrum of all chitosan films with AAE extract show overlaps of bands at 1256 cm^{-1}, 1151 cm^{-1}, 1063 cm^{-1} and 1020 cm^{-1}; these peaks were present in each component of the film (chitosan and AAE extract). Other characteristic bands of the extract such as 712 cm^{-1} associated to the vibrational mode of O–N–O and the monounsaturated in the aromatic ring, and 694 cm^{-1} due to C-H bending vibration [46] were conserved after of the incorporation into chitosan matrix. A new signal at 787 cm^{-1} showed up in the films with AAE incorporated, this signal was not observed previously in both components of the film (chitosan and extract). This last signal may be assigned to a change in the substitution grade of aromatic compounds presents in the extract [52].

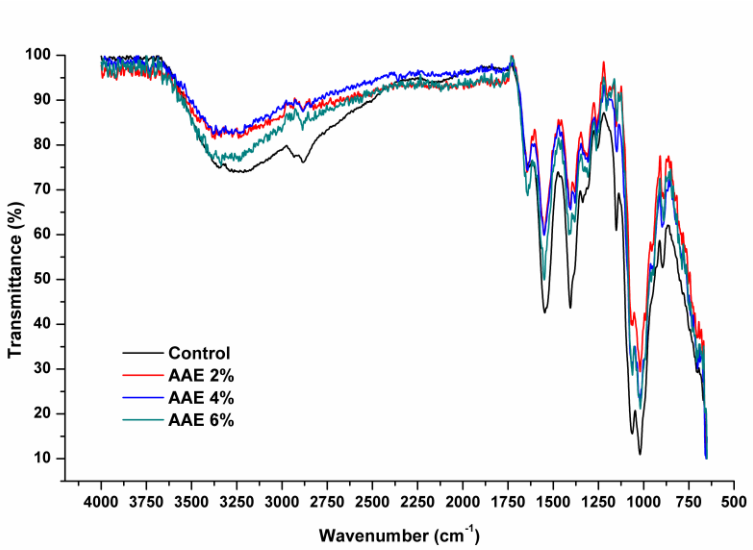

Figure 3.14 FTIR spectra of chitosan films with AAE extract at different concentrations.

Differential Scanning Calorimetry (DSC)

The DSC thermogram of the chitosan control film (**Figure 3.15**) showed a maximum endothermic peak at 86.35 °C with an enthalpy of 354.64 J/g and a maximum exothermic peak at 287.92 °C with an enthalpy of 166.41 J/g. These results (**Table 3.6**) coincide with some authors [53, 54] that have mentioned that the endothermic peak corresponds to evaporation of residual water in the film and the exothermic peak is associated with disruption and degradation of polymer chains of the chitosan. Other authors [55, 56] have identified a third peak in chitosan films between 156 and 170 °C that corresponds to the glass transition temperature of the chitosan, such as a result of a α relaxation of the chains of this biopolymer; this kind of relaxation is related to the effect of acetic acid and water on the amorphous portion of the chitosan.

In the case of the chitosan films incorporated with diverse concentrations of AAE was observed in the thermogram an maximum endothermic peak between 90.76 and 93.12°C with an enthalpy between 303.51 and 336.08 J/g and a maximum exothermic peak between 268.07 and 270 °C with an enthalpy value between 159.09 and 189.15 J/g. These values were similar to the chitosan control film, and the effect of concentration may be considered no significant (**Table 3.6**).

Concerning the chitosan films incorporated with different concentrations of HAECa was observed differences in the thermograms about the concentration of the extract used (**Figure 3.15**). When the concentration of 8% of HAECa was incorporated may be observed clearly in the thermogram three peaks, two endothermic peaks at 84.85°C (maximum peak) and 172.32 °C (small

peak) with values of enthalpy of 262.18 J/g and 18.43 J/g respectively, which coincided with the results of investigations of others authors [56]; these authors attributed the second endothermic peak to chemisorbed water in the film through hydrogen bonds and the elimination reaction of NH_3. The maximum exothermic peak was observed at 300.56°C with an enthalpy of 344.36 J/g that correspond to the decomposition of the film. With the concentrations of 10 and 12% of HAECa, the second endothermic peak decreased in size significantly, but was possible localized, for the first concentration was observed at 175.38°C with an enthalpy of 1.89 J/g and for the second concentration was observed at 175.22 °C with an enthalpy of 1.54 J/g; the decrement in size of the second endothermic peak may associate with a saturation of the binding sites in the chitosan structure caused by the effect of the concentration of the extract. Also was observed the maximum endothermic peak again in both concentrations, at 85.16 °C with an enthalpy of 228.89 J/g and 91.55 °C with an enthalpy of 210.72 J/g respectively (corresponding to lose moisture and compounds of low molecular weight from the extract, such as volatile compounds). The exothermic peaks were localized at 300.72 °C with an enthalpy of 276.80 J/g and 326.61 °C with an enthalpy of 233.34 J/g, respectively.

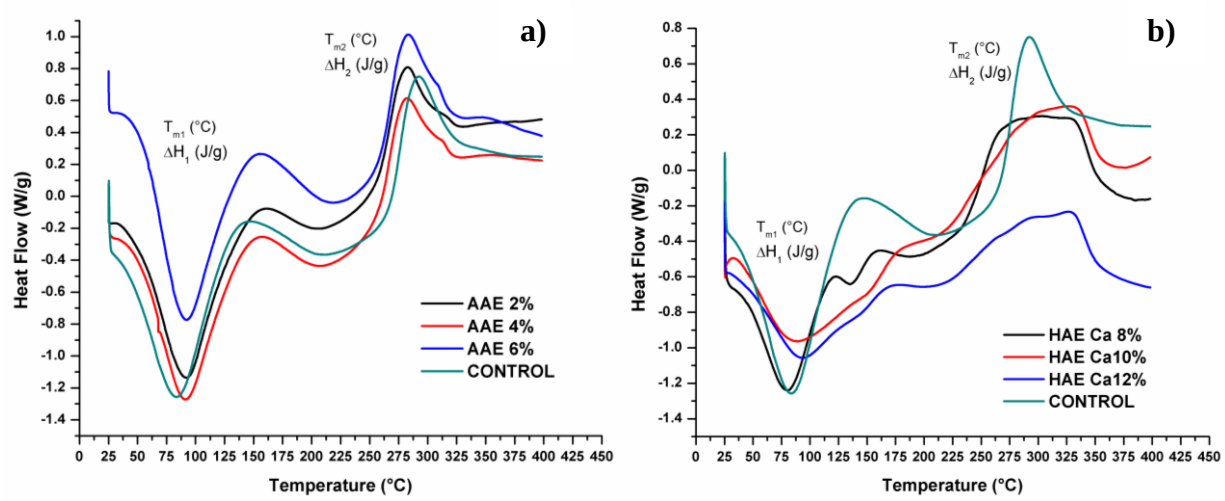

Figure 3.15. Behavior in DSC test of chitosan film with AAE and HAECa extracts (**a**) AAE (**b**) HAE Ca.

Table 3.6 Thermal characterization by DSC of chitosan films with HAECa and AAE.

FORMULATION	Endothermic phase				Exothermic phase			
	T_0 (°C)	T_{m1} (°C)	T_c (°C)	ΔH_1 (J/g)	T_0 (°C)	T_{m2} (°C)	T_c (°C)	ΔH_2 (J/g)
CONTROL	41.02 ± 0.52	86.35 ± 2.84	149.25 ± 2.58	354.64 ± 57.92	263.87 ± 4.85	287.92 ± 4.66	345.14 ± 7.60	166.41 ± 29.91
HAECa 8%	43.81 ± 3.90	84.85 ± 6.83	173.41 ±16.82	262.18 ± 79.18	225.67 ± 9.99	300.56 ± 25.20	386.17 ± 5.80	344.36 ± 36.73
HAECa 10%	39.63 ± 0.85	85.16 ± 6.20	176.06 ± 15.50	228.89 ± 39.36	225.25 ± 4.42	300.72 ± 0.08	359.89 ± 8.35	276.80 ± 0.78
HAECa 12%	41.67 ± 1.47	91.55 ± 2.07	186.52 ± 0.001	210.72 ± 22.64	222.55 ± 2.30	326.61 ± 0.19	381.21 ± 5.20	233.34 ± 13.36
AAE 2%	47.70 ± 2.73	91.04 ± 1.33	158.11 ± 3.12	334.00 ± 11.19	258.12 ± 1.07	270.00 ± 17.87	349.48 ± 20.21	189.15 ± 59.02
AAE 4%	52.68 ± 4.91	93.12 ± 2.90	155.15 ± 0.77	303.51 ± 23.04	255.91 ± 0.58	268. 07 ± 17.78	341.88 ± 12.28	159.09 ± 42.00
AAE 6%	50.70 ± 4.36	90.76 ± 0.65	159.53 ± 0.69	336.08 ± 35.09	256.60 ± 1.19	268.86 ± 18.53	339.29 ± 20.84	161.56 ± 73.26

T_0: Onset temperature

T_m: Peak melting temperature

T_c: Conclusion temperature

To compare the values obtained in DSC study can be observed that in the exothermic phase, the chitosan films incorporated with HAECa had a displacement to higher decomposition temperature and higher enthalpies than chitosan control and chitosan films incorporated with AAE. This behavior could be indicating a chemical interaction between this extract and the chitosan matrix, where the creation of new linkages has been carried out. Also in the endothermic phase of the study, the effect of the addition is notable, to generate a new peak by chemisorption phenomena.

Termogravimetric Analysis (TGA)

In TGA characterization (**Table 3.7**) of chitosan control film, three steps of decomposition were observed; the first was localized at 77.24°C with a weight loss of 6.86% that represent the loss of free water in the film, the second at 173.09°C with a weight loss of 14.07% that correspond to chemisorbed water (57) and the third at 288.39°C with a weight loss of 35.42% is related to dehydration, depolymerization, pyrolytic decomposition of polysaccharide backbone (58). Some authors (62) have been reported only two steps of decomposition in chitosan films and others (59) four steps, the first at 140°C (10% of weight loss), the second between 275 and 335°C (30% of weight loss), the third at 450°C (10% of weight loss) and the fourth at 550°C (15% of weight loss).

Table 3.7 TGA characterization of chitosan films incorporated with HAE Ca and AAE.

Formulation	Peak 1		Peak 2		Peak 3	
	Temperature (°C)	Weight loss (%)	Temperature (°C)	Weight loss (%)	Temperature (°C)	Weight loss (%)
Control	77.24 ± 4.37	6.86 ± 0.61	173.09 ± 0.58	14.07 ± 0.40	288.39 ± 0.32	35.42 ± 0.03
AAE 2%	74.13 ± 4.25	6.92 ±2.33	NA	NA	286.08 ± 1.48	33.71 ± 1.14
AAE 4%	75.40 ± 0.27	5.38 ± 0.09	NA	NA	287.57 ± 4.18	33.11 ± 1.75
AAE 6%	74.22 ± 0.15	5.89 ± 0.32	NA	NA	289.71 ± 3.62	33.13 ± 0.37
HAECa 8%	90.77 ± 7.21	5.43 ± 0.84	143.64 ± 2.52	10.75 ± 0.48	286.81 ± 2.38	31.47 ± 0.77
HAECa 10%	82.67 ± 5.42	3.18 ± 0.49	146. 76 ± 3.18	9.79 ± 1.12	294.53 ± 1.07	33.25 ± 0.22
HAECa 12%	86.08 ± 1.03	2.59 ± 0.05	145.92 ± 1.09	9.37 ± 0.51	290.61 ± 5.67	32.97 ± 2.03

Formulation	Peak 4		Peak 5	
	Temperature (°C)	Weight loss (%)	Temperature (°C)	Weight loss (%)
Control	NA	NA	NA	NA
AAE 2%	NA	NA	NA	NA
AAE 4%	NA	NA	NA	NA
AAE 6%	NA	NA	NA	NA
HAECa 8%	453.32 ± 7.42	55.06 ± 0.04	594.55 ± 4.90	61.41 ± 1.07
HAECa 10%	457.38 ± 5.91	55.13 ± 0.53	591.71 ± 7.98	61.51 ± 0.51
HAECa 12%	429.10 ± 11.48	53.44 ± 1.87	581.16 ± 3.90	61.50 ± 1.63

NA: Not applicable

The TGA study also showed a clear difference between the chitosan films incorporated with AAE (**Figure 3.16**) and HAECa (**Figure 3.17**). The chitosan films with AAE presented only two steps of decomposition, the first localized between 74.13°C and 75.40°C and the second localized between 286.68°C and 289.71°C; these peaks correspond to the process of losing moisture and the decomposition process, a significant concentration effect was not observed. The weight loss of each stage show in **Table 3.7**.

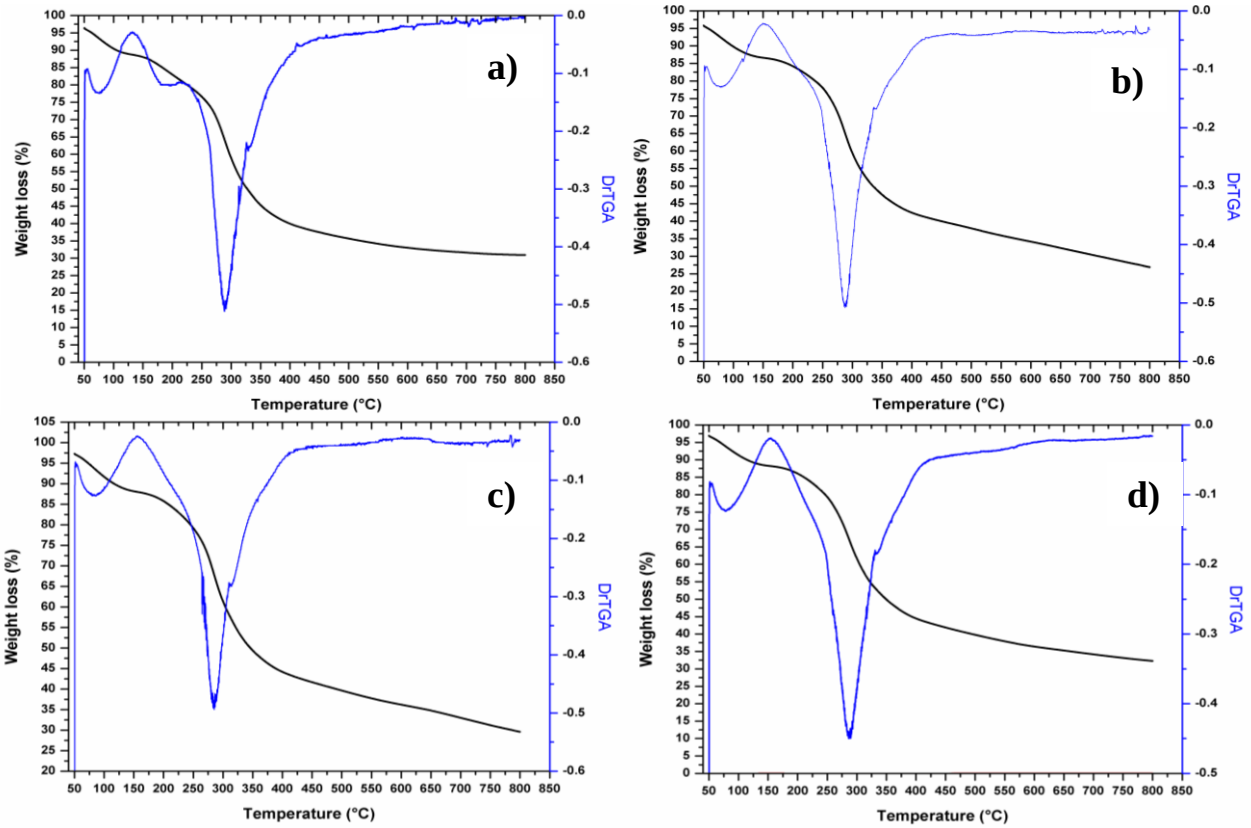

Figure 3.16. Behavior of the thermal decomposition of chitosan film incorporated with AAE (**a**) Control (**b**) AAE 2% (**c**) AAE 4% (**d**) AAE 6%

The chitosan films with HAECa shown five steps of decomposition, the first localized between 82.67 °C and 90.77°C, the second localized between 143.64°C and 146.76, the third localized between 286.81°C and 294.53°C, the fourth localized between 429.10°C and 457.38°C and the fifth localized between 581.16°C and 594.55°C. The peaks correspond to the process of free water loss, water chemisorbed loss, dehydration, depolymerization and pyrolytic backbone decomposition of the biopolymer [57, 60]. The shift in the decomposition temperature, as well as the generation of more steps of decomposition, may be attributed to the interaction between the amino groups of chitosan with hydroxyl groups of the extract [53], also to the existence of aromatic compounds in the HAECa, as the resonance of benzene ring gives thermal stability which results in an increment of the decomposition temperature [61]. Other authors observed that the presence of compounds, such as polyethylene glycol methyl ether, into chitosan matrix increase the offset of the decomposition temperature until 453°C [62]. The weight loss of each stage show in **Table 3.7**.

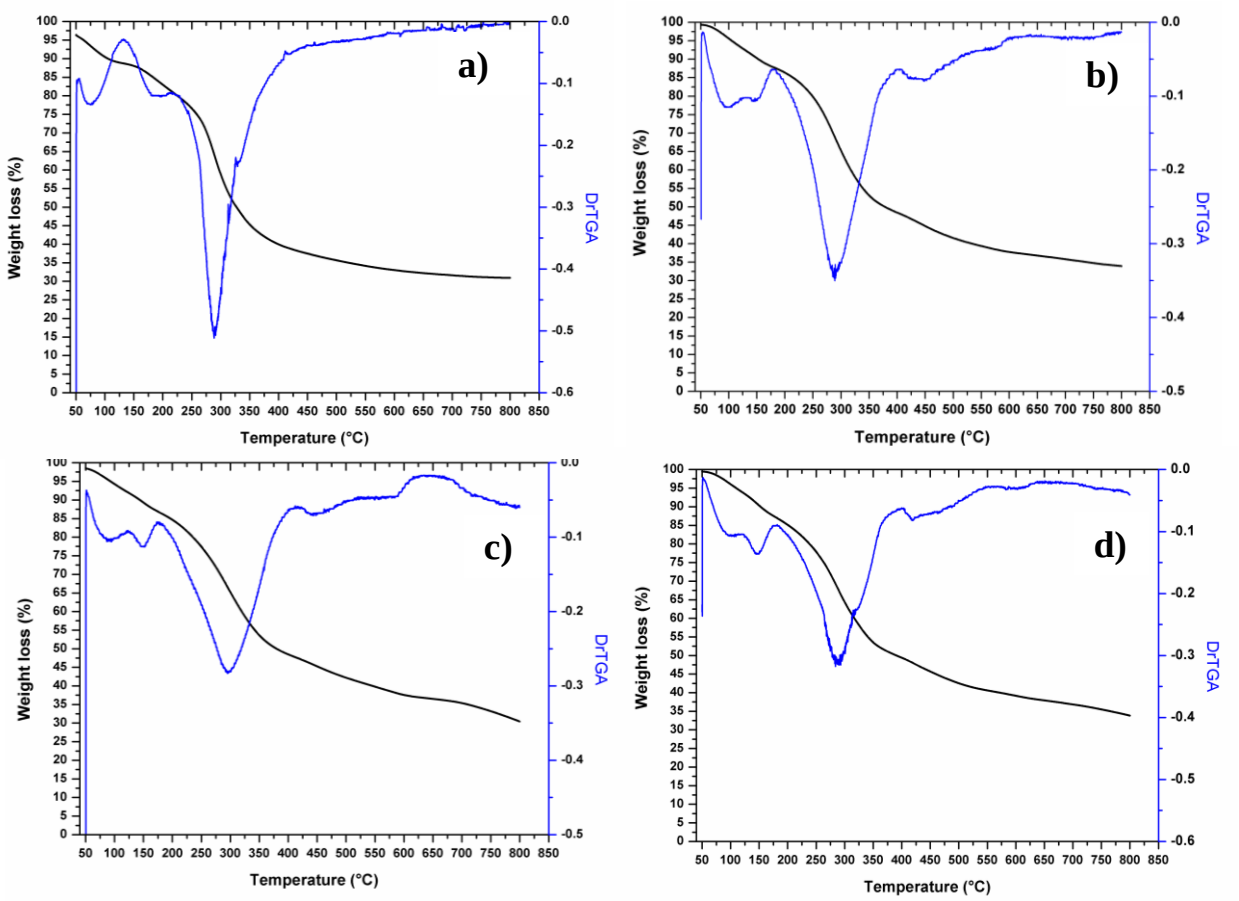

Figure 3.17. Behavior of the thermal decomposition of chitosan film with HAE Ca (**a**) Control, (**b**) HAE Ca 8%, (**c**) HAE Ca 10% (**d**) HAE 12%.

Water content by isotherm in TGA equipment

The graphs of the isotherm of the chitosan films with AAE and HAECa obtained in the water content test show in **Figure 3.18**. In both graphs can be observed two phases, a dynamic (from 30°C to 120°C) and other isothermal (120°C). In the last, was observed that the chitosan films with AAE showed a minor drop than the films with HAECa.

Also is notable the difference in the form of the curve developed, the control and chitosan films with AAE took convex form and the chitosan films with HAECa took a concave form. The convex form indicates that when the temperature was increased in the dynamic phase, the loss of components in the film (such as free water and volatile compounds) was more quickly, while that the concave form indicates a paused loss of components, which denote higher stability during this phase, which may be associated that HAECa had best interaction with the chitosan matrix and can generate new bonds.

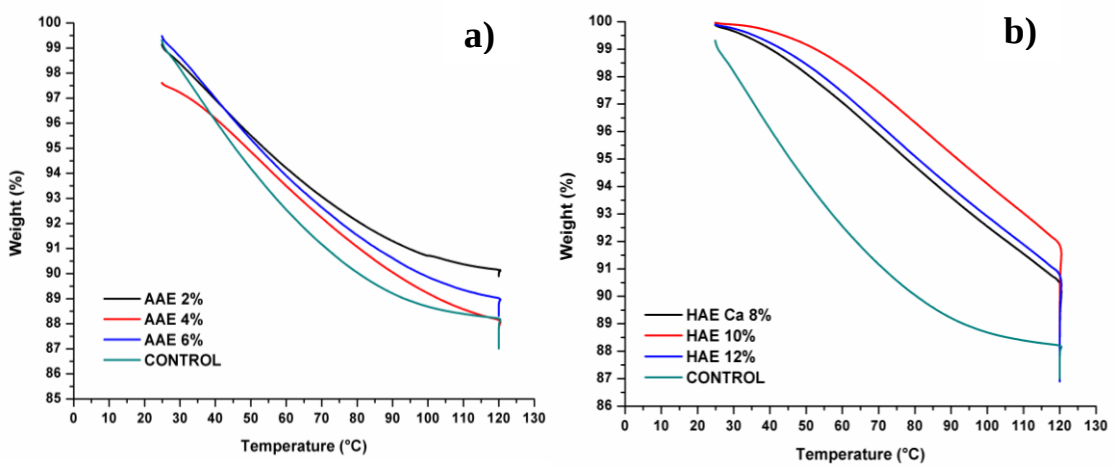

Figure 3.18 Behavior of the isotherm in the water content test of chitosan films incorporated with **(a)** AAE **(b)** HAECa

In **Figure 3.19** can be observe the values of weight loss percentage by phase (dynamic and isothermal) in control films and chitosan films with extracts. In the dynamic phase, it was not observed a significant difference between the control and the chitosan films with AAE, while among the chitosan films with HAECa only the concentration of 10% showed a significant difference ($P<0.05$) in comparison to control film. In the isothermal phase, the weight loss percentage in the chitosan films with AAE was lower (0.35 to 0.58 %) than the chitosan films with HAECa (2.73 to 3.95 %), which denote a significant difference between these extracts and confirm the observation carried out previously in the **Figure 3.18**.

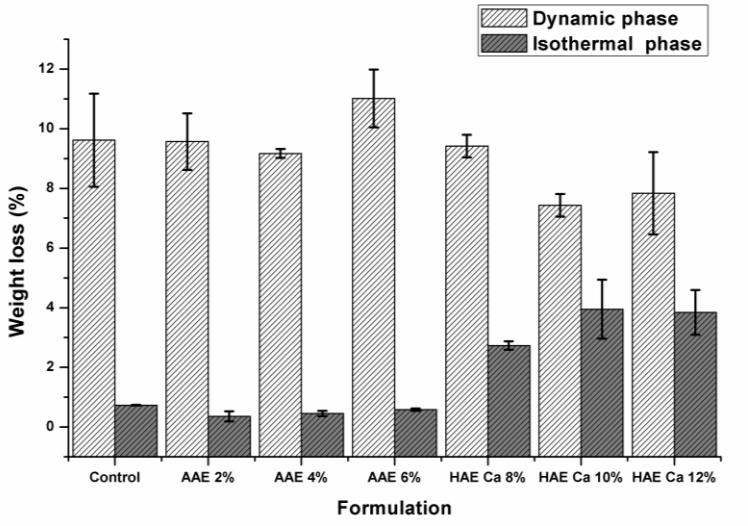

Figure 3.19 Weight loss (%) by phase in the water content test of chitosan films incorporated with AAE and HAE Ca

This behavior may be associated with the results obtained by other authors in previous studies [11]. These authors indicate that due to chitosan structure, water molecules can be bound by two polar groups, hydroxyl, and amine, present in the molecule.

FTIR studies carried out previously [63, 64] showed that the interaction of the water with OH groups is stronger than the amine groups and that when the chitosan films present low water content, it is bonded weakly to the chitosan through of the N-H group and that in a thermal analysis this water is removed at temperatures below 100°C.

While that when the water molecules bonded to chitosan through of the O-H group, the thermal analysis shows peaks attributed to the loss of water at temperatures above 100°C. The affinity of the molecules of water by the O-H group of the chitosan structure causes a chemisorption phenomenon, which was observed previously in the DSC and TGA analysis of the present research, through of the presence of a peak between 173.4°C and 186.52 °C in the first study and 143.64 °C and 146.76 °C in the second test.

Scanning Electron Microscopy (SEM) with Chemical Analysis by Energy Dispersive Spectroscopy (EDS).

The **Figure 3.20** shows the SEM images of the chitosan films with AAE, where differentcannot be observed differences in the surface of these with the increment of the concentration of the extract, only some impurities of the chitosan were observed. In general, the surface of the control and the chitosan films with AAE were homogeneous and continuous and a separation of phases were not observed.

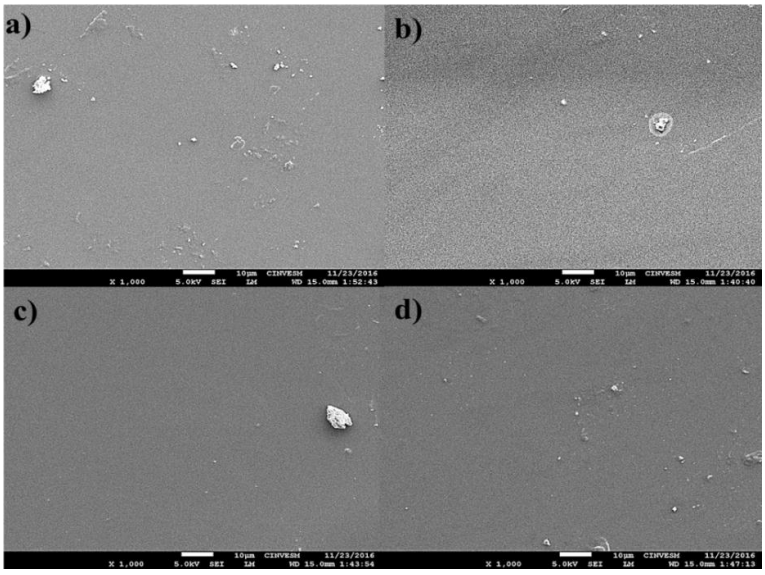

Figure 3.20. SEM images of chitosan films with AAE at different concentrations (**a)** Control (chitosan film) (**b)** 2% AAE (**c)** 4% AAE (**d)** 6% AAE. Magnification 1000 X

The SEM images of the chitosan films with HAECa (**Figure 3.21**) showed notable differences concerning the control films when the concentration of the extract increased. The difference consisted in the formation of small pores in the films; the distribution of these in the surface of the films was homogenous, and the amount of the pores increased to high concentrations of the extract. This characteristic of the surface of the chitosan films incorporated with HAECa explain the behavior observed in the cellular adhesion test. The formation of the pores in the surface of this kind of films may be associated with the interaction among the extract and the chitosan matrix during the process of incorporation and also to the drying process of the films.

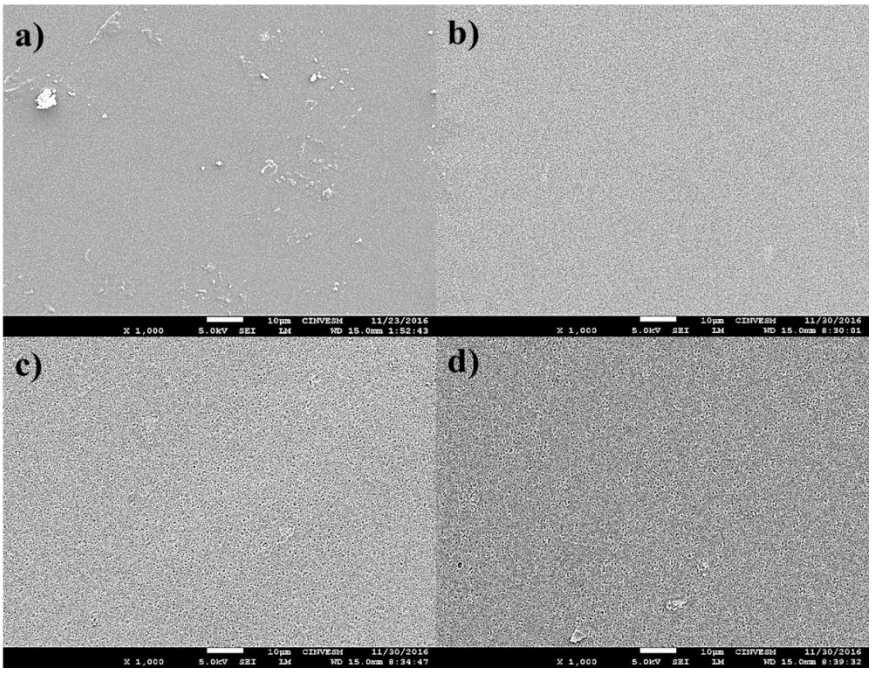

Figure 3.21 SEM images of chitosan films with HAECa at different concentrations: (**a)** Control (chitosan film), (**b)** 8% HAECa, (**c)** 10% HAECa, and (**d)** 12% HAECa. Magnification 1000 X

The **Table 3.8** shows the results of the EDS test of the chitosan films with AAE and HAECa comparing with the control, where can be the observed difference in both extracts. In chitosan films with AAE was observed a decrease in nitrogen percent and an increment in values of carbon percentage, which was more notable when the concentration of the extract increased. The chitosan films with HAECa showed a decrement in values of nitrogen percentage and oxygen percentage, but these films showed an increment in carbon percentage. These results confirm that

the last extract had a high interaction with the chitosan matrix than the other extract (AAE), which modified several properties of the films, which have been described previously.

Table 3.8 EDS results of the chitosan film control and chitosan films with AAE and HAE Ca at different concentrations.

Element	Weight%						
	Control	**AAE 2%**	**AAE 4%**	**AAE 6%**	**HAECa 8%**	**HAECa 10%**	**HAECa 12%**
C	47.35	48.62	54	53.45	59.92	57.87	57.88
N	7.42	6.66	**ND**	**ND**	5.73	5.17	5.02
O	44.66	44.05	44.73	44.62	34.14	36.59	36.71
Na	0.2	0.19	0.23	0.44	**ND**	**ND**	**ND**
Cl	0.38	0.48	0.59	0.69	0.21	0.37	0.38
K	**ND**	**ND**	0.28	0.55	**ND**	**ND**	**ND**
Ca	**ND**	**ND**	0.18	0.24	**ND**	**ND**	**ND**
Totals	100	100	100	100	100	100	100

ND: Not detected

components with the goal of to observe changes and interaction grade between these. For instance, chitosan films with polyvinyl alcohol (PVA), where was observed through of this technique, the blends of these components experimented a physical and chemical interaction and that the crosslink of the networks was a success [65].

3.2.3 Conclusions

The addition of HAECa into chitosan matrix exerted changes in the thickness of chitosan films, as well as in surface characteristics as the color. Also, modified the mechanical properties of the chitosan films, which suggest a possible chemical interaction between the extract and the biopolymer.

The addition of HAECa into chitosan matrix affected the parameters of color (increase of ΔE and C*), transparency-opacity (decrease), contact angle (change of hydrophobic to hydrophilic character) and water transmission rate (increase) of the films obtained, which indicate a good grade of chemical interaction between the biopolymer and the extract. These changes in ΔE and C* may be a result of the chemical interaction between some compounds of the extract (such as carotenoids) and the biopolymer. The changes in the contact angle and water transmission rate may be the cause for the action of some functional groups (such as OH) from the extract on the chitosan matrix.

The shift and overlap of some bands in the FTIR spectrum of chitosan films with HAECa and AAE indicate a grade of interaction between these components. These changes were mainly in the bands between 3100-3500 cm^{-1}, which show that the interaction was carried out through O-H and N-H bonds, probably with hydrogen bonds. In the case of HAECa another important change in bands was at 1643 cm^{-1} (chlorophyll that overlaps to C=O signal of amide type I of the chitosan), indicating interaction also through amino groups; while that with AAE, this band only suffered a slight displacement. On the other hand, the films with these extracts conserved particular compounds after adding in the chitosan matrix; in the case of HAECa, conserved the band at 1373 cm-1 (β- carotene pigment), and the peak at 1092 cm^{-1} (terpenoid or flavonoids compounds) while that AAE conserved bands associated to monounsaturated aromatic ring that may be indicate the presence of compounds such as eugenol.

The incorporation of the HAECa into the chitosan matrix caused significant thermal changes in the films, which could be observed through DSC, TGA tests and also caused changes in the isothermal behavior test. These results indicate a strong interaction between the chitosan matrix and the extract that resulted in the better thermal stability of the films obtained with respect to the control films. Moreover, the incorporation of AAE into chitosan matrix was not produced essential changes in the thermal properties of the films obtained.

The SEM images and the EDS results confirm that the HAECa extract had a high interaction with the chitosan matrix, which was previously observed in others tests such as DSC, and FTIR. This interaction was through of both bond groups of the chitosan, NH, and OH.

3.2.4 References

1. Rana VK, Pandey AK, Singh RP. Enhancement of thermal stability and phase relaxation behavior of chitosan dissolved in aqueous *l*-Lactic acid: using 'silver nanoparticles' as nano filler. Macromol Res. 2010.18 (8): 713-720.
2. Rubilar JF, Cruz RMS, Silva HD, Vicente AA, Vieira MC, Khmelinskii I J. Physico-mechanical properties of chitosan films with carvacrol and grape seed extract. Food Eng. 2013.115: 466-474.
3. Zivanovic S, Chi S, Draughon F. Antimicrobial activity of chitosan films enriched with essential oils. J Food Sci. 2005. 70(1): M45-M51.
4. Vimala K, Murali Mohan K, Sivudu S, Varaprasad K, Ravindra S, Narayana R, Padma Y, Sreedhar B, Mohana Raju K. Fabrication of porous chitosan films impregnated with silver nanoparticles: A facile approach for superior antibacterial application. Colloids Surf. B. 2010. 76: 248-258.

5. Noel SP, Courtney H, Bumgardner JD, Haggard WO. Chitosan Films. A potential local drug delivery system for antibiotics. Clin Orthop Relat Res.2008. 466:1377–1382.
6. Khoshgozaran-Abras S, Azizi MH, Hamidy Z, Bagheripoor-Fallah N. 2012. Mechanical, physicochemical and color properties of chitosan based-films as a function of *Aloe vera* gel incorporation. Carbohyd Polym. 2012. 87: 2058-2062.
7. Da Silva S, Amorim M, Fonte P, Madureira R, Ferreira D, Pintado M, Sarmento B. Natural extracts into chitosan nanocarriers for rosmarinic acid drug delivery. Pharm Biol, 2015. 53(5): 642–652.
8. Butnariu M, Coradini CZ. Evaluation of biologically active compounds from *Calendula officinalis* flowers using spectrophotometry. Chem Cent. J. 2012; 35 (6):1–2.
9. Vieira P, M de Morais S, Bezerra HQF, Travassos-Ferreira PA, Oliveira IR, Silva MGV. Chemical composition and antifungal activity of essential oils from *Ocimum* species. Ind. Crop. Prod. 2014; 55: 267–271.
10. Shiku Y, Hamaguchi PY, Tanaka M. Effect of pH on the preparation of edible films based on fish myofibrillar proteins. Fish Sci. 2003. 69(5):1026–1032.
11. Fang Y, Tung MA, Britt IJ, Yada S, Dalgleish DG. Tensile and barrier properties of edible films made from whey proteins. J Food Sci. 2002. 67: 188-193.
12. Han JH, Floros JD. Casting antimicrobial packaging films and measuring their physical properties and antimicrobial activity. J. Plast Film Sheet. 1997. 13: 287–298.
13. Abugoch LE, Tapia C, Villamán MC, Yazdani-Pedram M, Díaz-Dosque M. Characterization of quinoa protein chitosan blend edible films. 2011. J Food Hyd. 25: 879-886.
14. Moradkhani S, Salehi I, Abdolmaleki S, Komaki A. Effect of *Calendula officinalis* hydroalcoholic extract on passive avoidance learning and memory in streptozotocin-induced diabetic rats. Anc Sci Life. 2015; 34(3):156-161.
15. Khoshgozaran-Abras S, Azizi MH, Hamidy Z, Bagheripoor-Fallah N. 2012. Mechanical, physicochemical and color properties of chitosan based-films as a function of *Aloe vera* gel incorporation. Carbohyd Polym. 2012. 87: 2058-2062.
16. Wang Q, Tian F, Feng Z, Fan X, Pan Z, Zhou J. Antioxidant activity and physicochemical properties of chitosan films incorporated with *Lycium barbarum* fruit extract for active food packaging. Int J Food Sci Tech. 2015. 50: 458-464.
17. Garcia MA, Pinotti A, Zaritzky NE. Physicochemical, water vapor barrier and mechanical properties of corn starch and chitosan composite films. Starch. 2006. 58(9), 453– 463.

18. Altiok D, Altiok E, Tihminlioglu F. Physical, antibacterial and antioxidant properties of chitosan films incorporated with thyme oil for potential wound healing applications. J Mater Sci Mater Med. 2010.21(7):2227-36.
19. Siripatrawan U, Harte BR. Physical properties and antioxidant activity of an active film from chitosan incorporated with green tea extract. Food Hydrocoll. 2010. 24: 770–775.
20. Kobaisi M.A., Murugaraj, P., Mainwaring, D.E. Origin and influence of water-induced chain relaxation phenomena in Chitosan biopolymers. J. Polym. Sci. Part B. 2012. 50:403-414.
21. Kaminski K, Kaminska E, Ngai KL, Paluch M, Wlodarczyk P, Kasprzycka A, Szeja W. Identifying the origins of two secondary relaxations in polysaccharides. J Phys Chem B. 2009.113: 10088-10096.
22. Moradi M, Tajik H, Rohani SMR, Oromiehie AR, Malekinejad H, Aliakbarlu J, Hadian M. Characterization of antioxidant chitosan film incorporated with *Zataria multiflora Boiss* essential oil and grape seed extract. LWT - Food Sci Technol. 2012. 46:477–484.
23. Siripatrawan U, Harte BR. Physical properties and antioxidant activity of an active film from chitosan incorporated with green tea extract. Food Hydrocoll. 2010. 24: 770–775.
24. Wang L, Wang Q, Tong J, Zhou J. Physicochemical properties of chitosan films incorporated with honeysuckle flower extract for active food packaging. J Food Process Eng. 2015. 40.
25. Martins JT, Cerqueira MA, Vicente AA. Influence of α-tocopherol on physicochemical properties of chitosan-based films. Food Hydrocoll. 2012. 27(1): 220-227.
26. Andrady AL, Torikai A, Kobatake T. Spectral sensitivity of chitosan photodegradation. J Appl Polym Sci. 1996. 62: 1465-1471.
27. Sionkowska A, Wisniewski M, Skopinska J, Kennedy CJ, Wess TJ. The photochemical stability of collagen–chitosan blends. J. Photochem Photobiol: Chem. 2004. 162: 545–554.
28. Bunghez IR, Ion RM. Complex spectral characterization of active principles from Marigold. J Sci Arts. 2011. 14 59-64.
29. Mandal S, Bhattacharya S. Uv-Vis and FTIR spectroscopic analysis of phytochemicals and functional group in *ocimum sanctum* and a few medicinal plants. Romanian J Biophys. 2015. 25(4):
30. Archana D, Dutta J, Dutta P.K. Evaluation of chitosan nano dressing for wound healing: Characterization, *in vitro* and *in vivo* studies. Int. J. Biol. Macromol. 2013. 57: 193-203.
31. Hosseinkazemi H, Biazar E, Bonakdar S, Ebadi MT, Shokrgozar MA, Rabiie M. Modification of PCL electrospun nanofibrous mat with *Calendula officinalis* extracts for improved interaction with cells. Int J Polym Mater Polym Biomater. 2014. 64: 459-464.

32. Welti-Chanes J, Velez-Ruiz J, Barbosa-Canovas G. Transport phenomena in Food processing. Food Preservation Technology Series. CRC-Press. Taylor & Francis. 2002. Pp. 225.

33. Kampeerapappun P, Aht-ong D, Pentrakoon D, Srikulkit K. Preparation of cassava starch/montmorillonite composite film. Carbohydr Polym. 2007. 67: 155–163.

34. Bangyekan C, Aht-Ong D, Srikulkit K. Preparation and properties evaluation of chitosan-coated cassava starch films. Carbohydr Polym. 2006. 63: 61–71.

35. Queen D, Gaylor JDS, Ebans JH, Courtney JM. The preclinical evaluation of the water vapour transmission rate through burn wound dressings. Biomaterials. 1987. 8: 367- 371.

36. Vimala K, Mohan YM, Sivudu KM, Varaprasad K, Ravindra S, Reddy NN, Padma Y, Sreedhar B. Fabrication of porous chitosan films impregnated with silver nanoparticles: A facile approach for superior antibacterial application. Colloids Surf B Biointerfaces. 2010.76: 248–258.

37. Archana D, Dutta J, Dutta PK. Evaluation of chitosan nano dressing for wound healing: Characterization, *in vitro* and *in vivo* studies. Int J Biol Macromol. 2013. 57: 193-203.

38. El-Kemary M, Ibrahim E, A-Ajmi MF, Khalifa SAM, Alanazi AD, El-Seedi HR. *Calendula officinalis*-mediated biosynthesis of Silver Nanoparticles and their Electrochemical and Optical Characterization. Int J Electrochem Sci.2016. 11: 10795 – 10805.

39. Bunghez I.R., Ion R.M., Complex spectral characterization of active principles from marigold

(*Calendula Officinalis*). J Sci Arts. 2011. 14: 59-64.

40. Fierascui I, Bunguez IR, Fierascui R, Ion RM, Dinu-Pîrvu CE, Nuţă D. Characterization and antioxidant activity of phytosynthesised silver nanoparticles using *Calendula officinalis* extract. Farmacia. 2014 62(1): 129-136.

41. Hosseinkazemi H, Biazar E, Bonakdar S, Ebadi MT, Shokrgozar MA, Rabiie M. Modification of PCL electrospun nanofibrous mat with *Calendula officinalis* extracts for improved interaction with cells. Int J Polym Mater Polym Biomater. 2014. 64: 459-464.

42. Mandal S, Bhattacharya S. UV-VIS and FTIR spectroscopic analysis of phytochemical and functional group in *Ocimum sanctum* and a few medicinal plants. Romanian J Biophys. 2015. 25 (4): 247–257.

43. Ruju RS, Sakuntala P, Jaleeli KA. FTIR Spectroscopic analysis of *Ocimum gratissimum* leaves. IJETER. 2017. 5(4): 131-133.

44. Aynul Rifaya M, Meyyapan RM. The antibacterial effect of phyto-mediated silver nanoparticles produced from *Ocimum sanctum* L. (Lamiaceae) leaf extract. Afr J Microbiol Res. 8(1): 118-128.

45. Mallikaljona K, Narasimha G, Dillip GR, Praveen B, Shreedhar B, Lakshmi CS, Reddy BVS, Raju BDP. Green synthesis of silver nanoparticles using *Ocimum* leaf extract and their characterization. Dig J Nanomater Biostruc. 2011. 6(1): 181-186.

46. Balamurughan MG, Muhanraj S, Kodhalyolli S, Pugalenthl V. Ocimum sanctum leaf extract mediated green synthesis of iron oxide nanoparticles: Spectroscopic and microscopic studies. J Chem Pharm Sci. 2014. 4: 201-204.

47. Raot S, Thorat PV, Thakre R. Green synthesis of zinc oxide nanoparticles using *Ocimum tenuiflorum* leaves. IJSR. 2015. 4(5): 1225-1228.

48. Kulkarni VD, Kulkarni PS. Green synthesis of copper nanoparticles using Ocimum sanctum leaf extract. Int J Chem. 2013. 1(3): 1-4.

49. Anuradha G, Syama Sundar B, Ramana MV. *Ocimum americanum* L. leaf extract mediated synthesis of silver nanoparticles. A novel approach towards weed utilisation. Arch Appl Sci Res. 2014. 6(3): 59-64.

50. Anuradha G, Syama Sundar B, Sreekanthkuma J, Ramana MV. Synthesis and characterization of silver nanoparticles from *Ocimum basilicum* L. var. thyrsiflorum. EJAE.2014. 1(5): 5-9.

51. Joshi S, Karna AK. Analysis of phytoconstituents and cytotoxic activities of different parts of *Ocimum sanctum*. Int J Appl Sci Biotechnol. 2013. 1(3): 137-144.

52. Coates J. Interpretation of Infrared Spectra, A Practical Approach. Encyclopedia of Analytical Chemistry. R.A. Meyers (Ed.). John Wiley & Sons Ltd, Chichester. 2000. pp. 8.

53. Rodriguez LB, Leite HF, Yoshida MI, Saliba JB, Cunha Junior AS, Faraco AAG. In vitro release and characterization of chitosan films as dexamethasone carrier. Int J Pharm. 2009. 368: 1-6.

54. Guinesi LS, Cavalheiro ETG. The use of DSC curves to determine the acetylation degree of chitin/chitosan samples. Thermochim Acta. 2006.444:128-133.

55. Mucha M, Pawlak A. Thermal analysis of chitosan and its blend. Thermochim Acta. 2005. 427: 69-76.

56. Peng Y, Wu Y, Li Y. Development of tea extracts and chitosan composites for active packaging materials. Int J Biol Macrom. 2013. 59: 282-289.

57. Martins JT, Cerqueira MA, Vicente AA. Influence of α-tocopherol on physicochemical properties of chitosan-based films. Food Hydrocolloids. 2012: 27: 220-227.

58. Zohuriaan MJ, Shokrolahi F. Thermal studies on natural and modified gums. Polymer Testing. 2004. 23: 575-579.

59. Archana D, Dutta J, Dutta PK. Evaluation of chitosan nanodressing for wound healing: Characterization, in vitro and vivo studies. Int J Biolog Macromoleculas. 2013. 57: 193-203.

60. Khalid MN, Agnely F, Yaguubi N, Grossiord JL, Covarraze G. Water state characterization, swelling behavior thermal and mechanical properties of chitosan based networks. European J Pharmaceutical Sciences. 2002. 15: 245-432.

61. Pelissari FM, Grossmann MVE, Yamashita F, Pineda EAG. Antimicrobial, Mechanical, and Barrier Properties of Cassava Starch-Chitosan Films Incorporated with Oregano Essential. J Agric Food Chem. 2009. 57: 7499–7504.

62. Sarwar MS, Ghaffar A, Islam A, Yasmin F, Oluz Z, Tuncel E, Duran H, Qaiser AA. Controlled drug release behavior of metformin hydrogen chloride from biodegradable films based on chitosan/poly(ethylene glycol) methyl ether blend. Arab J Chem. 2017.

63. Neto CGT, Giacomelti JA, Job AC, Ferreira FC, Fonseca JLC, Pereira MR. Thermal Analysis of Chitosan Based Networks. Carbohyd Polym. 2005. 62: 97-103.

64. Rueda DR, Secall T, Bayer RK. Differences in the interaction of water with starch and chitosan films as revealed by infrared spectroscopy and differential scanning calorimetry. Carbohyd Polym. 1999. 40: 49–56.

65. De Souza Costa-Junior E, Pereira M, Mansur HS. Properties and biocompatibility of chitosan films modified by blending with PVA and chemically crosslinked. J Mater Sci: Mater Med. 2009. 20:553–561.

3.3 Antimicrobial activity of films based on chitosan, aqueous extract of *Ocimum micranthum* Willd leaves and hydro-alcoholic extract of *Calendula officinalis* L. flowers.

3.3.1. Experimental Methods

Microbial strains

The microorganisms used to evaluate the antimicrobial activity of the chitosan film added with AAE and HAECa included two species of Gram-positive bacteria (*Staphylococcus aureus* ATCC® 25973TM and *Bacillus subtilis* ATCC® 465 TM); one species of Gram-negative bacteria (*Pseudomonas aeruginosa* ATCC ® 27853 TM) and a yeast-fungus (*Candida albicans* ATCC® 14053 TM).

Treatment of samples for antimicrobial activity test

The films added with AAE (2% % and 6% v/v) and HAECa (8% 10% and 12%) extracts, and chitosan films controls were exposed to UV light for 30 min.

Agar disc-diffusion test

The antimicrobial activity of the chitosan film added with AAE and HAECa was determined through the agar disc-diffusion method. For this purpose, Mueller Hinton agar (Merck VM556437 329) was prepared according to the manufacturer's instructions and deposited in Petri dishes, which were submitted to the sterility test. After, the Petri dishes with Mueller Hinton (a total of six) were inoculated with 100 μL of a dilution at 1.5 x 10^8 CFU/mL (equivalent to 0.5 of the McFarland scale) of each microorganism tested. Then, the inoculum was dispersed in the Petri dishes through of the extension technique using digralski spreader, after were deposited discs of 5mm of diameter of each formulation of chitosan films with extracts (by triplicate) on the extremes of the Petri dishes, which were incubated at 35°C for 24 h *(S. aureus, B. subtilis* and *P. aeruginosa*) and 48 h (*C. albicans*). Also were deposited disc with amikacin (4 mg/L) and Nystatin (2 mg/L) such as positive controls and controls of chitosan film. Finished the incubation time, the Petri dishes were reviewed searching inhibition growth. In the case where inhibition growth zones were present, the diameter was measured.

Complementary tests

Two samples of chitosan films with extracts were taken of the Petri dishes where the effect of the contact against microorganism growth was observed. These were placed in other Petri dishes

with Mueller Hinton agar and incubated at 35°C for 24 h (*S. aureus, B. subtilis,* and *P. aeruginosa*) and 48 h (*C. albicans*). Once the incubation period had lapsed, in the Petri dishes where the effect by the contact against microorganism growth was observed again, the films were covered with a solution of iodonitrotetrazolium chloride 0.25 mg/mL (58030-1g-F Sigma Aldrich®), after the Petri dishes were incubated at 35 °C for 1 h. Finished the incubation time, these were reviewed to observe if present or not a color change. A change in pink color indicates the presence of viable microorganisms, while that the absence of change in color indicates the absence of microorganism growth.

In the particular of *C. albicans*, of the Petri dishes where this microorganism was grown, samples of chitosan films with extracts were taken, and these were soaked in saline solution (0.85%) and washed two times with PBS 1X. After, the films were treated with alcoholic solutions (50, 70, 90 and 100%) and submitted to a process of critical point drying (equipment Quorum K850 model) during 1 h. Finally, some samples were observed in an optical microscope Labomed TCM 400 LM-7125000 model with 4X objective and others were covered with a layer of gold through a metallization process (equipment Quorum Q150R ES model) and these were observed in an SEM microscope Phillips XL-30 Series using 5 kV of voltage, SEM mode, a magnification of 1500 X. Photographic records were taken. This test was carried out with the purpose of to observe possible cell adherence of this microorganism onto chitosan films with extracts, due to in part to its eukaryote nature.

3.3.2. Results and discussions.

Agar disc-diffusion test and complementary tests

Table 3.9 summarizes the results of the agar disc-diffusion test, where the chitosan film control and chitosan films with AAE and HAECa did not present inhibitory effect by diffusion against the test microorganisms. However, the chitosan films with HAECa presented an effect by contact against *P. aeruginosa*, microorganism Gram-negative, which was observed in all formulations with this extract. On the other hand, the chitosan films with AAE also presented an effect by contact, in this case, against *B. subtilis,* microorganism Gram-positive. Amikacin (positive control) showed a better inhibition capacity against *P. aeruginosa* (gram-negative) than *S. aureus* (gram-positive). The other positive control (Nystatin) also showed the capacity of inhibition, in this case against *C. albicans*, a yeast fungus. The chitosan film control did not show the inhibitory effect by diffusion or contact against all test microorganisms. Diverse authors [1,2] have mentioned the antimicrobial activity of the chitosan in solutions, which depends on many factors such as deacetylated degree, molecular weight, concentration in a solution, pH and ionic strength. However,

some authors [3, 4] have reported loss of antimicrobial activity of chitosan films, which attributed to the low capacity of diffusion on the agar of the amino groups into of the film structure; this functional group is responsible for the antimicrobial activity of the chitosan, because its interaction with the negatively charged microbial cell membranes (electrostatic forces model) causes an increase of bacterial membrane permeability and cell growth inhibition [5, 6]. The capacity for diffusion is affected by the chemical structure and crosslinking level of the films as well as the size, shape, and polarity of the diffusing material [7].

Table 3.9 Agar disc-diffusion results of positive controls, the chitosan film control and chitosan films with AAE and HAE Ca at different concentrations.

FORMULATION	*S. aureus Gram*(+)		*B.subtillus* Gram (+)		*P. aeruginosa* Gram (-)		*C. albicans* (yeast-fungus)	
	Inhibitory (mm)	Contact	Inhibitory (mm)	Contact	Inhibitory (mm)	Contact	Inhibitory (mm)	Contact
CONTROL FILM	0	-	0	-	0	-	0	-
AMIKACIN	10.50 ± 0.71	+	21 ± 1.41	+	30.50 ± 0.71	+	NA	
NYSTATIN	NA		NA		NA		5.50 ± 0.70	+
HAECa 8%	0	-	0	-	0	+	0	-
HAECa 10%	0	-	0	-	0	+	0	-
HAECa 12%	0	-	0	-	0	+	0	-
AAE 2%	0	-	0	+	0	-	0	-
AAE 4%	0	-	0	+	0	-	0	-
AAE 6%	0	-	0	+	0	-	0	-

Mean ± standard deviation (n=3). Inhibitory is inhibitory zone surrounding film discs ; Contact is contact area under disc on agar surface.- indicates growth in the area, + indicates no growth; Control film is a film disc without extract; **NA:** Not applicable

In **Figure 3.22**, it can be observed the inhibition effect that chitosan films with HAECa have against *P. aeruginosa.* It can be observed that the film avoided the growth of microorganism into the area under the disc on the agar surface. This effect was presented in all concentrations of the extract. This result indicates that the HAECa conserved its antimicrobial effect against this microorganism showed in a previous test (CMI), but when it is incorporated into the chitosan matrix this effect cannot diffuse around in the sample area. This lack of the diffusion capacity of the extract may be associated with the chemical interaction grade reached with the chitosan matrix, due to probably to its ethanolic nature, as well as its chemical composition.

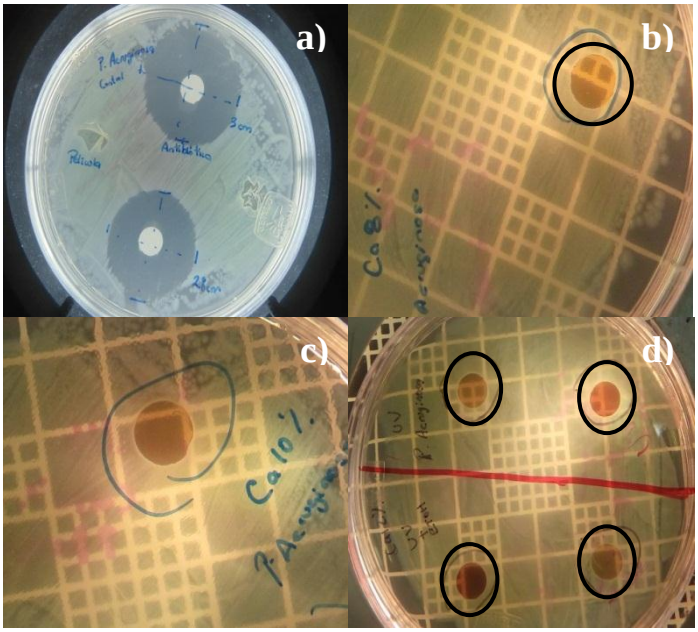

Figure 3.22 Images of the agar disc-diffusion test of chitosan films with HAE Ca at different concentrations using *P. aeruginosa* microorganism (**a)** Positive control (amikacin 4mg/mL) (**b)** 8% (**c)** 10% (**d)** 12%.

The **Figure 3.23** shows the confirmation of the effect by contact of the chitosan films with HAECa against *P. aeruginosa*, which was carried out through staining with a solution of iodonitrotetrazolium chloride 0.25 mg/mL. In this test, the change to pink color denote the presence of viable microorganisms, which in the image only can be observed this change around the sample of film, but not in the contact area with the agar surface. The change of color around the sample of the film may be attributed to a few cells of the microorganism that remained adhered to the edge of the film when was passed to Petri dish with Mueller-Hinton agar in the confirmation test of the effect by contact.

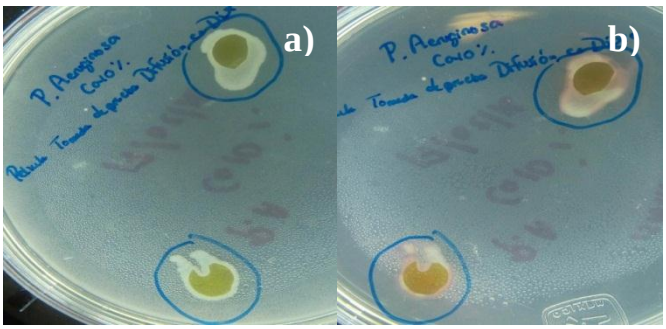

Figure 3.23 Verification of the effect by contact against *P. aeruginosa* of the chitosan films with HAE Ca (**a)** Films on Mueller Hinton agar after 24 hours of incubation at 35°C, (**b)** Films on Mueller Hinton agar with a solution of iodonitrotetrazolium chloride 0.25 mg/mL after 1 h of incubation at 35 °C.

Figure 3.24 shows the effect by contact of the chitosan films with AAE against *B. subtilis*, Gram-positive microorganism. This effect was presented in all concentrations of the extract, which means that the AAE conserved its antimicrobial effect against this microorganism showed in a previous test (CMI), but when incorporates it into chitosan matrix, this effect loss the capacity of diffusion. The principal reason for this behavior is associated with partial loss of volatile compounds [8, 9] such as eugenol and methyl-eugenol, which were identified in a previous study [10] and with tried antimicrobial activity [11, 12] during the drying process of the films.

In general, has been observed that the Gram-positive microorganisms are more sensitive to the volatile compounds contained in essential oil and extracts added to chitosan films than Gram-negative microorganisms, which may be due to the chemical composition of its cell wall [13]. Nevertheless, also has been observed cases where Gram-negative microorganisms were more sensitive than Gram-positive [14, 15], which was related to the kind of volatile compounds contained in the essential oil used, such as monoterpenes and oxygenated monoterpenes. In the present study, in the specific case of the chitosan films with AAE, the probable compound related to antimicrobial activity was eugenol, which mechanism of action consists in that its hydroxyl group could bind proteins and prevent enzyme activity, in addition to causing cell wall deterioration and cell lysis [11, 16]. The above in part is favored by the chemical composition of the Gram-positive microorganism that comprises peptidoglycan and teichoic acid [2].

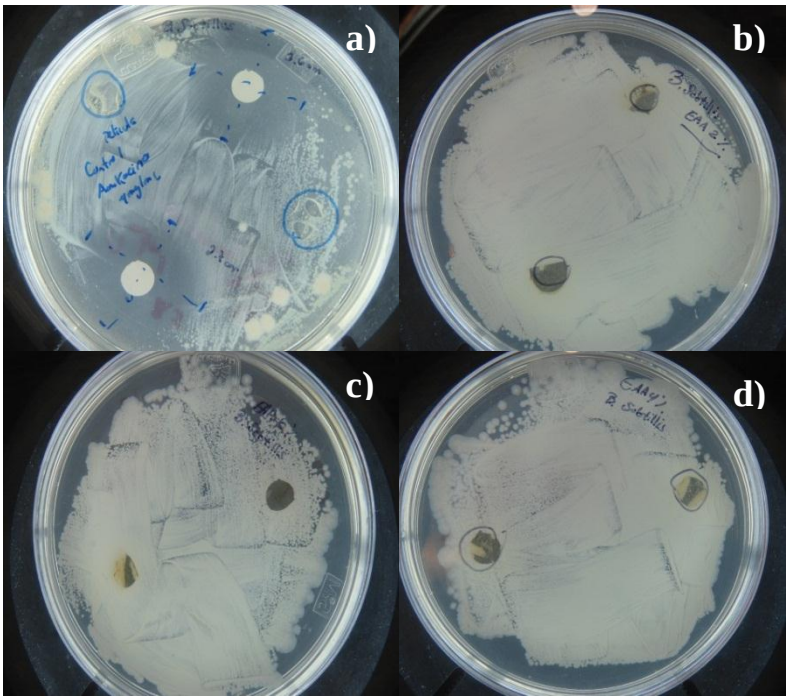

Figure 3.24 Images of the agar disc-diffusion test of chitosan films with AAE at different concentrations using *B. subtilis* microorganism (**a)** Positive control (amikacin 4mg/mL), (**b)** 2%, (**c)** 4%, and (**d)** 6%.

Figure 3.25 shows the confirmation of the antimicrobial activity by contact effect of the chitosan films with AAE against *B. subtillis* through of the test with a solution of iodonitrotetrazolium chloride 0.25 mg/mL. In the images can be observed a change of color (to pink) only around sample film, but there is not growth in the contact area with agar surface. The change of color is associated with the growth of microorganisms.

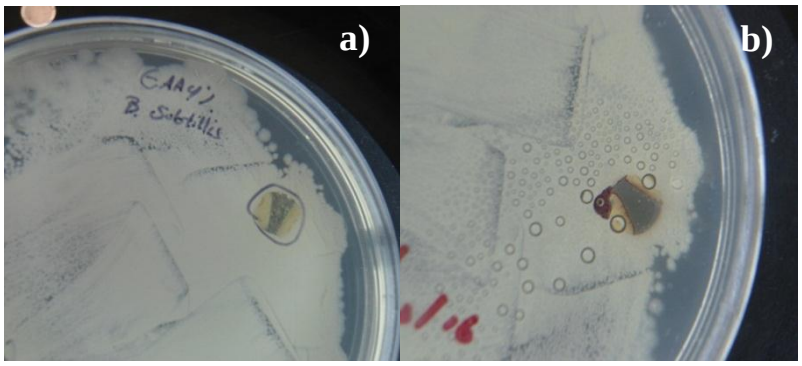

Figure 3.25 Verification of the effect by contact against *B. subtilis* of the chitosan films with AAE (**a)** Films on Mueller Hinton agar after 24 h of incubation at 35°C (**b)** Films on Mueller Hinton agar with a solution of iodonitrotetrazolium chloride 0.25 mg/mL after 1 h of incubation at 35°C.

Figure 3.26 shows the images of the disc diffusion test in chitosan films incorporated with HAECa against *C. albicans*, a yeast-fungus. In all concentrations of the extract, inhibition by diffusion or by contact was not observed, which indicates that when was incorporated into chitosan matrix, the extract had a total loss of the antimicrobial activity showed previously in another assay (MIC). This behavior may be due to that the compounds with antifungal activity were inactivated of any form when were incorporated in the structure of the biopolymer, which indicates a high grade of interaction between these components of the film.

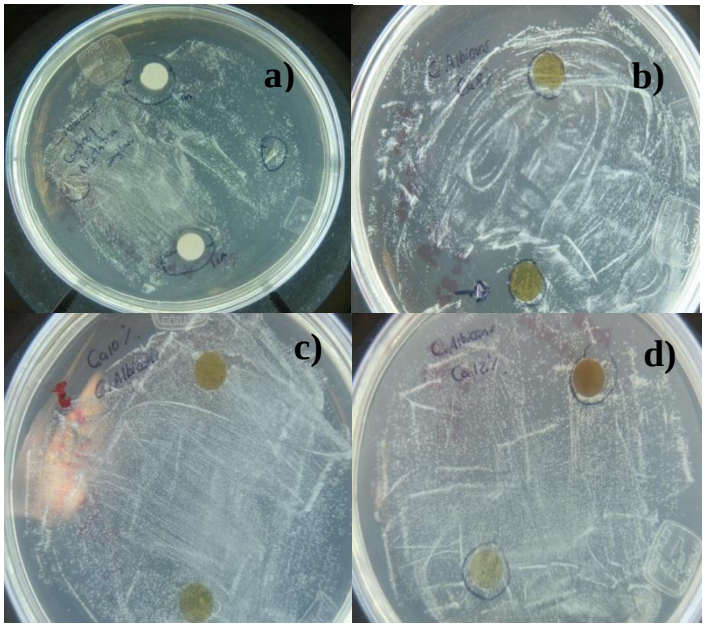

Figure 3.26 Images of the agar disc-diffusion test of chitosan films with HAECa at different concentrations using *C. albicans* microorganism (**a)** Positive control (Nystatin 2mg/mL) (**b)** 8% (**c)** 10% (**d)** 12%.

As *C. albicans* is a microorganism constituted of eukaryote cells, was taken such as a model to observe a probable cell adhesion in the chitosan film with HAECa. This was evidenced by optical and SEM microscopy (**Figure 3.27**). Both kinds of microscopy show the characteristic morphology of *C. albicans*, which indicates that when the extract was incorporated into chitosan matrix, the film obtained not only lost the antimicrobial activity of the extract, also chemical changes were carried out that conferred to the film the capacity of to allow the adhesion of eukaryote cells. This behavior may be associated with changes in the surface of the films, such as the character hydrophilic-hydrophobic of these.

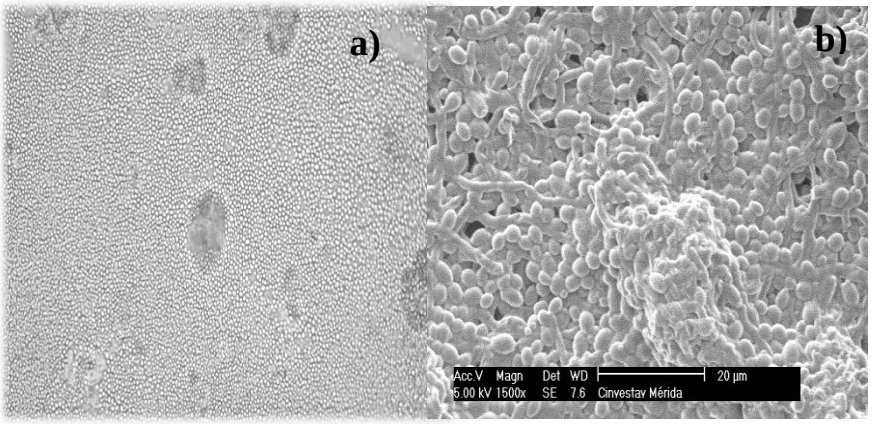

Figure 3.27 Verification of cell adhesion by microscopy of *C. albicans* in chitosan films with HAE Ca after the agar disc-diffusion test (**a)** Optical microscopy (**b)** SEM microscopy with a magnification of 1500X.

3.3.3. Conclusions

The incorporation of the AAE and HAE into chitosan matrix, in general, caused loss of antimicrobial activity in the films obtained against all test microorganisms. Only an effect of contact in some cases can be observed. The above may be attributed to interaction grade between the chitosan and the extracts, also to the chemical composition of these last. The relevant result of these tests was that the incorporation of EHACa also caused a chemical change that conferred to the obtained film the capacity of to allow the adhesion of eukaryote cells, in this specific case of *C. albicans*. These results are of great interest to investigate another eukaryote cells such as the fibroblasts.

3.3.4. References

1. Malinowska-Pańczyk E, Staroszczyk H, Gottfried K, Kolodziejska I, Wojtasz-Pająk A. Antimicrobial properties of chitosan solutions, chitosan films and gelatin-chitosan films. Polimery. 2015. 60: 735-741.
2. Kong M, Chen XG, Xing K, Park HJ. Antimicrobial properties of chitosan and mode of action: A state of the art review. Int J Food Microbiol. 2010. 144:51-63.
3. Pranoto Y, Rakshit SK, Salokhe VM. Enhancing antimicrobial activity of chitosan films by incorporating garlic oil, potassium sorbate and nisin. LWT. Food Sci Tech. 2005. 38:859-865.
4. Coma V, Martial-Gros A, Garreau S, Copinet A, Deschamps A. Edible antimicrobial films based on chitosan matrix. J Food Sci. 2002.67 (3): 1162-1169.
5. Goy RC, Assis OBG. Antimicrobial of films processed from chitosan and N,N,N-trimethylchitosan. Braz J Chem Eng. 2014. 31 (3): 643-648.
6. Lin WC, Lien CC, Yeh HJ, Yu CM, Hsu SH. Bacterial cellulose and bacterial cellulose-chitosan membranes for wound dressing applications. Carbohydr Polym. 2013. 94: 603-611.
7. Cagri A, Ustunol Z, Ryser ET. Antimicrobial, mechanical, and moisture barrier properties of low pH whey protein-based edible films containing p-Amminobenzoic or sorbic acid. 2001. J Food Sci. 66(6): 865–870.
8. Remya S, Mohan CO, Bindu J, Sivaraman GK, Venkateshwarlu G. Effect of chitosan based active packaging film on the keeping quality of chilled stored barracuda fish. J Food Sci Technol. 2016. 53 (1): 685-693.
9. Higuera-Barraza OA, Soto-Valdez H, Acedo-Félix E, Peralta E. Fabrication of an antimicrobial active packaging and its effect on the growth of pseudomonas and aerobic mesophilic bacteria in chicken. VITAE. 2015. 22 (2): 111-120.

10. Caamal-Herrera IO, Muñoz-Rodríguez D, Madera-Santana T, Azamar-Barrios JA. Identification of volatile compounds in essential oil and extracts of *Ocimum micranthum* Willd leaves using GC/MS. Int J Appl Res Nat Prod.2016; 9(1): 31-40.
11. Marchese A, Barbieri R, Coppo E, Orhan IE, Daglia M, Nabavi SF, Izadi M, Abdollahi M, Nabavi SM, Ajami M. Antimicrobial activity of eugenol and essential oils containing eugenol: A mechanistic viewpoint. Crit Rev Microbiol. 2017. DOI: 10.1080/1040841X.2017.1295225.
12. Joshi RK. Chemical Composition, *In Vitro* Antimicrobial and Antioxidant Activities of the Essential Oils of *Ocimum Gratissimum*, *O. Sanctum* and their Major Constituents. Indian J Pharm Sci. 2013.75(4): 457–462.
13. Yuang G, Chen X, Li D. Chitosan films and coatings containing essential oils: The antioxidant and antimicrobial activity, and application in food systems. Food Res Int. 2016. 89: 117-128.
14. Hafsa J, Smach MA, Khedher MRB, Charfeddine B, Limem K, Majdoub H, Rouatbi S. Physical, antioxidant and antimicrobial properties of chitosan films containing Eucalyptus globulus essential oil. LWT- Food Sci Tech. 2016. 68: 356-364.
15. Altiok D, Altiok E, Tihminlioglu F. Physical, antibacterial and antioxidant properties of chitosan films incorporated with thyme oil for potential wound healing application. J Mater Sci: Mater Med. 2010. 21: 2227-2236.
16. Bevilacqua A, Corbo MR, Sinigaglia M. *In Vitro* Evaluation of the Antimicrobial Activity of Eugenol, Limonene, and Citrus Extract against Bacteria and Yeasts, Representative of the Spoiling Microflora of Fruit Juices. J Food Protect. 73 (5): 888-894.

3.4 Cell adhesion and cell viability tests of films based on chitosan, aqueous extract of *Ocimum micranthum* Willd leaves and hydro-alcoholic extract of *Calendula officinalis* L. flowers.

3.4.1 Experimental Methods

Cell line and cell culture

The biocompatibility of the chitosan films with extracts (HAECa and AAE) was tested using hFB cells. This cell line was used previously in the MTT and Trypan Blue assay with the HAECa and AAE extracts to determine its cytotoxicity. The cells were grown previously in DMEM F12 medium (Gibco, USA) supplemented with 10% fetal bovine serum (Gibco, USA) and incubated at 37 °C in a humidified atmosphere of 5% CO_2.

Treatment of films for cell adhesion assay

Chitosan films added with HAECa (8% 10% and 12%) and AAE (2% 4% and 6%) were cut in a square shape of approximately 1 cm^2 and placed in plates of 24 wells (Corning). Then, these were washed two times with phosphate buffer solution (PBS 1X Gibco). The PBS was removed and the samples exposed to 15 min of UV light by each side. Later, 1 mL of 1X PBS sterilized and supplemented with amikacin (4mg/L), and Fluconazole (1.5 mg/L) was added. The films were incubated for 24 h at 37 °C, 5% CO_2 and humidified atmosphere. Finished the incubation time, the supplemented PBS was removed, and three washes were made with sterilized PBS. The films were used immediately after the washing. This treatment was also applied to the controls. Three samples per each formulation were treated.

Cell adhesion assay

The wells that contained the films and controls were inoculated with 1 mL of culture medium prepared at $5x10^4$ cells/mL. Positive adhesion controls (Thermanox™, Thermo Fisher Scientific), pure chitosan film control, cell controls in wells without film, and well controls with cell free medium were used. The plate was incubated for 72 h under culture conditions (at 37 °C and 5% CO_2).

Cell morphology by optical microscopy

After 24, 48 and 72 h of incubation, the plates from the cell adhesion test were observed under an inverted phase contrast microscope (Labomed TCM 400 LM-7125000 model) with 4X and 20X objectives and the hFB cells adhered on the surface of the chitosan films were photographed.

Cell morphology by SEM microscopy

Scanning electron microscopy (SEM) was used to observe the morphology of cells adhered to the films. For this purpose, at 72 h of incubation time, the culture medium that covered the samples was retired and washed two times with sterilized PBS 1X. Then, a glutaraldehyde 3% in Sodium Cacodylate 0.1 M buffer was added to the samples and the plates were incubated at 4°C and in darkness for two hours. Finished the incubation time, the films were washed two times with PBS 1X solution. Later, the films were dehydrated in increasing concentrations of ethanol (50%, 70%, 90% and 100%) for 15 min. Finished the dehydration, the samples of films were placed with tweezers in a sample holder, which was soaked in ethanol. Then, the sample holder was submitted to a process of critical point drying (equipment Quorum K850 model) for 1 h. Later, the samples were fixed on stubs of carbon tape of double-sided fixed previously on a sample holder. Finally, the samples were coated with a layer of gold through a metallization process (equipment Quorum Q150R ES model) to make them more conductive allowing the surface visualization.

The morphology of the fibroblast cell adhered to positive adhesion control (Thermanox™, Thermo Fisher Scientific), chitosan film control, chitosan films with AAE and HAECa were observed using a Field Emission Scanning Electron Microscope JEOL JSM-6390LV model (Tokyo, Japan). The images were obtained by LEI detector, under high vacuum, 5 kV of voltage with a working distance of approximately 8 mm and a magnification of 1500X. For to observe as the fibroblast cells covered the surface of the chitosan films with extracts, images were obtained using LEI detector, 5 kV of voltage, under high vacuum, LM mode and a magnification of 250X.

Cell viability by the fluorescence method

Some samples of films that were recovered at 72 h of incubation time and used to determine the viability to adhere cells by the method of fluorochrome staining. The Live/Dead kit for mammalian cells was used (Thermo Fisher Scientific); this kit contains calcein AM and ethidium homodimer-1, which show the living cells in green color and the dead cells in red color, respectively. The preparation of the reagent was performed according to the manufacturer's instructions. For the staining process, the culture medium was removed from the wells with the samples, two washes were performed with PBS I X, after 200 μL of the reagent prepared previously was added to the surface of the films. The films were incubated for 45 min under standard culture conditions, finished the incubation time, the films were placed on slides, and these were observed with a fluorescence microscope (Zeiss LSM 510 META) with a 4X and 10X objectives and photographic records were registered.

3.4.2. Results and discussion

The chitosan films with extracts (HAECa and AAE) showed different biocompatibility characteristics. Next, the results are described by each kind of film evaluated.

Chitosan films with HAECa

In the case of chitosan films with HAECa was observed cell adhesion since of 24 h and this was proportional to extract concentration. The cell adhesion was confirmed at 72 h, at this time the cells showed the spindle shape characteristic (**Figure 3.28**). While that the fibroblast cells adhered to the chitosan control film (without extract) presented a rounded shape, which means that the attachment of these on the surface of films was weak, and did not reach to spread and to grow. The above observation indicates that the initial attachment plays a most important role in the cell affinity for surfaces [1, 2]. In the case of the chitosan films with HAECa, suggests that the extract caused chemical and physical changes in the chitosan matrix, which allowed that the fibroblast cells could spread and grow. This behavior of the fibroblast cells may be related to characteristics of the surface of the chitosan films such as surface energy, roughness, and surface chemistry [2,3]. The wettability of a surface in part reflects its chemistry, a form to determine this parameter is with angle contact measurement [3]. The contact angle average value showed by chitosan films with HAECa was 50°, which indicates that the surface of this type of film is hydrophilic. Some authors have mentioned that the hydrophilic properties of the polymer lead to increased cell spreading and adhesion [3].

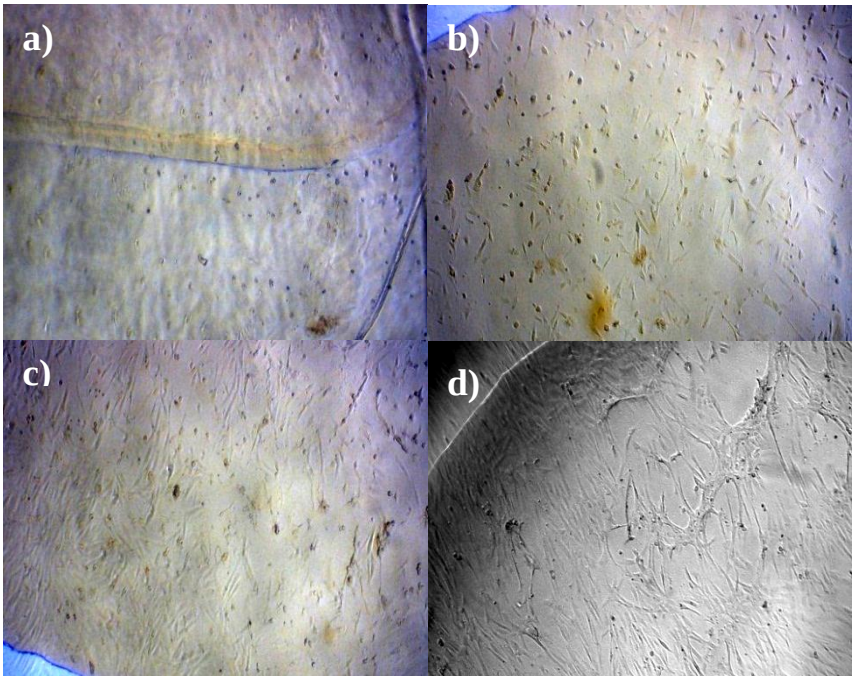

Figure 3.28 Images of the optical microscopy of the cell adhesion test of chitosan films with HAE Ca at different concentrations at 72 h of culture, using a magnification 4X **a)** Chitosan film control) **b)** 8% **c)** 10% **d)** 12%.

The SEM images evidenced the morphology of the fibroblast cells attached to the surface of chitosan films with HAECa, the characteristic shape of a spindle, spread and grew on the surface of the films in all concentrations of the extract (**Figure 3.29**). These cells were spreading until to form a monolayer on the surface of the film at a high concentration of the extract (HAECa 12%), as well as was observed with the control ThermanoxTM, that is a polymer treated for cell adhesion. By other hand, in the chitosan control film (without extract), the fibroblast cells took a round and spherical shape, without spread or growth; the above behavior has been observed in other previous studies with NIH-3T3 cells, where these presented cell growth inhibition, resulted from their inability to attach to a hydrogel of chitosan-PVP [4]. This occurred in spite of that the chitosan is a biopolymer with many physical and chemical properties, conferred by its functional groups, which do it an ideal material for the cell adhesion [5]. However, must be considered the existence of other factors that could affect the process of cell adhesion, such as the nature of cell kind, growth factors present into the medium or the extract.

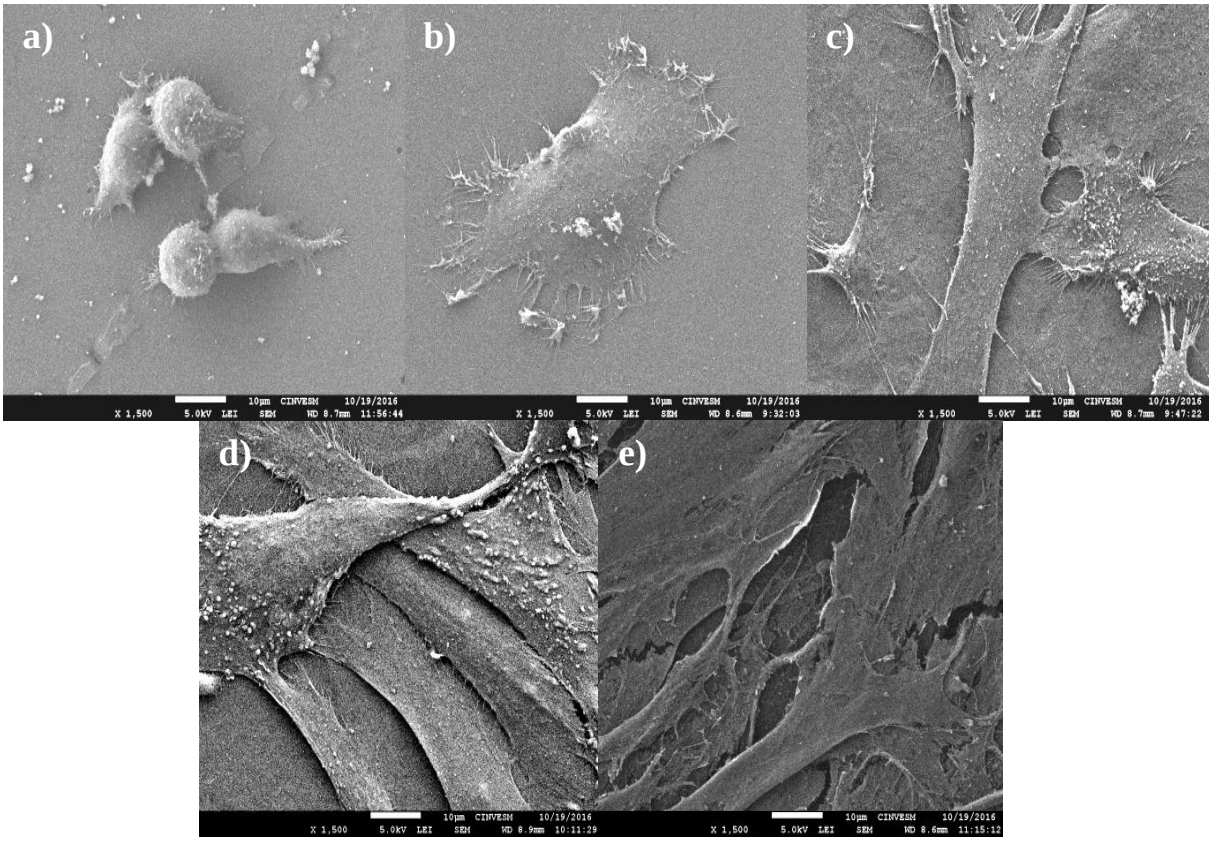

Figure 3.29 Micrographs SEM of the cell adhesion test of chitosan films with HAE Ca at different concentrations, 72 h of culture, using LEI detector and SEM mode with a magnification of 1500X (**a)** Chitosan film control **b)** 8% **c)** 10% **d)** 12% **e)** Thermanox ™.

Micrographs were taken with SEM equipment at a magnification of 250X to visualize at a greater distance the monolayer formation of the fibroblast cells on the surface of films with HAECa. The images show the low density of fibroblast cells with a rounded shape on chitosan control film, while that in chitosan films with HAECa at 12%, the fibroblast cells congregated and grew as an adherent spreading monolayer, as well as in the ThermanoxTM polymer used as positive control (**Figure 3.30**).

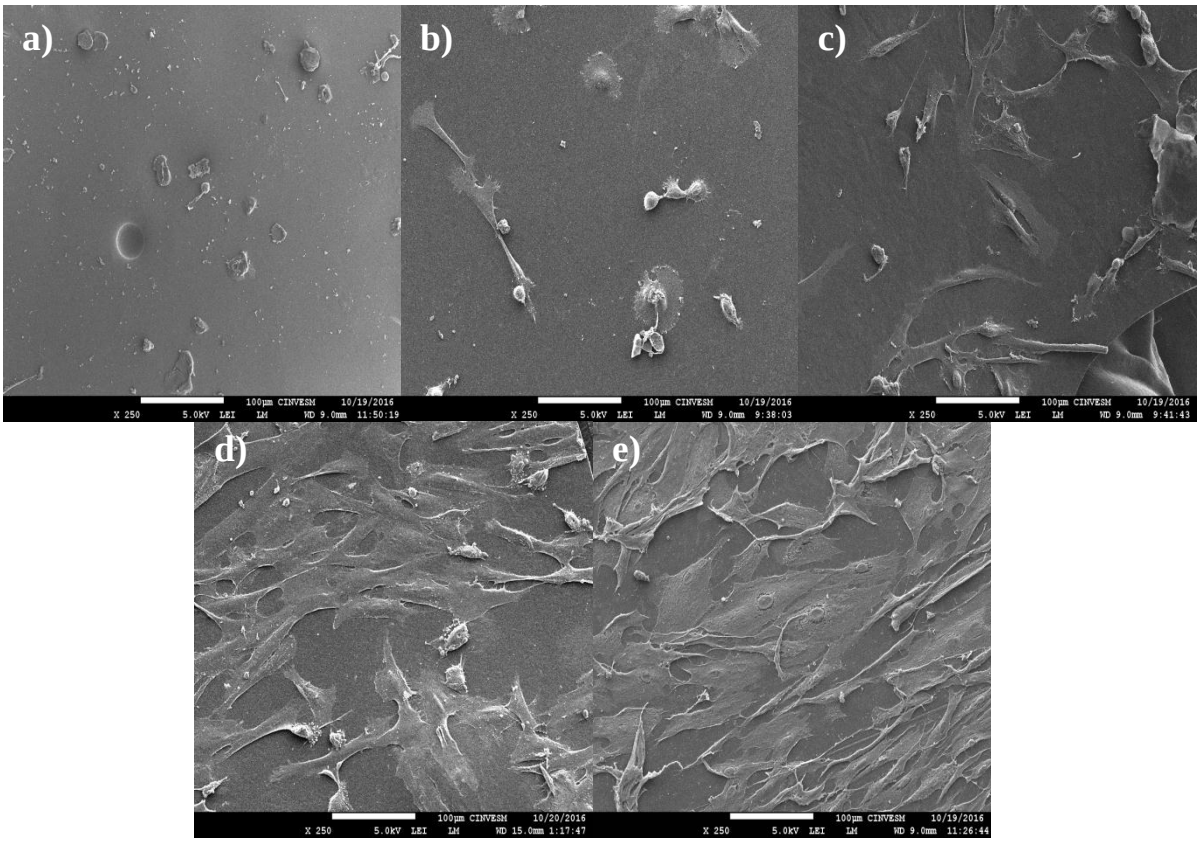

Figure 3.30 Micrographs SEM of the cell adhesion test of chitosan films with HAE Ca at different concentrations, at 72 h of culture using LEI detector and LM mode with a magnification of 250X (**a)** Chitosan film control) (**b)** 8% (**c)** 10% (**d)** 12%
e) Thermanox ™.

Some authors reported the use of an alcoholic extract from *Calendula officinalis* in the formulation of PCL nanofibers, with the purpose to improve the cell adhesion capacity of this material [6]. The results of this study indicated that the incorporation of the extract caused changes in chemical and physical properties of the PCL nanofibers, and fibroblast line (L929) showed good growth on this substrate. On the other hand, another authors have mentioned that the serum albumin used such as part of the medium in the adhesion assay, can provide binding proteins (such as fibronectin and vitronectin), which are first absorbed into the substrate and allow the attachment of the fibroblasts, being that these have no natural recognition sites on the surface of the polymeric

materials [1, 7]. The above does of the residual protein in chitosan a relevant parameter, which that may exert a significant influence on the biocompatibility of this biopolymer because may to influence binding/adsorption of other proteins and have potential to elicit immunological reactions [7].

The viability of the fibroblasts adhered to the chitosan films with HAECa was verified at 72 hours of contact, through a fluorescence test where the cells that fluoresce in green are living cells, and the cells that fluoresce in red are dead cells. The Figure 3.31 shows the images obtained by fluorescence microscopy.

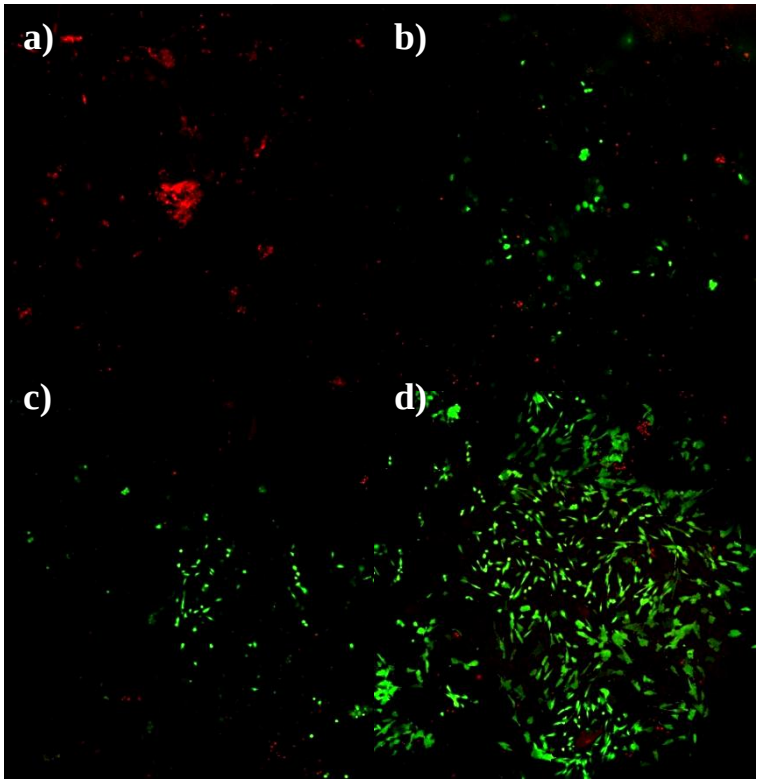

Figure 3.31 Images of the Fluorescence microscopy of the cell viability test of chitosan films with HAE Ca at different concentrations, at 72 h of culture using magnification 4x (**a)** Chitosan film control (**b)** 8% (**c)** 10% (**d)** 12%

The images show how the density of fibroblast cells in chitosan films with HAECa increased when the concentration of the extract incremented and these also show the viability of the cell line at all concentrations. In contrast, the fibroblast cells adhered to chitosan control films presented low density and loss of viability. The anchorage form of the cell line in the surface of the films may influence the viability [8]. However, other studies have revealed that chitosan films without additional factors have allowed to maintaining the viability of the bone marrow derived

mesenchymal stromal cells (BMSCs) [9] and other cases where with the help of additional factors conserved the viability of MC3T3 osteoblast cells [8].

Chitosan films with AAE

Chitosan films with AAE showed a low cell adhesion and proliferation at 24 h. Optical microscope images also show cell adhesion at 72 h, but the fibroblasts presented a rounded shape, as well as in the chitosan control film. Another fibroblast cells achieved spread and growth but in an irregular shape (**Figure 3.32**).

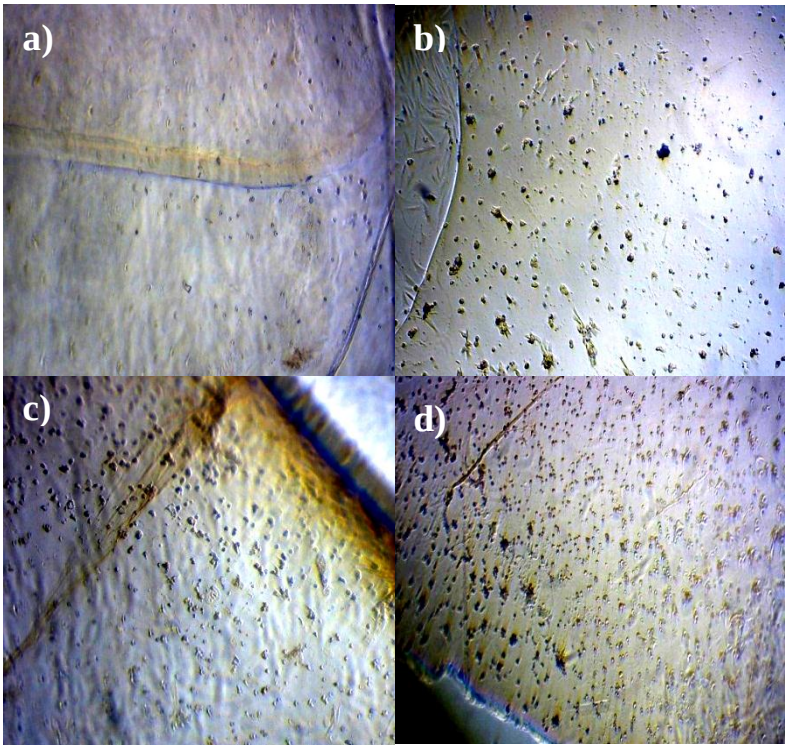

Figure 3.32 Images of the optical microscopy of the cell adhesion test of chitosan films with AAE at different concentrations at 72 h of culture, using a magnification 4X (**a)** Chitosan film control) (**b)** 2% (**c)** 4% **(d)** 6%.

Several authors have mentioned that adhesion and proliferation of cells on biomaterials depend on the surface properties such as cleanliness, surface charge, surface free energy, surface topography, wettability, and density [2,8]. The results of the contact angle test in the present research exert that the wettability property may be the reason for the behavior of the fibroblast cell line. Chitosan films with AAE conserved the contact angle of the chitosan control films (90°) while the addition of HAECa decreased the contact angle (50°) of the chitosan films. Values of contact angle below 90° denote the hydrophilic nature of the surface, which is an essential factor that influences in the cytocompatibility of biomaterial [10]. The cell adhesion and growth are directly

affected by the wettability of the surface, due to most of the cells prefers to anchor in hydrophilic surfaces [10].

The SEM images evidence the morphology of the fibroblasts attached to the surface of chitosan films with AAE. These cells took a round and spherical shape in all concentrations of the extract (as well as in the chitosan film control) with a tendency to form aggregates and some cells reached to spread in an irregular form that did not correspond to a characteristic shape of this kind of cells (**Figure 3.33**). This behavior may be attributed in part to the hydrophobic surface of the films, which was demonstrated through its value of contact angle (90°).

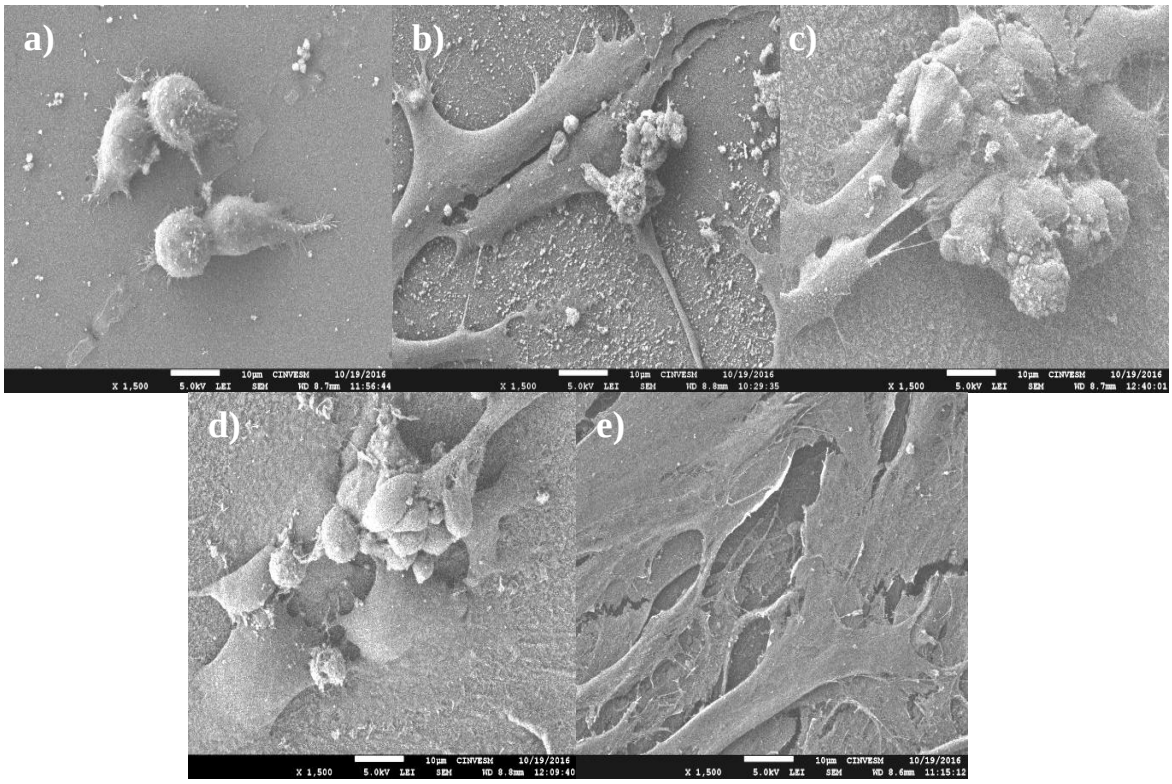

Figure 3.33 Micrographs of SEM of the cell adhesion test of chitosan films with AAE at different concentrations, 72 h of culture, using LEI detector and SEM mode with a magnification of 1500X (**a)** Chitosan film control) (**b)** 2% (**c)** 4% (**d)** 6% **e)** Thermanox ™.

Some authors have mentioned that the biomaterial surface characteristics are critical because may regulate the cell function and cell expression [8]. The above is due to that when the cells adhere and grow on substrates, the cells sense, interpret and integrate the extracellular signals and respond to them [8]. The images showed that is likely that the fibroblast cells suffered stress when adhered to a surface with a hydrophobic character. The presence of some compounds in the

extract (AAE) may increase the cell stress, which was reflected in the form that these adhere to the material.

Micrographs of chitosan films with of AAE at a magnification of 250X showed the low density of fibroblast cells on the surface (**Figure 3.34**). The adhered cells formed small aggregates, and the most of these did not grow or spread on the surface, which indicates a weak adhesion and low biocompatibility with the material.

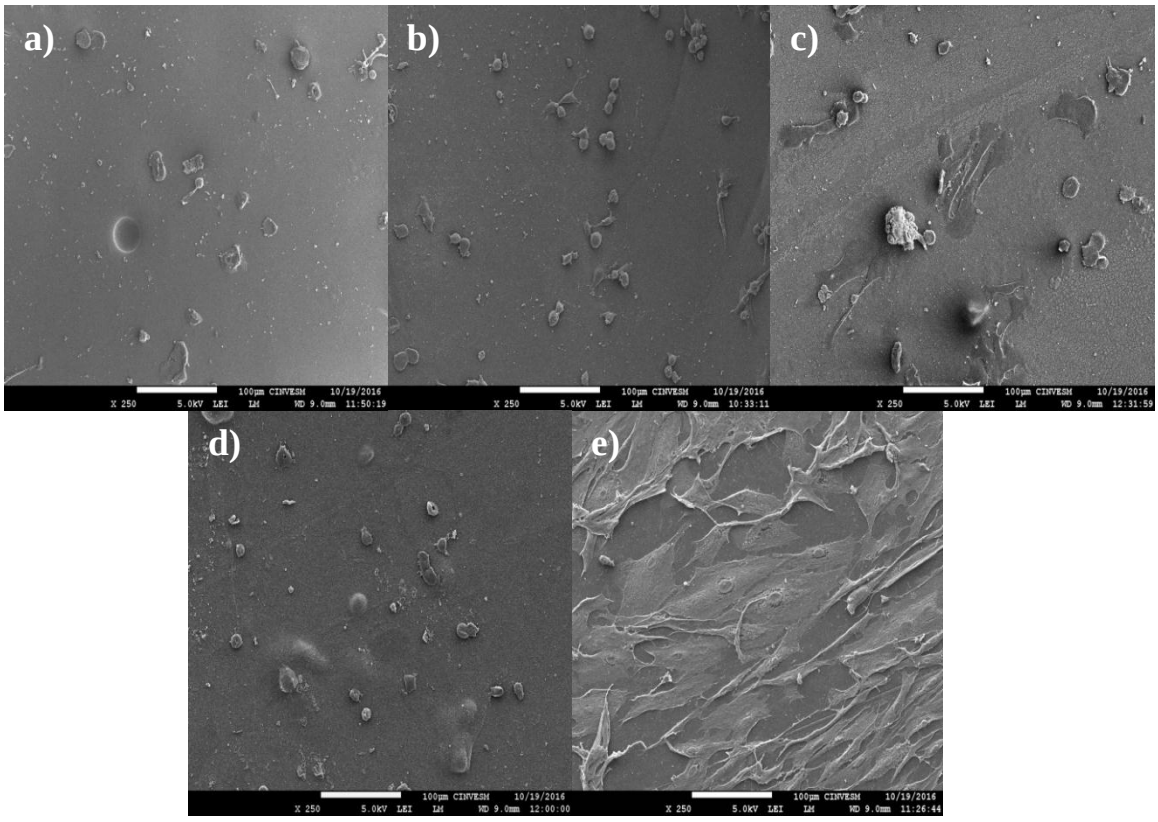

Figure 3.34 Images of the SEM microscopy of the cell adhesion test of chitosan films with AAE at different concentrations, at 72 h of culture, using LEI detector and LM mode Chitosan film with a magnification of 250X : (**a)** Control) (**b)** 2% (**c)** 4% (**d)** 6% **e)** Thermanox ™.

Chitosan films with AAE did not analyze with fluorescence microscopy because showed low adherence, growth and irregular spread of the fibroblast cell line on the surface, characteristics not appropriate for a material with application in the biomedical area.

3.4.3 Conclusions

The addition of HAECa into chitosan matrix caused chemical and physical changes in the films which allowed the adhesion, growth, and viability of the fibroblast cell line. The addition of AAE in chitosan films with as well as the films control (only chitosan) did not propitiate proper

attached of fibroblast and therefore its growth and viability. These results allow state that the chitosan films incorporated with HAECa are a biomaterial with viable application into the biomedical area.

3.4.4. References

1. Ghanem A, Katalinich M. Characterization of chitosan films for tissue engineering applications. Appl Bionics Biomech. 2005. 2(1): 9-16.
2. Zhu X, Chian KS, Chan-Park MB, Lee ST. Effect of Argon-plasma treatment on proliferation of human-skin-derived fibroblast on chitosan membranes in vitro. J Biomed Mater Res A. 2005.73 (3): 264-74.
3. Dowling DP, Miller IS, Ardhaoui M, Gallagher WM. Effect of surface wettability and topography on the adhesion of osteosarcoma cells on plasma-modified polystyrene. J Biomater Appl. 2011 Sep;26(3):327-47.
4. Risbud M, Hardikar A, Bhonde R. Growth modulation of fibroblasts by chitosan-polyvinyl pyrrolidone hydrogel: implications for wound management? J Biosci. 2000. 25(1):25-31.
5. Rodríguez-Vázquez M, Vega-Ruiz B, Ramos-Zúñiga R, Saldaña-Koppel DA, Quiñones-Olvera LF. Chitosan and its potential use as a scaffold for tissue engineering in regenerative medicine. BioMed Res Int. 2015. 1-15.
6. Hosseinkazemi H, Biazar E, Bonakdar S, Ebadi MT, Shokrgozar MA, Rabiee M. Modification of PCL electrospun nanofibrous Mat with *Calendula officinalis* extract for improved interaction. Int J Polym Mat Polym Biomat. 2014. 64: 459-464.
7. Hamilton V, Yuan Y, Rigney DA, Puckett AD, Ong JL, Yang Y, Elder SH, Bumgardner JD. Characterization of chitosan films and effect on fibroblast cell attachment and proliferation. J Mater Sci Mater Med. 2006. 17(12):1373-81.
8. Zheng Z, Zhang L, Kong L, Wang A, Gong Y, Zhang X. The behavior of MC3T3-E1 cells on chitosan/poly-L-lysine composite films: Effect of nanotopography, surface chemistry and wettability. J Biomed Mater Res A. 2009. 89(2):453-65.
9. Wrobel S, Cristina Serra SC, Ribeiro-Samy S, Sousa N, Heimann C, Barwig C, Grothe C, Salgado AJ, Haastert-Talini K. In Vitro Evaluation of Cell-Seeded Chitosan Films for Peripheral Nerve Tissue Engineering. Tissue Eng : Part A. 2014. 20 (17-18): 2339-2349.
10. Archana D, Dutta J, Dutta PK. Evaluation of chitosan nanodressing for wound healing: Characterization, *in vitro* and *in vivo* studies. Int J Biol Macromol. 2013. 57: 193-203.

GENERAL CONCLUSIONS

The chemical compounds identified by GC/MS in the essential oil and ethanolic extract from leaves of *O. micranthum* and the hydro-alcoholic extract of *M. tenuiflora* bark could be the reason of the antimicrobial activity against *S. aureus*, *B. subtilis*, *P. aeruginosa* and *C. albicans* but also of the anti-proliferative effect observed on hFB cell line at lower concentrations. Only the hydro-alcoholic extract of *C. officinalis* flowers (HAECa) and the aqueous extract of *O. micranthum* leaves (AAE) showed a special activity against *C. albicans* at same concentration (80 µl/ml) and a minor anti-proliferative effect on hFB cell line at concentrations evaluated.

The hydro-alcoholic extract of *C. officinalis* flowers lost its antimicrobial effect that showed previously when was incorporated it in the chitosan matrix; however its proliferative effect was conserved. The increase of the concentration of the hydro-alcoholic extract of *C. officinalis* in the chitosan matrix caused a higher proliferative impact on fibroblast cell line. By the other hand, the incorporation of the hydro-alcoholic extract of *C. officinalis* flowers produced changes in the chitosan matrix, therefore in mechanical, physical and thermal properties of the films. The modification of the contact angle of chitosan films could be one of the principal factors of its proliferative effect on fibroblast cell line.

The aqueous extract of *Ocimum micranthum* Willd leaves lost the antimicrobial effect and the proliferative effect when it was incorporated into the chitosan matrix. The physical and thermal properties of the chitosan films were significantly modified with the incorporation of this extract. Furthermore, some mechanical parameters of the chitosan films were changed by the presence of the extract.

These results indicate that the chitosan films with HAECa could be used for biomedical, although before is necessary confirming its proliferative behavior on hFB cell line through of *in vivo* models and clinical assays.

By the other hand, the extracts and oils from *O. micranthum*, *M. tenuiflora* and *A. indica* that showed anti-proliferative effect on hFB cell line could be evaluated in other kind of cell line, for example cancer cells.

PERSPECTIVES

The proliferative effect of the chitosan films with hydro-alcoholic extract of *Calendula officinalis* flowers on fibroblast cell line must be confirmed with in vivo tests. If this kind of test will result success, could be consider a clinical assays. By the other hand, a surface charge test in the chitosan films with hydro-alcoholic extract of *Calendula officinalis* flowers is necessary for a better understanding of proliferative mechanism and the adhesion of the fibroblast cells in this material.

According with the results of the proliferative essay on fibroblast cell line, the anti-proliferative effect of the ethanolic extract and essential oil from *Ocimum micranthum* Willd leaves must be studied in cancer cell lines. Also this effect must be studied in the hydro-alcoholic extract of *Mimosa tenuiflora* bark and the oil of *Azadirachta indica* A. Juss seeds. The purpose is to use those extract always for a biomedical application as the treatment against cancer cells, a disease that represent a challenge in the field of the medicine today.

PUBLICATIONS DERIVED FROM THE THESIS

1.- Caamal-Herrera IO, Muñoz-Rodríguez D, Madera-Santana T, Azamar-Barrios JA. Identification of volatile compounds in essential oil and extracts of *Ocimum micranthum* Willd leaves using GC/MS. Int J Appl Res Nat Prod.2016; 9(1): 31-40.

2.- Caamal-Herrera IO, Muñoz-Rodríguez D, Madera-Santana T, Azamar-Barrios JA. Identification of volatile compounds in hydro-alcoholic extracts of *Calendula officinalis* L. flowers and *Mimosae tenuiflorae* bark using GC/MS. Int J Appl Res Nat Prod.2016; 9(1): 20-30.

3.- Caamal-Herrera IO, Carrillo-Cocom LM, Escalante-Réndiz DY, Aráiz-Hernández D, Azamar-Barrios JA. Antimicrobial and antiproliferative activity of essential oil, aqueous and ethanolic extracts of *Ocimum micranthum* Willd leaves. BMC Complement Altern Med. 2018; 18 (1):55.

4.- Caamal-Herrera IO, Carrillo-Cocom LM, Escalante-Réndiz DY, Aráiz-Hernández D, Azamar-Barrios JA. *In vitro* Antimicrobial and Anti-proliferative Activities of a Commercial Hydro-alcoholic Fluid Extract of *Mimosa tenuiflora* (Willd) Poiret Bark. **Pending submission.**

5.- Caamal-Herrera IO, Gónzalez-Burgos A, Madera-Santana T, Azamar-Barrios JA. Material based on chitosan and natural extracts for biomedical application: Effects of the extracts on mechanical, thermal, chemical, physical and functional properties. **In process.**